Physiological evidence for climate limitations of oak distributions at local and regional scales

A Dissertation

SUBMITTED TO THE FACULTY OF THE

UNIVERSITY OF MINNESOTA

BY

Beth Fallon

IN PARTIAL FULFILLMENT OF THE REQUIREMENTS

FOR THE DEGREE OF

DOCTOR OF PHILOSOPHY

ADVISOR Jeannine Cavender-Bares

November 2017

Acknowledgements

My dissertation work would not have been possible without the thoughtful guidance and incredible scientific experience of my graduate advisor, Jeannine Cavender-Bares. My committee members, David Moeller, Andy Hubbard, Rebecca Montgomery, and Walid Sadok, provided valuable feedback to make this work better. Ken Kozak and George Weiblen contributed comments to my initial research proposal that improved my subsequent work.

Many funding and management groups made this research possible. The National Science Foundation (DEB-1146380, PI Jeannine Cavender-Bares) provided funding for acorn collection, common garden supplies, and a semester research position. The Charles J. Brand Fellowship generously supported my work for a year, and the University of Minnesota Graduate Department of Plant Biological Sciences provided summer funding and travel support. The University of Minnesota Graduate School Thesis Research Travel Grant, the Dayton Bell Museum Fund, and the Carolyn M. Crosby Fellowship provided funds for research in Arizona and greenhouse work at the University of Minnesota. The Southwestern Research Station (American Museum of Natural History) provided ample logistical support (Dawn Wilson and Gary Wisdom once drove up the mountain to clear the road of some trees downed after high winds so that I was not stuck in Barfoot Park overnight) and lab and living space for field work within the Chiricahua Mountains, as well as providing funding for reduced cost of living during research trips. The United States Forest Service's Chiricahua National Forest (Douglas Ranger District) provided a permit for temporary installations of temperature monitoring apparatuses within the Chiricahuas.

Many people directly contributed to data collection and this work would not have been possible without their kind assistance. Sally Ratliff and Chip Blackburn assisted with initial site selection and measurements within the Chiricahuas. Greg Goodrum, Chris Walker, and many Southwestern Research Station volunteers helped out with field collections, often before dawn. Antonio Gonzalez-Rodriguez, Frank Hoerner, and Esau Zuniga collected acorns from wild populations and provided them for this research. Matthew Kaproth and Jose Ramírez Valiente donated their expertise in establishing and caring for an oak garden experiment. Ian Carriere, Alec Scollard, and Melat Weldesalasie helped plant and measure oaks in the greenhouse common garden experiment. The staff of the University of Minnesota Plant Growth Facility, especially Pam Warnke and Roger Meissner, helped me greatly in setting up and maintaining a successful greenhouse garden. José Eduardo Meireles was instrumental in the development of ideas for research on oak cooling responses and hyperspectral detection, collected the hyperspectral reflectance data, and was an incredible resource in analyzing that data. Anna Schweiger, Shan Kothari, and Vinicius Marcilio-Silva generously volunteered their time for hyperspectral data collection.

I benefited from the time of generous colleagues in the Cavender-Bares lab who provided feedback on this research as I developed it into its current form. Jake Grossman, Laura Williams, Dudu Meireles, Nick Deacon, Anna Schweiger, Shan Kothari, Jen Teshera-Levye, Xiajoing Wei, Matt Kaproth, Will Pearse, Jose Ramírez Valiente, and Alyson Center have made suggestions on research questions, methods, analyses, and framing of the results that has made my work exponentially better. Jake and Nick also provided thorough feedback on an earlier version of Chapter 2. Cathleen Nguyen helped me work

through some of my initial confusion on the pneumatic method of measuring xylem vulnerability.

Many friends have made me a better scientist and a happier person throughout graduate school. Allison Haaning, Diana Trujillo, and Christina Smith are incredible scientists and very funny friends and traveling companions, and graduate school would not have been very much fun without them. Leland Werden, Derek Nedveck, and Eli Krumholz joined us frequently at happy hour to talk about new science and nonsense. Mandy Waters, Erin Treiber, and Stephanie Erlandson and I started out in the same class of Plant Biological Sciences graduate students and I have learned so much from them and have been inspired by their progress in their research and their lives. Jake Grossman is a patient and thoughtful scientist, a good role model, and a kind friend. Mohamed Yakub is an incredible force of ideas and enthusiasm. He has been inspirational to me in trying to go out and communicate science. He co-founded Market Science, a direct-to-public science outreach platform, and I have been happy to be a part of continuing to organize that project with him, Ryan Briscoe Runquist, and John Benning.

Finally, my family has always been very supportive of education and finding work that I find important. My parents, Michael and Deborah Fallon, encouraged my siblings and me to try many things and kept us outside and engaged as much as possible, through road trips to different national parks or camping trips in the upper Midwest. My husband, Henry Brock, has been an incredibly supportive partner while I pursued my graduate education and has helped make life easier (including some copyediting) and better for me while continuing his own education to become a secondary school science teacher.

Dedication

This work is dedicated to my grandmother, Margaret Fallon.

Abstract

Understanding the extent to which physiological tolerances of climate may limit plant distributions is critical to predicting the effects of a changing climate. This dissertation research focuses on how responses to drought and cooling influence species ranges among oaks (*Quercus* L.), a globally-distributed woody genus that is highly diverse within the Americas. I used functional and physiological traits to investigate correlations between cold and drought resistances and climate at two scales: 1) local species elevation limits in a semi-arid montane system and 2) regional range limits among North and Central American oaks. In Chapter 1, I found that a trade-off between the leaf-level drought resistance traits of avoidance (leaf abscission) and desiccation recovery (leaf capacitance), and not stem freezing tolerance, influenced species sorting by elevation in a semi-arid mountain system in the southwestern US. In Chapter 2, I found that stem drought tolerance (xylem vulnerability) is correlated with aridity of climate of origin among oaks from across the Americas, but that the seasonality of precipitation best predicted leaf level drought avoidance (leaf habit and stomatal closure). Finally, in Chapter 3, I found that oak species in the Americas have different leaf level cooling responses (chlorophyll fluorescence measurements of photosynthetic stress and yield) that were correlated with minimum temperatures in their climate of origin, but that ability to acclimate to cold temperatures was best predicted by leaf phenology, not climate of origin. I also found that we could predict chlorophyll fluorescence measurements with models created from hyperspectral reflectance data measured on the same leaves. These models included regions of important biological significance, including wavelengths corresponding with reflectance of photosynthetic and protective pigments. Overall, there

I found significant evidence that species distributions are strongly influenced by climate. Oak species have suites of traits as mechanisms of drought resistance, and these strategies are correlated with not only overall aridity in their current habitats, but with the seasonality of precipitation. Oak species may also be able to acclimate to cooler temperatures outside of those commonly experienced in their current range. Oak species within the Americas and the mountainous, arid southwest US, may be vulnerable to range shifts as global temperatures continue to rise and precipitation regimes change.

Table of Contents

List of Tables

List of Figures

Introduction

It is not overly simplistic to summarize a large part of ecological investigations as primarily concerned with why any species grows or lives where it does. While the factors that can influence species ranges are numerous, they can be broadly split into abiotic and biotic causes. The abiotic climate factors, especially temperature and precipitation, have long been a topic of research and are increasingly important as global climate change alters long-standing climatic patterns and thus alters the habitats of current species ranges. In this dissertation, I report on research into how physiological resistances to long and short term drought and cold temperatures structure oak (*Quercus* L.) species ranges on both the relatively small scales of mountain elevation ranges and within the wider landscape of continental ranges.

Researchers have long observed the coincidence of species distributions and climatic gradients (Merriam 1894, Shreve 1915, Livingston and Shreve 1921, Whittaker and Niering 1965, MacArthur 1972, Stephenson 1990). At global scales, species distributions were thought to be limited at the polar latitudes by ability to tolerate increasingly cold temperatures and growing season limits, while at more equatorial latitudes limitations were due to increasing temperatures (Merriam 1894, MacArthur 1972). Available water, which varies within continents more locally than on latitudinal gradients, is a highly important factor in shaping distributions as well, especially those of plants (Stephenson 1990). Research into how physiological limitations relate to these limits shows that plants have both growth and survival limitations due to cold and lowered physiological function

in high heat (Osmond et al. 1987). However, limitations at warm edges may be more complicated by biotic factors, as, for example, more cold tolerant plants have slower growth rates and thus may be simply less successful in warmer climates than their less tolerant neighbors (Koehler et al. 2012).

At continental scales, climatic factors can be used to accurately model species distributions, but local range boundaries, like species turnover along an elevation gradient, may be less clearly influenced by climate envelopes (Pearson and Dawson 2004). However, there are analogies between continental limits and local elevation. Elevational tree lines and latitudinal tree lines have been found to be analogous to one another in European trees (Randin et al. 2013). Additionally there have been many documented shifts in species elevation ranges as temperatures increase and precipitation regimes shift (Lenoir et al. 2008, Kelly and Goulden 2008, Crimmins et al. 2011, Brusca et al. 2013, Harsch and HilleRisLambers 2016). However, not all shifts track changes in climate. For example, some elevation range shifts may be the result of biotic interactions or due to demographic causes (Schwilk and Keeley 2012) or idiosyncratic movements of particular species (Lenoir et al. 2008). This leaves open the question of how much physiological tolerances influence local species distributions within mountain ranges.

The physiological limitations of individual plants are categorized by their degree of resistance to particular stressors. Species that cannot resist a common climatic stress in any area simply cannot occupy that space. Stress resistance can be achieved through

several different pathways (Levitt 1980). Annual plants may employ an escape strategy and avoid adverse environmental conditions, while perennial plants must avoid or tolerate any potential ill effects of stresses. Woody plants must maintain their longer lived lignified stems. Species may tolerate ill-effects from freezing by increasing the freezing resistance of the tissue (Sakai 1970, Friedman et al. 2008), or they may withstand the effects of increasing water stress by reducing their vulnerability to xylem dysfunction (Sperry et al. 1988). The leaves of woody plants may be either tolerant or avoidant of stress. Species may tolerate water or cold stresses through adjustment of osmotic potentials to avoid freezing or desiccation damage (Medeiros and Pockman 2011, Bartlett et al. 2012), they can avoid short-term water stress by closing stomata (Brodribb et al. 2003, Bartlett et al. 2016), or they can avoid the stresses altogether, and possibly reduce the stress on the rest of the plant, with seasonally-timed leaf loss (Chabot and Hicks 1982, Tyree et al. 1993). Woody plant physiological limitations must be considered as the complex sum of parts, and, possibly, contrasting strategies in both leaves and stems.

The oaks (*Quercus* L.) are a highly diverse woody genus that is especially abundant in North and Central America (estimated to be 243 species within the Americas, Nixon 2006, Cavender-Bares 2016). The genus occupies a wide range of habitats within the Americas (see for example Whittaker and Niering 1964, Abrams 1990, Nixon 2002, Romero Rangel et al. 2002, Cavender-Bares et al. 2004b, Aguilar-Romero et al. 2017) and has diversified within the Americas, with oaks of the two most abundant subgenera (red, *Lobatae*, and white, *Quercus*) diversifying in parallel, while the live oaks, *Virentes*, occupy the subtropical to tropical areas of North and Central America (Hipp et al. 2017).

Additionally, oaks exhibit a range of leaf habits, from winter deciduous, to evergreen, and drought deciduous, often within broadly sympatric areas (Nixon 1997). This broad range of habitats, leaf strategies, and phylogenetic history, makes them a useful system for investigations of how physiological limitations may underlie their distributions.

I use the oaks to investigate physiological limitations and species distributions, with the goals of a) understanding how distributions in woody plants may be linked to climate and b) whether different physiological strategies may be more successful in different climatic conditions. I specifically ask: 1) Do physiological limitations to drought and/or freezing correspond with elevation limits among a set of red and white oaks of different leaf habits in semi-arid mountains? 2) Are stem and leaf drought resistance strategies correlated with species distributions among a group of red, white, and live oaks from warm regions of North and Central America? 3) Do leaf photosynthetic responses to cooling differ across a group of live, white, and red oak species, and can we detect those responses accurately with hyperspectral reflectance?

Chapter 1. Leaf-level trade-offs between drought avoidance and desiccation recovery drive elevation stratification in arid oaks

Summary

The extent to which climate limitations drive the stratification of species by elevation is integral to understanding past and current range shifts, as well as predicting the impacts of climate change. Zonation patterns of species within mountains have been well-documented, and shifts in these patterns have been correlated with recent warming. However, the physiological mechanisms that explain these zonation patterns are not well understood. We used a system of broadly sympatric oak species within semi-arid mountains to 1) investigate the extent to which species elevation ranges correlate with climate, 2) test for associations of cold and drought resistances and trade-offs between resistances with upper and lower elevation limits, and 3) examine the extent to which species-wide climatic ranges predict patterns of local community assembly along elevation gradients. We found that aridity gradients but not winter minimum temperatures predict oak stratification. Species differed in drought resistance, demonstrating a trade-off between drought avoidance and drought recovery. At lower elevations species avoided drought stress during the dry season through leaf abscission while at upper elevations they maintained transpiration but recovered from daily desiccation via higher leaf storage capacity (rather than tolerated via lower turgor loss points). Stem electrolyte leakage was not correlated with elevation differences. These results indicate that environmental filtering is linked to drought resistance rather than freezing resistance. We found evidence of niche partitioning closely-related oaks that was correlated with differences in leaf phenology. The functional, phenological, and physiological traits important to elevation stratification were not correlated with aridity at the wider species range, but

rather overall precipitation and precipitation seasonality. Our findings indicate that drought resistance along a leaf avoidance-recovery trade-off is integral to species stratification within this semi-arid montane system. Additionally, environmental filtering is acting on traits and strategies conserved at the species level. Species within this system are likely vulnerable to range retraction under increased drought as a consequence of this functional-physiological trade-off.

Introduction

Pronounced poleward or upward elevation range shifts in many organisms have been attributed to modern climate change (Parmesan and Yohe 2003, Lenoir et al. 2008, Freeman and Class Freeman 2014), presumably due to a retreat from warming and drying central latitudes or lower elevations. However, montane species elevation limitations are not solely restricted by climatic tolerances and the consequent range shifts may be due to other demographic or disturbance factors (see for example, Kelly and Goulden 2008 and the response by Schwilk and Keeley 2012). Deciphering the mechanisms that can explain plant elevation limits is critical to understanding species distributions and predicting the consequences of climate change.

The effects of climate on range limitations have been central to the study of plant ecology (Shreve 1915, Grinnell 1917, MacArthur 1972). However, range limitations can be attributed to a mix of abiotic, both climatic and edaphic, and biotic factors (as reviewed in Sexton et al. 2009), complicating the understanding of climatic influence and

predictions of effects of global warming. At large, continental scales, plant ranges may be well predicted with only bioclimatic models (Pearson and Dawson 2004, Araújo and Pearson 2005). Yet, even at these broad scales, minimal thermal tolerances may be the best predictors of poleward limits, and biotic factors may be more important at warmer edges (MacArthur 1972, Koehler et al. 2012). The topography of mountains may make elevation range limits analogous to latitudinal limits, and physiological limitations may be more important at only one range edge. Upper elevation range limits within mountains can be due to minimal thermal tolerances (Randin et al. 2013), while lower elevations may be limited by physiological tolerances to warmer temperatures and associated drought (Adams et al. 2009, Gifford and Kozak 2012).

Patterns of range shifts correlated with climate change support underlying physiological mechanisms for elevation limits within mountains (Parmesan and Yohe 2003), but may not clearly identify whether cold or heat related stresses underlie the limits, as shifts in ranges may both demonstrate contraction from warming or expansion at upper elevations. Reconstructions of mountain edge vegetation communities during and after the last glacial maximum in the unglaciated American southwest revealed shifts in species composition aligned with overall warming (Betancourt et al. 1990, Van Devender 1990, Holmgren et al. 2006) and Lenoir et al. (2008) found significant mean upward shifts in alpine vegetation correlated with modern warming. A recent study revisiting the historic vegetation gradient study of Whittaker and Niering (1965) within the Santa Catalina Mountains of Arizona found that many species had shifted upslope, but not all had done so uniformly (Brusca et al. 2013). Differences in shift direction or magnitude may either

show that physiological mechanisms are not establishing some species elevation limits or may simply expose different stressors. Modern down slope shifts in California plant species were not predicted solely by warming but rather by associated water stress (Crimmins et al. 2011). Differences in shifts may show prevailing regional climatic stresses: in the American west, northern plant species were more likely to shift downward while plants of the central and southern regions had greater proportions of species shifting upward (Harsch and HilleRisLambers 2016). Some elevation shifts may confound physiologically established limits with other factors: elevation range contractions in arid systems in southern California were tightly correlated with warming (Kelly and Goulden 2008), but one documented species shift was also partly due to demography and fire effects (Schwilk and Keeley 2012). Deciphering the physiological mechanisms that underlie plant elevation limits is critical to understanding species distributions and predicting the consequences of climate change.

Whether the physiological mechanisms that influence species elevation range limits can be directly inferred from wider species distributions remains an open question. Processes of community assembly do act upon species physiological and functional traits and result in vegetation sorting along elevational gradients (Harrison et al. 2010, Randin et al. 2013). However, direct relationships between those traits and mean climate of origin can be muddied by intraspecific diversity, causing overestimation of the suitable climatic range of individuals of the same species in both broadly overlapping populations (Banta et al. 2012) and along range edges (Davis and Shaw 2001). Additionally, it may be more difficult to predict climate envelopes of species with broad niche distributions (Kadmon

et al. 2003), increasing errors in predicting small scale elevation distributions. Correctly linking the physiological mechanisms that influence elevation limits with the mean climate of broader species ranges increases our ability to accurately infer local physiological mechanisms from broadly accessible climate data.

Perennial plants exposed to stress must have resistance strategies, which can fall along a spectrum from avoidance, physiological responses meant to reduce exposure of specific tissues to stress, to tolerance, responses that expose tissue to stress but mitigate damages (Levitt 1980). Different types of resistance may be more advantageous in responding to different qualities of stresses. For example, McDowell et al. (2008) proposed that plants may avoid short term drought stress while tolerating low intensity water shortages. In semi-arid mountain systems plants may experience both cold and drought, and the two stress factors may be most extreme on opposite ends of the elevation gradient (MacArthur 1972), where plants may already be near the edge of their physiological limits. Across elevation gradients, trade-offs in physiological functions may be expected, for example, drought avoidance may be most important in the extreme droughts of low elevations while drought tolerance is most effective in the low intensity droughts of the higher elevations.

Drought and freezing stresses impose critical limitations that long-lived species may resist through a number of responses. Drought stresses may cause leaf tissue desiccation and wilting or disrupt water flow in plant vasculature. Species may avoid water loss in

the short term by closing stomata (McDowell et al. 2008, Skelton et al. 2015), while drought deciduousness may be more valuable under longer-term stress to avoid leaf damage and to protect stems vulnerable to drought-induced embolism (Tyree et al. 1993, Wolfe et al. 2016). Conversely species may tolerate drought in multiple ways: lower turgor loss points, or more negative pressures at which the leaf wilts (Lenz et al. 2006), have been found to correlated with aridity, while leaf capacitance, a measure of available water storage in leaf tissue, has been found to be negatively correlated with resistance to water loss (in leaves) and may speed tissue recovery from desiccation (Nobel and Jordan 1983, Lamont and Lamont 2000, Sack et al. 2003). Cold stresses may cause tissue damage through freezing, through either ice crystal formation or ice-induced embolism (Cavender-Bares 2005). Species may avoid critical freezing damage to leaf tissue through cold deciduousness, which may also consequently reduce vascular damage to the whole plant (Cavender-Bares and Holbrook 2001). Cold tolerant species must prevent ice crystal formation in long-lived perennial tissues and may have increase osmotic content in their cells, during a cold acclimation period, to avoid ice formation and cell death (Sakai 1970, Friedman et al. 2008).

We used a system of six species of broadly sympatric oak species (*Quercus* L.) that co-occur in southeastern Arizona, USA (Fig. 1a,b) to test for species climatic differences and trade-offs in physiological stress responses to drought and cold. We specifically examine mechanisms of stress avoidance (timing of leaf abscission), drought tolerance (leaf turgor loss point, Ψ_{TLP}, and leaf capacitance, C_{leaf}), and freezing tolerance (temperature causing 50% cell injury, T_{50}). We asked: 1) Do the oak species occupy habitats that differ in

minimum temperatures and drought conditions? 2) Do the oak species have different stem tolerances to freezing or differences in leaf drought resistance that are correlated with elevation? 3) Can the stratification of species in the mountains be explained by their species-wide climatic niches?

Methods

Study system

The Sky Islands of southeastern Arizona are part of an archipelago of isolated mountain ranges surrounded to the north by the high elevation Colorado Plateau and the south by the Sierra Madre Occidental and flanked to the east and west by the Chihuahuan and Sonoran Deserts (Warshall 1995). Annual precipitation in the region is bimodal: dry periods are interrupted by steady, widespread winter precipitation, and the strong, unpredictable storms of the North American monsoons in the summer (Rodwell and Hoskins 2001, Sheppard and Comrie 2002). Mountain elevations are stark in comparison to the surrounding valleys (Barton and Teeri 1993, Mitchell and Ober 2013) and the elevation gradient is associated with sharp climatic slopes. Temperatures can decline by up to 3^{o}C with every 400m rise in elevation: the highest elevations have an average annual maximum temperature of 13^{o}C, while the lowest intermountain zones average 30^{o}C. High elevations receive over 1.1m of annual precipitation compared to the 0.3m delivered to the valley floors (Mitchell and Ober 2013).

This system is rich in oak species with at least ten species native to most mountain ranges. The elevational stratification of several species has been historically documented (Blumer 1909, Shreve 1915, Whittaker and Niering 1965) and both climatic and fire-regime related reasons for the environmental filtering have been proposed (Poulos 2009, Schwilk et al. 2013). We used six of the most commonly occurring species within Sky Islands as a basis for this study. *Quercus emoryi* (EM, Torrey 1848) and *Q. hypoleucoides* (HY, A Camus 1932) are within the red oak section *Lobatae*. *Q. grisea* (GR, Liebmann 1854), *Q. arizonica* (AZ, Sargent 1895), *Q. rugosa* (RG, Née 1801), *Q. gambelii* (GM, Nuttall 1848) are within the white oak section *Quercus* (Nixon 1997).

All of the field studies took place in the Chiricahua Mountains (peak 2980m elevation). This range is situated in grasslands and converted rangeland (1300m elevation) in the southeastern corner of Arizona and extends 80km north from the southern USA border (Fig. 1, Barton and Teeri 1993). We focused our study on the eastern part of the mountain range accessible from a network of maintained forest roads in the Coronado National Forest, managed by the United States Forest Service. The surficial geology of the study area is primarily volcanic, either tuff and rhyolite from an Oligocene caldera eruption in the same range or rhyolite rocks predating that eruption but still of the Oligocene era (Du Bray et al. 1995).

Site selection and establishment

We surveyed a set of elevationally stratified random sites first for oak vegetation cover by elevation and selected a subset to use as longer term temperature and physiological data collection sites. We generated a point data set that included only high irradiance sites, on either north (337.5 to 22.5^{o}) or south-facing (and 157.5 to 202.5^{o}) slope aspects, to avoid the influence of differing microclimates (Boyko 1947, Holland and Steyn 1975), and excluded areas near streams or roads. We stratified the points by elevation (bands of 200m starting at 1400m) and randomly selected 5 sites in each band of each aspect (Appendix S1 Methods).

We visited the prioritized sites in May 2014 (sites=74, most very low elevation sites on private land) and collected data on: 1) predominant aspect of site, 2) slope degree, 3) oak species present within 50m radius of point, 4) growth form, 5) estimated vegetative cover of each oak species, and 6) a relevé-type description of vegetation present. From among these sites, we selected 12 sites, one of each elevation by aspect, that included all oak species found within that elevation band and met our aspect criteria (Appendix S1: Table S1.1). We excluded the sites in the 1400-1600m elevation band because oaks were only present within the stream buffers at that low elevation. At each site, we selected six healthy individuals (recent leaf cohorts, live buds, few dead branches) of each oak species present that were closest to the center of the plot. We excluded obvious hybrid individuals using Nixon (1997) for identification and collected seasonal samples of the white oak section (*Quercus*) to confirm identification. On a single site (south, 1600m) we had to alter identification of 4 of 6 individuals of *Q. arizonica* to its relative *Q. grisea.* We identified 138 individuals and used these for all subsequent trait measurements.

Site temperature, water availability, leaf transpiration

We installed a temperature monitoring network of thermochron iButtons (model DS1920, Maxim Integrated Products, Sunnyvale CA USA) in May 2014 at all 12 established sites and an additional 5 temperature-only sites and measured air temperature every three hours (Appendix S1 Methods, Appendix S1: Table S1.1). We corrected the temperature data from calibration readings at 0^{o}C and we used the average of three readings per site per time for air temperature. We also interpolated long term mean bioclimatic variables from high resolution (30 arc second) publicly available data, focusing on mean annual temperature (BIO1, ^{o}C *10), minimum temperature of the coldest month (BIO6, ^{o}C *10), (Hijmans et al. 2005) and an aridity index (AI, the ratio of mean annual precipitation to mean annual evapotranspiration, lower values are more arid, Zomer et al. 2007, 2008, CGIAR-CSI 2008), using spatial analysis tools in ArcMap v10.1 (ESRI 2011).

We collected leaves and measured leaf predawn water potential (Ψ_{PD}) and mid-day water potential (Ψ_{MD}) to examine differences in plant water status and change in plant water status ($\Delta\Psi = \Psi_{MD} - \Psi_{PD}$) between pre-dawn and mid-day during dry and rainy seasons. We use Ψ_{PD} as both a possible indicator of abiotic soil water availability, because plants are assumed to be reasonably well equilibrated with soil water potential after several hours of stomatal closure at night, and biotically-controlled plant water access, as plants of different rooting depth can achieve different access to ground water. $\Delta\Psi$ is a measure of daily water loss; more negative values indicate actively transpiring leaves. We collected leaves pre-dawn (before nautical twilight, Ψ_{PD}) and between 11am – 1pm (Ψ_{MD}) in both June and October 2014 from all study plants (Appendix S1 Methods, Kramer and

Boyer 1995). We tested leaf water potentials in positive pressure chambers (40 and 100bar models, Soilmoisture Equipment Corporation, Goleta, CA, USA) within 2 hours of sampling (Scholander et al. 1965). We measured individuals for Ψ_{PD} and Ψ_{MD} on the same day and finished all measurements among sites within a 5 day period.

Phenology

Leaf habit differs among species in this system, with three species classified as evergreen or consistently retaining leaves (*Q. hypoleucoides, Q. rugosa, Q. emoryi*), one as winter-deciduous (*Q. gambelii*), and two as sub-evergreen (*Q. grisea, Q. arizonica*) (Nixon 1997). We monitored differences in the timing of leaf loss over one year, starting immediately after the summer monsoons, on each study individual using a marked cohort of recently mature leaves (Appendix S1 Methods). We monitored leaf retention during all subsequent seasons (winter, drought, post-monsoons).

To find both mean percentages of leaf retention of the previous year's cohort and shape of leaf loss over time, we fit nonlinear and linear models to percent of marked leaves retained by leaf age since marking using both species level and species by site level (intraspecific) data subsets. We used the Akaike information criterion score of each model to determine the best fit. For each species and intraspecific model, we calculated the percentage of marked leaves retained and standard error of model fit for each season (winter, dry, and wet seasons, package nlstools Baty et al. 2015). All analyses were done in R version 3.2 or greater (R Core Team 2016).

Turgor loss point and leaf capacitance

We determined leaf turgor loss point for each study individual from collections immediately following the rainy season in 2014. We collected stems with recent, fully-expanded, healthy, full-sun leaves at the shoulder times of the day to minimize xylem cavitation, rehydrated the stems for up to 18 hours, and determined Ψ_{TLP} (MPa) and C_{leaf} (mol m^2 MPa^{-1}) using the bench dry method (Appendix S1 Methods, Koide et al. 1989, Sack et al. 2013). We used ImageJ (Schneider et al. 2012) to determine leaf area and calculated specific leaf area (SLA, mm^2 mg^{-1}). To find Ψ_{TLP}, we removed saturated points from the pressure volume curves and fit isoclines using reduced major axis regression, which accounts for error in both axes (Smith 2009). We calculated C_{leaf} as the product of saturated leaf water content and relative leaf water content decline before turgor loss, normalized by leaf area (Bartlett et al. 2012, Appendix S1 Methods).

Freezing injury

We measured freezing injury to stems as electrolyte leakage induced by different experimental temperatures following the methods of Flint et al. (1967), and expanded by Friedman et al. (2008), and Koehler et al. (2012). Because perennial plants will harden in the cold, increasing their ability to tolerate lower freezing temperatures before cellular damage (Sakai 1970), we collected twigs in two seasons: winter (January 2015) to examine freezing tolerance after hardening, or cold acclimation, and late summer (September 2015) to examine inherent, or unacclimated, tolerances to freezing. We

collected live, leaf- or bud- bearing twigs of the most recent flush from study individuals and kept them in water in the dark. We shipped stems from Arizona field sites to the University of Minnesota and processed them within four days. We sectioned stems and subjected each to different declining experimental temperatures (-5, -10, -15, -20, -25, and -38^{o}C), and calculated index of injury at each temperature as electrolyte leakage compared to an unfrozen stem section, normalized by total stem conductivity (Appendix S1 Methods).

To directly compare freezing vulnerabilities, we found the temperature inflicting 50% injury (T_{50}). We first calculated the index of injury (I_t) for each stem at each freezing temperature as a normalized percentage of control specific conductivity (Flint et al. 1967, Friedman et al. 2008). We removed individuals from the analyses with two or more negative I_t values, as these indicated a greater injury in the control than in the freezing treatments. We also excluded any I_t values that were greatly out of range (<-25% or >125%). We then fit models of mean experimental temperatures by I_t for each combination of species, site, collection season, and test Round to find T_x. We compared simple linear, quadratic polynomial, and non-linear models and chose the model with the best fit as the lowest AIC score and then predicted T_{50} (^{o}C) for each combination (package nlstools, Baty et al. 2015).

Data analysis

Site temperature and bioclimatic variables

We examined responses of locally collected site annual mean temperatures, summer (months 6-9) mean and maximum temperatures (average daily maximum), and winter (months 11-2) mean and minimum (average daily minimum) temperatures in multiple regression models of elevation and aspect (factor, north or south). We tested Pearson's r correlations of locally collected temperatures against derived (and interpolated) bioclimatic variables at each site and adjusted significance values for false discovery rates in multiple comparisons (Benjamini and Hochberg 1995, Hijmans et al. 2005, CGIAR-CSI 2008).

Species occurrence and elevation optima

We converted species cover from site surveys into presence and absence data and used logistic regression to estimate mean (peak of distribution) species elevation, mean aridity index and mean minimum temperature of the coldest month, testing model fits between a null, linear, and quadratic model (Lenoir et al. 2008), and excluding all sites that were not within 30^{o} of either direct north or south (as measured on ground) . We tested for single elevation means for each species and different means on north and south facing aspects. We also used species cover estimates to visually compare two dimensional density of occurrence along aridity and cold temperature (package MASS, Venables and Ripley 2002). We tested for niche differentiation, both within our whole oak system and within oak subgenera, against a null model, along an elevation, aridity, and cold temperature gradient using cover estimates from the site surveys using the NicheOverlap function in the EcoSim R 1.00 packages (Gotelli and Ellison 2013).

Leaf water potential, TLP, and freezing injury models

We used linear multiple regression and ANOVA (type III to allow unbalanced data) to test the effect of two climatic variable predictors (mean temperature of coldest month or aridity index, both highly correlated with elevation, see results) and species on responses (leaf water potentials (Ψ_{PD}, $\Delta\Psi$) in both dry and post-rain seasons), Ψ_{TLP}, C_{leaf}, and T_{50}). In addition, in models for T_{50}, we included collection season (summer or cold unacclimated stems) and testing round (as stems were processed in two batches) as predictors. We included all possible interaction terms and reduced each model by removing terms from the full model when not significant ($\alpha = 0.05$). We examined all models fits for homoscedasticity and normality. We also fit separate simple linear models between response variable and climatic variables and tested for pairwise differences among species using post-hoc Tukey tests (95% CI).

Climate of species range and trait correlations

We found two sets of mean values for all measured traits, species means (N=6) and species means at each collection site (N=24). We obtained mean climate values for each species range from subsampled occurrence data, which were confirmed with identified specimens or in the literature, using the dismo package in R (GBIF 2013, Hijmans and Elith 2013, Hijmans et al. 2016). We tested for the correlation of species mean trait values with mean climatic values of each species range using both Pearson's r, for linear relationships, and Spearman's rho, for nonlinear, but monotonic relationships correlations (package Hmisc, Harrell Jr and Dupont 2016), and adjusted for multiple comparisons by reducing false discovery rates (Benjamini and Hochberg 1995). In order to compare

timing of leaf loss in different seasons, to mean values of other traits, we dropped any species from analysis if the likelihood of it retaining its leaves through the previous season was less than 0.01. This resulted in dropping *Q. gambelii* from comparisons of dry season leaf loss and wet season leaf loss. We also examined local trait data for inter-trait correlations (species x site).

Results

Minimum temperatures do not correspond to elevation

Local MAT and summer temperatures were significantly predicted by elevation, while minimal winter temperatures were not (Appendix S1: Fig. S1.1). Local MAT was significantly predicted by both elevation ($p = 0$) and aspect ($p = 0$), without an interaction ($R^2 = 0.93$, $F_{3,13} = 94.07$). MAT declined with elevation by $0.005^oC\ m^{-1}$ while the warmer south-facing aspect increased the intercept by 1.46^oC. A model of elevation alone was still strongly predictive of MAT ($R^2 = 0.80$, $F_{1,15} = 61.5$, $p = 0.0001$). Average maximum summer temperatures were predicted strongly by an additive model of elevation ($p < 0.0001$) and aspect ($p = 0.001$, $R^2 = 0.90$, $F_{2,14} = 66.1$). Summer mean temperatures had a similarly significant relationship and the slopes of both were steeper than the MAT. Average winter mean temperatures were also significantly predicted by elevation ($p<0.0001$) and aspect ($p<.0001$, $R^2 = 0.82$, $F_{2,14} = 34.8$) but winter absolute minimum temperatures were not significantly predicted by elevation ($R^2 = 0.20$, $F_{1,15} = 3.644$, $p = 0.076$, Appendix S1: Fig. S1.1c). Winter minimum temperatures did drop below freezing (to -13 to -17^oC on average since 1992) and historically reached a record minimum of -23^oC at 1640m (since 1955) and -25^oC at 2902m (since 1992, NOAA 2016).

Elevation and local temperatures highly correlated with long-term climate variables

Elevation and locally measured mean and maximum temperatures were significantly correlated with interpolated long-term climatic variable (Appendix S1: Table S1.2). The aridity index was positively correlated with elevation (higher MAP/MAE ratios at higher elevations) and temperature variables were negatively correlated with elevation. All locally collected temperature data, with the exception of winter minima, were significantly ($p < 0.01$) correlated with interpolated long term bioclimatic data, although the strongest correlations ($r > |0.85|$, $p < 0.001$) were between summer and annual temperature measures (Appendix S1: Table S1.2). The average difference between two fitted models of temperature (either long term mean annual temperature or local annual temperature) by elevation was 1.93^{o}C, which is in near agreement with temperature anomalies (over historic averages) recorded for the region during the collection period (Appendix S1: Fig. S1.2, Kalnay et al. 1996, NOAA 2016). Because of the highly supported relationships between site level elevation, temperature data, and long-term climatic variables, we use the latter in the rest of the results to show the relationship between species location and the longer term climate variables.

Oak species have overlapping distributions but different mean elevations

All oak species were found to have different mean elevations (and mean aridity, mean cold temperatures, Fig. 2). All species except *Q. rugosa* had overlapping elevation distributions on north- and south-facing aspects. The quadratic generalized linear model

predicted all optima (or elevation of highest likelihood of occurrence) better than a null model (Appendix S1: Table S1.3). All species except *Q. gambelii* and *Q. rugosa* were found to have mean elevations strongly predicted by a quadratic fit, and the model prediction likely suffer from the low number sites at which individuals were observed (Appendix S1: Table S1.3). Because the simple mean elevation of presence data for both species (*Q. gambelii:* 2500.5m ±132.4, *Q. rugosa*: 2315 m ± 258.4) overlapped with the quadratic maxima, we used the maxima for comparing species means for simplicity. When presence was analyzed by aspect, all species had slightly lower optima on north-facing slopes than their south-facing counterparts. Despite the differences in optima, we found no significant niche differentiation by elevation, AI, or BIO6 (mean temperature of coldest quarter) among the full set of oak species. The standardized effect sizes of each model compared to a null distribution were close to zero (SES_{elev}= -0.83, p < null = 0.194; SES_{AI} = -0.83, p < null = 0.194; SES_{BIO6} = -0.80, p < null = 0.217), indicating that while the species are occupying different elevational means, there is significant overlap among species inconsistent with niche differentiation. However, when the oak species were split into their respective subgenera, *Quercus* (white) and *Lobatae* (red), overlap was low indicating significant niche differentiation across elevation among species within the same clades (SES_{white} = -2.54, p < null = 0; SES_{red} = -1. 61, p < null = 0.001).

Plant water access differences are greatest in the dry season

Dry season Ψ_{PD} was significantly predicted by an interaction of aridity index with species (R^2 = 0.70, $F_{10,124}$ = 29.0, p = 0, Appendix S1: Table S1.4); dry season Ψ_{PD} showed significantly lower water availability in the most arid sites compared to higher elevation

sites (Fig. 3a). The interactive effect was significant in two higher elevation species that had either more moderate intraspecific responses to changing aridity index (*Q. rugosa*) or an opposite sign (*Q. gambelii*). Pairwise-species differences are correlated with species mean elevation, with the exception of the two lowest elevation species (Fig. 3b). Wet season Ψ_{PD} had a negative relationship with AI when both AI and species were included in the model ($R^2 = 0.36$, $F_{6, 131} = 12.2$, $p = 0$), but the effect of the climate gradient was small compared to species (Appendix S1: Table S1.4). The range of Ψ_{PD} was quite small after rains (-0.96 - -0.01MPa) while during the dry season, the lowest elevation individuals often differed substantially from the highest elevations (-4.49 - -0.44MPa).

Differences in daily transpiration are primarily species driven and greater in the dry season

Diurnal changes in leaf water potential were also correlated with aridity index in the dry season, but not in the wet season (Appendix S1: Table S1.4). Dry season $\Delta\Psi$ had a negative relationship with aridity index but species level differences had a larger effect (slope = -4.0, $R^2 = 0.30$, $F_{6, 128} = 9.3$, $p = 0$). *Q. gambelii* had significantly greater dry season $\Delta\Psi$ than both *Q. hypoleucoides* and *Q. arizonica* ($p<0.001$) and *Q. rugosa* also had greater diurnal change than *Q. hypoleucoides* ($p<0.05$). Wet season $\Delta\Psi$ was not significantly correlated with aridity index, but species level differences were significant ($R^2 = 0.1$, $F_{6,131} = 131$, p, 0.02). *Q. rugosa* had significantly greater daily change $\Delta\Psi$ than *Q. hypoleucoides, Q. gambelii, Q. arizonica* ($p < 0.05$).

Leaf capacitance, not turgor loss point, is predicted by site aridity and species

Ψ_{TLP} is best fit in an interactive AI by species model (R^2 = 0.24, $F_{10,118}$ = 3.6, p = 0.000, Appendix S1: Table S1.4). The non-significant slope of Ψ_{TLP} by AI (Fig. 3c) was positive, but not large (less negative Ψ_{TLP} at low aridity), but there were significant species by AI interaction effects. There were no significant species-level differences in Ψ_{TLP} (Fig. 3d). C_{leaf} was best predicted by an additive model of species and AI, where species-level differences had the largest effect (R^2 = 0.30, $F_{6,122}$ = 8.6, p = 0, Appendix S1: Table S1.4). C_{leaf} increased significantly with AI, and species-level differences were driven by comparisons between mid-elevation *Q. hypoleucoides* and lower elevation *Q. arizonica* and *Q. emoryi* (Fig. 3e,f).

All species can acclimate to local cold extremes

Simple linear models were most commonly the best model to find T_x in acclimated stems (64% of models, N = 47, mean correlation = 0.90 ± 0.06), while non-linear exponential models were the best fit for unacclimated stems (88%, N = 48, mean correlation = 0.83 ± 0.09). We removed *Q. grisea* from further analyses because it never experienced 50% injury.

An overall, additive model of collection season, test group, and species best predicted T_{50} (R^2 = 0.81, $F_{8, 82}$ = 44.7, p = 0). Collection season and species were both large effects, indicating cold acclimated stems were less vulnerable (T_{50} was lower) than summer, unacclimated, stems, and *Q. emoryi* and *Q. hypoleucoides* were significantly more

vulnerable to freezing than other species (Appendix S1: Table S1.5). Test group, or the time of stem processing before experimental freezing, did affect T_{50}: on average, stems tested a day later had T_{50} values 2.5^{o}C higher than stems tested the day prior. This experimental effect was only significant in unacclimated stems. Species was the largest effect in acclimated stems (Appendix S1: Table S1.5). Neither BIO6 (mean minimum temperatures of the coldest month), nor mean prior temperature, were significant in the larger models of seasonal T_{50} (Appendix S1: Table S1.5). In single predictor models, T_{50} was significantly predicted by prior mean temperatures at the collection site in unacclimated stems ($R^2 = 0.23$, $p = 0.019$) but not in acclimated stems (Fig. 4a,b). Species-level differences shifted between seasons: *Q. gambelii* was significantly less vulnerable to freezing than most other species in summer when stems were unacclimated, while *Q. hypoleucoides* was significantly more vulnerable in winter when stems were cold acclimated (Fig. 4c).

Leaf retention is correlated with SLA in all seasons and C_{leaf} in dry and wet seasons

Percentage of leaf retention (of previous year's cohort) during different seasons differed among species by mean elevation (Fig. 5). A non-linear, sigmoidal model was the best fit ($p < 0.01$ compared to null) for all species except *Q. rugosa*, *Q. hypoleucoides*, and *Q. gambelii*. Only the highest elevation species, *Q gambelii*, was winter deciduous; it retained no marked leaves in the cold season and simple linear models were a perfect fit to total leaf loss during that period (Fig. 5a). The lowest elevation species, *Q. grisea* and *Q. emoryi*, lost all marked leaves in the dry season while *Q. arizonica* lost most leaves (Fig. 5d). *Q. rugosa* and *Q. hypoleucoides*, both intermediate to higher elevation species,

retained a majority of their previous season leaves throughout the study period and linear model fits of leaf retention were not significant for most species by site combinations because leaf age since marking was not a significant predictor, indicating a true evergreen leaf habit.

Species mean SLA was negatively and significantly correlated with probability of retaining previous leaves through in all seasons (cold season: $R^2 = 0.86$, $p = 0.008$, dry season: $R^2 = 0.84$, $p = 0.029$, wet season: $R^2 = 0.84$, $p = 0.029$, Fig. 5). Species mean absolute leaf capacitance had a significant positive relationship with dry and wet season leaf retention (dry season: $R^2 = 0.9$, $p = 0.014$, Fig. 5f, wet season: $R^2 = 0.93$, $p = 0.009$), but no significant correlation with winter leaf retention ($p = 0.668$).

SLA, wet season $\Delta\Psi$, and leaf phenology are correlated with mean climate of species range

SLA, wet season $\Delta\Psi$, and cold season leaf phenology were linearly correlated with climate of species range (Table 1). Dry and wet season leaf retention had significant Spearman's rho correlations. SLA was positively correlated with temperature seasonality ($r_s = 0.94$, $p < 0.05$) and precipitation in the dry season and negatively correlated with temperature ($r_p = -0.92$, $p < 0.05$), overall precipitation ($r_s = -0.94$, $p < 0.05$), and precipitation seasonality ($r_p = -0.98$, $p < 0.01$). Wet season $\Delta\Psi$, where more negative values indicate greater transpiration, was lower in species of less arid wider ranges with higher precipitation seasonality (Table 1). Wet season $\Delta\Psi$ was positively correlated with

temperature seasonality (r_p = 0.90, p<.05) and negatively correlated with the aridity index (r_p = -0.97, p < 0.01), mean annual precipitation (r_p = -0.97, p < 0.01), and precipitation seasonality (r_s = -0.89, p < 0.05). Differences in leaf retention were significantly correlated (p < 0.1) to mean annual temperature (winter), temperature seasonality (dry and wet seasons), mean annual precipitation (dry and wet seasons), precipitation seasonality (all seasons), dry season precipitation (winter), and wet season precipitation (dry and wet seasons, Table 1). As *Q. gambelii* is the only winter deciduous species, with a much more northern distribution than the other species, we also check for correlations with *Q. gambelii* removed from the analysis. Without *gambelii*, mean species elevation and local aridity index and mean cold temperatures were significantly correlated with climatic variables of species ranges. Local elevation and aridity were positively correlated (p < 0.01) with mean annual precipitation, precipitation seasonality, and wet season precipitation, while local cold minima were negatively correlated with the same variables.

Discussion

We demonstrated that a trade-off between leaf level drought avoidance and desiccation recovery (tolerance) are more critical in explaining oak species distributions across the elevation gradients of the semi-arid Sky Islands, than physiological traits associated with freezing vulnerability or drought stress tolerance. We confirm classic studies of species distributions in this region showing that oak species are stratified across elevation gradients, though we found no evidence of niche partitioning among all oaks, but rather partitioning within oak subgenera (Shreve 1915, Wallmo 1955, Whittaker and Niering

1965, Sawyer and Kinraide 1980). Local climatic conditions vary significantly and predictably with elevation, and derived climatic values match our fine-scale temperature observations, however environmental variables associated with aridity, including pre-dawn water potential, and maximum temperatures, have stronger relationships with elevation than winter minimum temperatures. In concordance with this finding, freezing tolerance among all species is high and demonstrates a general ability of these oak species to acclimate to and tolerate common winter minimum temperatures. Turgor loss point, often considered a critical indicator of drought tolerance (Bartlett et al. 2012), varies only weakly across the elevation gradient and is not significantly different among species. The important mechanisms driving species distributions are drought avoidance strategies, leaf loss during the dry season in the lowest elevation species, contrasted with long leaf retention of species at mid-elevation and winter deciduousness at high elevation. The dry season leaf loss is also negatively with leaf water storage (absolute capacitance at full turgor) and positively associated with SLA. SLA, wet season transpiration, and timing of leaf loss are also the traits most strongly correlated with the range-wide climatic conditions of each species.

Abiotic effects: drought, not cold, limits elevation ranges

Our study confirms elevation zonation among the oaks as observed in this region by early scholars (Shreve 1915, Whittaker and Niering 1964, 1965). The zonation patterns we observed correlated with an aridity gradient but not with severity of freezing, suggesting two contrasting spatial scales of environmental filtering: aridity drives local elevation limits while minimum temperatures are important in filtering the regional species pool.

We found significant relationships of water access, mean and maximum temperature and species specific differences in water access, all correlated with elevation. These oak species may also mediate their water access to reduce the impact of local vapor pressure deficits: the lowest elevation species, occupying the highest aridity zones, have intermediate soil water potentials in the dry season (Fig. 3b), indicating that deeper root systems may moderate the more extreme environments. Additionally, *Q. gambelii,* the highest elevation species has been found to develop deep roots for water access (Ehleringer and Phillips 1996) and was found to have the highest dry season water potentials in our study. The differences in local climates and abiotic and biotic differences in dry season water access support drought resistance (avoidance and tolerance) as a primary mechanism of elevation range limits. These results agree with research that found different limitations to water stress among two elevationally stratified oaks in northern Mexico (Poulos et al. 2007) and support studies in semi-arid mountain systems that have demonstrated increased mortality associated with warming driving upward vegetation shifts (Kelly and Goulden 2008) and, within a system including many of the same oaks as in our study, upward movements correlated with increased drought (Brusca et al. 2013). Given that only long term average minimum temperatures vary along an elevation gradient, but absolute minimum temperatures do not, we conclude that physiological resistances to freezing are not a genus wide driver of species sorting into current elevations.

Drought resistance: a recovery avoidance-trade off in leaf-level strategies

We observed a general avoidance--desiccation recovery trade-off that reflects the leaf economic spectrum, but did not find any differences in drought tolerance of plastic strain (turgor loss points). Leaf stress avoidance strategies were found at both ends of the elevation gradient: winter deciduousness in the highest elevation species (*Q. gambelii*) and drought deciduousness in the lowest elevation species. These deciduous strategies, in both seasons, are strongly correlated with SLA and drought tolerance through desiccation recovery or leaf water storage (C_{leaf}) in the dry season. We propose that the contrasting patterns of winter and dry season leaf loss along the elevation gradient are still reflective of drought resistance, rather than a cold resistance spectrum. SLA declines significantly between the temperate winter deciduous Rocky Mountain *Q. gambelii,* occurring at the highest elevations, and the subtropical winter evergreens. This difference is expected following the global leaf economics spectrum wherein we expect lower SLA in more arid regions (Wright et al. 2004). The summer dry season most strongly affects the lowest elevation species, where we observed Ψ_{PD} as low as -4MPa, average maximum air temperatures near 30 ^{o}C, and transpiration ($\Delta\Psi$) near zero (whether because of leaf desiccation or stomatal closure is unclear). The high SLA, high wilting points, and the relatively short life span of the leaves of the winter deciduous species make it ill-suited for any prolonged summer drought stress. Among the non-winter deciduous species we observe a second negative relationship with SLA and dry season leaf retention, where SLA is highest among drought deciduous plants. This fast-slow life strategy divide is between drought dispensable leaves at the lowest elevations and long-lived leaves at the middle to high elevations (Reich 2014). The evergreen species do not have low enough wilting points to withstand the most extreme drought, nor can they shed their leaves to

avoid it. Conversely, the lowest elevation species maintain an intermediate SLA: leaves are less expensive to shed during droughts, yet may more readily withstand the daily vapor pressure deficits of a semi-arid region in any season.

Habitats at elevations of less water stress are not enough to protect the non-drought deciduous species, but rather the plants must still be able to tolerate summer water stress (even of lower magnitudes). Oaks have been observed to maintain open stomata longer during drought than co-occurring species and drought adapted oaks, even *Q. gambelii*, will continue to transpire well below their own turgor loss points and despite decreasing water access (Abrams 1990, Ehleringer and Phillips 1996). Vapor pressure deficits can still be very high in the dry season within the high elevations (Fallon, unpublished data), so actively transpiring species in our study also experienced Ψ_{MD} well below their wilting points. High leaf water storage has been associated with higher leaf hydraulic conductance, faster leaf recovery from water loss, and functions as a drought tolerance through stress recovery trait (Nobel and Jordan 1983, Sack et al. 2003). C_{leaf} acts as a safety margin after some leaf desiccation (Levitt 1980, Lamont and Lamont 2000), and is highly correlated in our study with dry season leaf retention and evergreen status (retention through wet season, Fig. 3f). However there is some evidence that the bulk leaf capacitance may not be the most accurate measure of xylem available water, so this safety margin may be less robust than drought avoidance strategies (Blackman and Brodribb 2011). While *Q. gambelii* did not maintain previous season leaves, through the year, all living plants flush in the spring and maintain summer season leaves and its leaf capacitance values are significantly higher than those of the dry season deciduous

species. Leaf capacitance serves a role in desiccation recovery of non-drought deciduous species.

Drought tolerance, as ability to withstand the strain of negative potentials, $\Psi_{TLP,}$ was not significantly different among species or reflective of the local or species-wide climatic zones, despite being a measure highly correlated with biome-level aridity (Bartlett et al. 2012). Ψ_{TLP} was measured on plants right after the rainy-season when all plants were well watered ($\Psi_{PD} > -1$ on all plants) and Ψ_{TLP} can shift seasonally within oaks (Abrams 1988). Bartlett et al. (2014) found that Ψ_{TLP} seasonal adjustments still reflect local environmental differences and the magnitude of those shifts were similar to osmotic adjustments observed in eastern oak species (Abrams 1990). Leaf level tolerances are moderate for all species to permit leaf retention in a semi-arid region (0.35 – 0.56 range of aridity index), but not a significant factor in environmental filtering.

Freezing tolerance due to range limits or other stress responses, but not elevation gradient

The oak species in this system showed significant ability to acclimate to winter temperatures and no evidence of elevation-related cold stress filtering. Unacclimated freezing vulnerability tracked temperatures of previous exposure (which were strongly confounded with elevation gradients) and only the deciduous species of the highest elevation sites was significantly less vulnerable to freezing damage. All species acclimated to cold temperatures with decreasing freezing vulnerability, though *Q.*

hypoleucoides was the most vulnerable species. *Q. hypoleucoides* would be the only species that would experience 50% injury during local record freezes (average of ten record minimum winter temperatures in the study system is -19.4^{o}C) and all species can withstand the average winter minimum (-14.3^{o}C (± 3), measured at 1645m since 1955, NCEI and NOAA).

A combination of different northern range limits, winter leaf phenology, and fire responses may explain the species level differences in freezing vulnerability. Lenz et al. (2013) observed, in a system of cold deciduous trees in the Swiss Alps, that freezing tolerances were significantly correlated to an elevation gradient, despite similar freezing pressures, on dormant twigs and primarily correlated with time of bud burst, but once leaves were developed, stems were similarly vulnerable. As most species in this system are winter evergreen, and only one breaks bud after winter, common leaf phenology may lead to similar freezing vulnerabilities along the elevation gradient. Despite these within mountain similarities, we have reason to suspect that stem tissue freezing vulnerabilities should differ among species. Freezing tolerance has been found to differ among oaks of different origins (Koehler et al. 2012) and stem embolism and photosynthetic vulnerabilities have been found to differ among oaks of different latitudinal limits (Cavender-Bares et al. 2005). Northern latitudinal limits may explain the significant species differences in our system (Fig. 1b). In our study, only *Q. gambelii*, has a northern temperate latitude range limit (41.5^{o}N) and is the only species to have significantly greater freezing tolerance in unacclimated stems. *Q. hypoleucoides* has the lowest northern range limit (33.8^{o}N) and is the most vulnerable stem.

While *Q. hypoleucoides* has the most southern upper latitude range limit, there may also be a secondary, explanation for its more vulnerable stems. All species in our study system have some fire resistance and recovery abilities. Schwilk et al. (2013) determined that *Q. hypoleucoides* had thinner bark and a faster estimated burn damage time than the other oaks in this study. We have personally observed this species to resprout vigorously following total above ground stem death and Barton (2002) found that this species was more successful in recovering after a fire than conifers within the same mountain range. Cavender-Bares et al. (2004) found that evergreen oak species may be less suited for fire prone areas, but in these semi-arid mountain ranges, all oaks may be adapted for frequent fires (Swetnam and Betancourt 1998, Barton 2002, 2008). As we have never observed *Q. hypoleucoides* living but without leaves, it may be that any foliar aboveground tissue death (as would likely happen in a fire or extreme freezing event) triggers stem above ground death and resprouting rather than maintenance of leafless stems.

Species range associations

SLA, leaf phenology, and wet season transpiration were highly correlated with climate of species range among all species and elevationally-associated climate zones are correlated with wider species ranges among the Madrean (non-winter deciduous oaks in this study) oaks. SLA was strongly associated with broad ecological differences (Díaz and Hodgson 2004, Wright et al. 2004) and the biggest differences are between winter deciduous species and Madrean oaks. SLA remained weakly ($p < 0.1$) correlated with temperature seasonality (positive) and precipitation seasonality (negative) among the winter

evergreens. Leaf phenology in the dry and wet seasons was also weakly correlated with temperature seasonality (negative) and mean annual precipitation (positive). When *Q. gambelii* was not considered, the species local elevation ranges and associated climate were correlated with species ranges as well, though not directly to aridity. Species with higher precipitation seasonality and higher wet season precipitation live at the highest elevations in the mountains, while species of lower seasonality occupy lower elevations. Similarly, wet season transpiration was strongly correlated, in all species and among winter evergreens, with mean annual precipitation, and larger changes occur among species with the highest precipitation. These are surprising relationships, as we might have expected the drought-deciduous low elevation species to be adapted to high seasonality. However, this may show differences in resource acquisition strategies. The higher seasonality and precipitation of the ranges of *Q. rugosa* and *Q. hypoleucoides* may influence the evergreen strategy, as species retain leaves longer and develop strategies, such as higher C_{leaf}, to avoid leaf loss during drought until the following rainy season. These species then increase transpiration and photosynthetic capacity during the wettest growing season, once they have greater water access and do not have to rely on the safety margin of leaf capacitance. The lower seasonality in the ranges of *Q. emoryi* and *Q. arizonica* shows species that experience overall less precipitation and so must be adapted to drought as severe without the seasonal high influx of water.

Species coexistence and niche partitioning within subgenera

Density dependent interactions may also be important in community assembly of the oaks in the sky islands. While we observed a high degree of overlap in the in elevation limits

among species, unsurprising given the broadly overlapping ranges of the oak species (Fig. 1), we found evidence for niche partitioning within species of the same subgenus. This supports the hypothesis that there are underlying competition or other density dependent interactions (common pests, for example) among the more closely related oaks and fits with previous observations of red-white oak pairs coexisting more frequently than those of the same subgenus (Mohler 1990, Cavender-Bares et al. 2004a). In our study, we find contrasting leaf phenology across the whole gradient within each subgenus. The red oaks, *Q. emoryi* and *Q, hypoleucoides* are drought-deciduous (to subevergreen) and true evergreen, respectively, while the white oaks shift from dry-deciduous (*Q. grisea*), semi-dry deciduous (*Q. arizonica*), true evergreen (*Q. rugosa*), and winter deciduous (*Q. gambelii*) along the slope. These contrasting phenologies along the gradient, rather than within sites, demonstrate niche differentiation within a wider species pool, rather than within local sites. The more closely-related species within the regional pool that occupy similar spaces (dry, often exposed, volcanic slopes) differ in leaf phenology. Species sorting along the gradient follows our findings of an avoidance-desiccation recovery trade-off, but within each subgenus, so that the true evergreens are red and white and have nearly similar mean elevations. This supports the findings of Cavender-Bares et al. (2004a), that co-occurring species within a Florida oak community were less likely to be related and that contrasting leaf phenology was common among closely-related co-occurring oaks. In the case of the red oaks with our study, *Q. emoryi* can access deeper water sources than its higher elevation relative *Q. hypoleucoides*, allowing it to persist longer throughout the higher vapor pressure deficits of low elevation dry seasons and may benefit from wet season water run-off, allowing it to quickly grow

new leaves. *Q. hypoleucoides*, with its longer lived leaves, may benefit less from a boom and bust cycle of the lower elevations. It's also possible that *Q. emoryi* is pushed downslope from its optimal elevation zone. It was found to be more vulnerable to drought induced mortality than either *Q. grisea* and *Q arizonica* in a long-term drought in Texas (Poulos 2014). Among the white oaks, *Q. rugosa* has been found to be a relatively shade tolerant species (Poulos et al. 2008), which may allow it to live a similarly conservative evergreen lifestyle at the middle elevations of the white oak gradient, while its relatives demonstrate different timing of deciduousness. While not part of our study on adult plants, differences in timing of acorn production have also been proposed to promote coexistence (Mohler 1990) among red and white oak pairs, as recruitment will occur at different times and acorn and seedling predators won't impact unrelated species. Red oaks usually produce acorns every two years, while white oaks have annual production. In our system, *Q. emoryi*, actually does produce acorns every year, but it does so during beginning of the summer monsoons, while its co-occurring white oaks do so in later summer (*Q. grisea*) and autumn (*Q, arizonica*), this would then separate recruitment timing by at least several months.

Changing climate and increasing drought: retreats and limits

This drought-filtered oak system may be particularly vulnerable to climate changes. Species shifts in response to past global cooling and warming have been well-documented in the region (Betancourt et al. 1990, Holmgren et al. 2006) and given our observations of low freezing vulnerabilities among the oaks, we may expect that many of the past movements have been range retractions upward away from increasingly arid low

land environments. All of the oak species in this study operate at minimum water potentials, or Ψ_{MD}, well below their turgor loss points and some can avoid the most extreme habitats and recover from the stress, while the lowest elevation species simply can tolerate leaf loss during drought periods. Local annual temperatures have increased dramatically in the 60 years of local recorded data. Mean minimum temperatures at the lowest elevations have increased by 4^{o}C and our snippet of temperature data found temperatures on the mountain were 1.5^{o}C greater than average (NCEI and NOAA, Appendix S1: Fig. S1.2). Weather extremes, that exacerbate drought and stress, have increased and are expected to continue to change under business as usual emissions scenarios (IPCC 2013). While there may be some density dependent interactions among closely related species and local adaptation among these oak species, as their mountain climate envelopes are not highly correlated with those of their wider range, there is strong evidence that environmental filtering is acting upon species-level conserved traits (SLA, leaf phenology) and that local elevation limits are correlated with precipitation of the species wider ranges. As we expect that these traits are less plastic than osmotic shifts that can adjust stem freezing vulnerability or leaf turgor loss point, we should expect selection against these traits, increased mortality at range edges, and range retractions, as have already been observed in a very similar system (Brusca et al. 2013) and other semi-arid mountains (Kelly and Goulden 2008).

Conclusions

Our research shows that aridity, and not cold, filters oak species within this semi-arid system and influences elevation limits. Leaf phenology and leaf drought recovery (leaf

capacitance) form a drought avoidance-desiccation recovery trade-off and highly associated with functional traits (SLA). The trade-off and associated traits are the primary factors in establishing species drought resistance and consequent elevation zones. These traits are not associated with the aridity of the species wider ranges, but rather with precipitation. We did find evidence of niche partitioning within oak subgenera where elevation differences among subgenera are closely related to leaf phenology.

Acknowledgements

This research was done with funding to BF from the Southwestern Research Station (SWRS, American Museum of Natural History), the University of Minnesota Charles J. Brand, Carolyn Crosby, and Dayton Bell Fellowships, and the Department of Plant and Microbial Biology. Additional funding was provided by NSF Award 1146380 (JCB PI). We performed all data collection under permit with the Coronado National Forest, Douglas Ranger District, managed by the United States Forest Service (USDA). We thank Sally Ratliff, Christopher Walker, and Chip Blackburn for extensive help with fieldwork, as well as the staff and many volunteers of the SWRS.

Chapter 1 Tables

Table 1. Trait and local elevation correlations with climate of species range, among all species and among only the winter evergreens (without Q. gambelii). Only traits with significant correlations are shown ($p < 0.001$ ***, $p< 0.01$**, $p<.05$*, $p< 0.1$†, significance values were adjusted for false discovery rates in multiple comparisons). Bioclimatic variables are Aridity Index (AI = MAP/MAE (CGIAR-CSI 2008)), and WorldClim variables from Hijmans et al. (2005): MAT (BIO1, ^{o}C*10), Temperature seasonality (BIO4), driest quarter temperature (BIO9, ^{o}C*10), temperature of warmest quarter (BIO10, ^{o}C*10), temperature of coldest quarter (BIO11, ^{o}C*10), MAP (BIO12, mm), precipitation seasonality (BIO15), precipitation in driest quarter (BIO17, mm), and precipitation in wettest quarter (BIO18, mm).

Table 1.

		AI	BIO1	BIO4	BIO9	BIO10	BIO11	BIO12	BIO15	BIO17	BIO18
Pearson's r	cold leaf retention	0.11	**0.87†**	-0.57	0.71	0.61	0.80	0.35	**0.89†**	**-0.93†**	0.66
	wet ΔΨ	**-0.97****	-0.44	**0.90***	-0.33	0.37	-0.67	**-0.97****	-0.50	-0.05	-0.70
	SLA	-0.28	**-0.92***	0.67	**-0.81†**	-0.57	**-0.88†**	-0.51	**-0.98****	**0.85†**	**-0.85†**
Spearman's rho	dry leaf retention	0.80	0.40	**-0.90†**	0.20	-0.10	0.70	**0.90†**	**0.90†**	0.20	**0.90†**
	wet leaf retention	0.80	0.40	**-0.90†**	0.20	-0.10	0.70	**0.90†**	**0.90†**	0.20	**0.90†**
	wet ΔΨ	-0.66	-0.71	**0.89***	-0.37	-0.09	-0.77	**-0.89***	**-0.89***	0.14	**-0.89***
	SLA	-0.71	-0.66	**0.94***	-0.54	-0.37	**-0.83†**	**-0.94***	**-0.94***	0.31	**-0.94***
Pearson's r without *gambelii*	wet ΨPD	-0.78	**-0.90†**	0.79	-0.72	0.15	**-0.97***	-0.85	**-0.96***	-0.23	**-0.95***
	wet ΔΨ	**-0.97***	-0.56	**0.99***	-0.27	0.64	**-0.91†**	**-0.98***	-0.76	-0.63	-0.78
	elev	0.76	0.75	-0.74	0.57	-0.22	0.85	0.79	**1.00****	0.32	**0.99****
Spearman's rho without *gambelii*	dry leaf retention	0.80	0.40	**-0.90†**	0.20	-0.10	0.70	**0.90†**	**0.90†**	0.20	**0.90†**
	wet leaf retention	0.80	0.40	**-0.90†**	0.20	-0.10	0.70	**0.90†**	**0.90†**	0.20	**0.90†**
	wet ΨPD	-0.80	**-0.90†**	**0.90†**	-0.30	0.10	**-1.00*****	**-0.90†**	**-0.90†**	-0.30	**-0.90†**
	wet ΔΨ	-0.70	-0.60	**0.90†**	0.00	0.40	-0.70	**-0.90†**	**-0.90†**	-0.30	**-0.90†**
	SLA	-0.80	-0.40	**0.90†**	-0.20	0.10	-0.70	**-0.90†**	**-0.90†**	-0.20	**-0.90†**
	elev	**0.90†**	0.70	-1.00***	0.10	-0.30	**0.90†**	1.00***	1.00***	0.40	1.00***

Chapter 1 Figures

Figure 1 Study system and sites. a) typical leaves of each oak species within the Chiricahua Mountains. b) Broader ranges of each oak species (Little Jr. 1971, USGS 2013) in bold colors and transparent colors showing scale of distribution probabilities as calculated with species distribution modeling (Hijmans et al. 2005, GBIF 2013, Hijmans and Elith 2013). c) Region map, with color gradient of log(Mean annual precipitation, Hijmans et al. 2005), box shows inset map of the Chiricahua Mountains, d) and circles denote sampling points for all physiological traits and local temperature data (color scale denotes only elevation). Digital elevation models via USGS (2009).

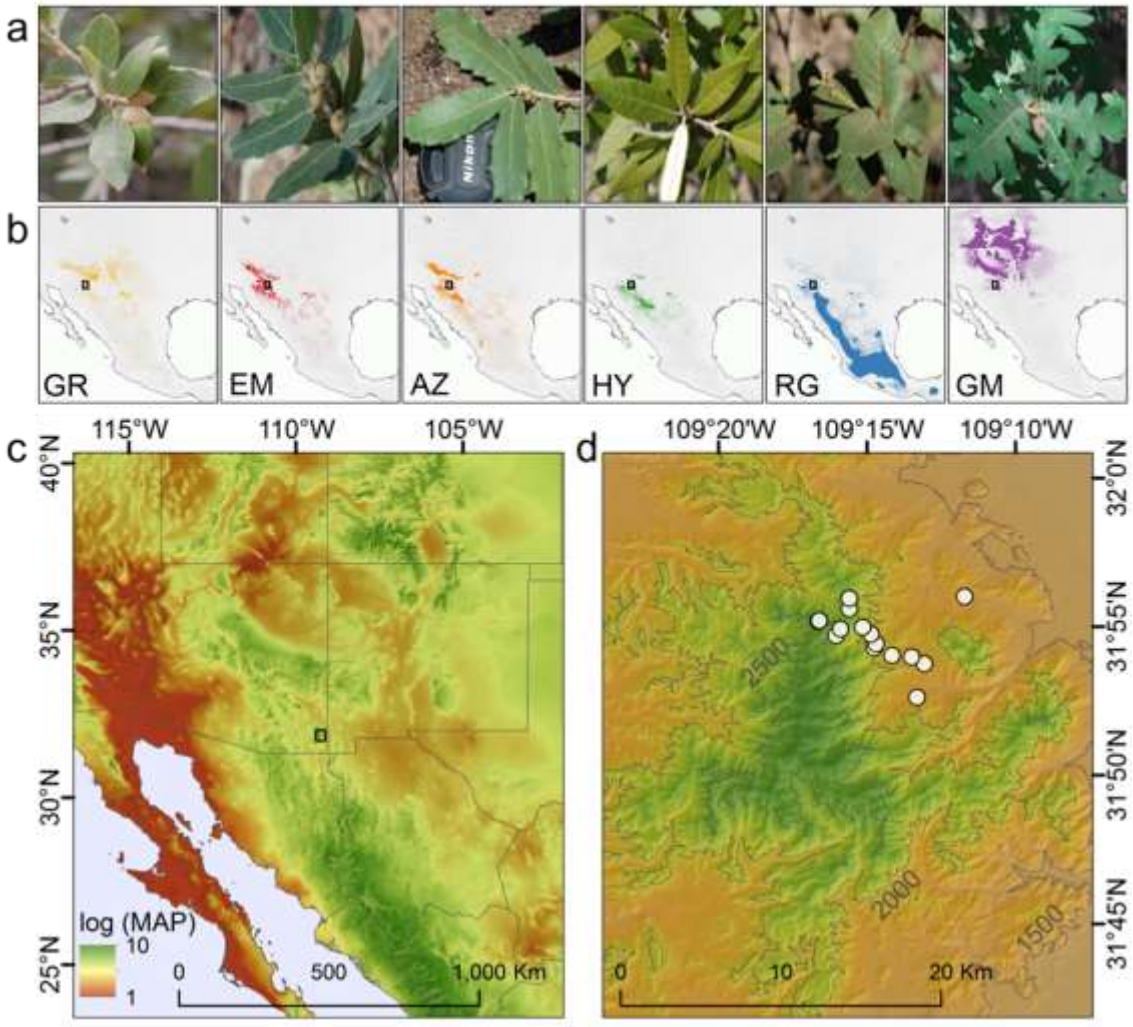

Figure 2. Species occurrences within Chiricahua Mountains, by elevation and local climate a) Species occurrence curves by elevation, dotted lines denote red oaks (section Lobatae) and solid lines denote white oaks (section Quercus). Species are Q. grisea (GR), Q. emoryi (EM), Q. arizonica (AZ), Q. hypoleucoides (HY), Q. rugosa (RG), Q. gambelii (GM). b) Presence points show observed locations of each species within survey sites in the eastern Chiricahua Mountains. c) Occurrence density by minimum temperature of coldest month, BIO6 (Hijmans et al. 2005) and a measure of aridity (the ratio of mean annual precipitation to mean annual evapotranspiration, CGIAR-CSI 2008).

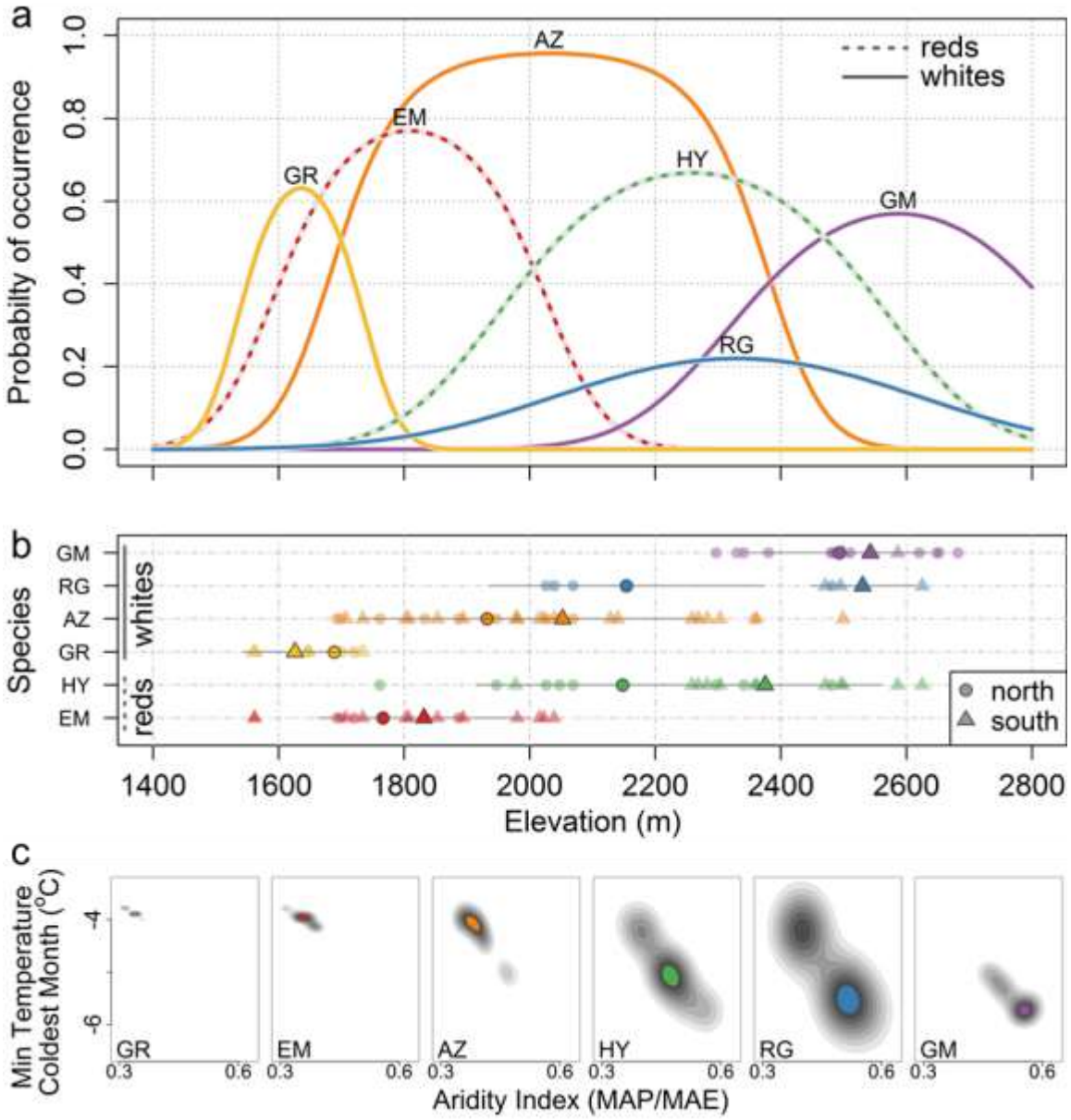

Figure 3. Plant water access measures and drought tolerance traits. All error bars show standard error of the mean and letters denote significant pairwise differences at $p<0.05$. Species are Q. grisea (GR), Q. emoryi (EM), Q. arizonica (AZ), Q. hypoleucoides (HY), Q. rugosa (RG), Q. gambelii (GM). a, c, e) Dry season Ψ_{PD} (N=135), Turgor loss point (Ψ_{TLP}, N=127), and absolute leaf capacitance (C_{leaf}, N=127) by aridity index, MAP/MAE (CGIAR-CSI 2008) at each site. b, d, f) Species means of Ψ_{PD}, Ψ_{TLP}, C_{leaf} by mean elevati on of occurrence.

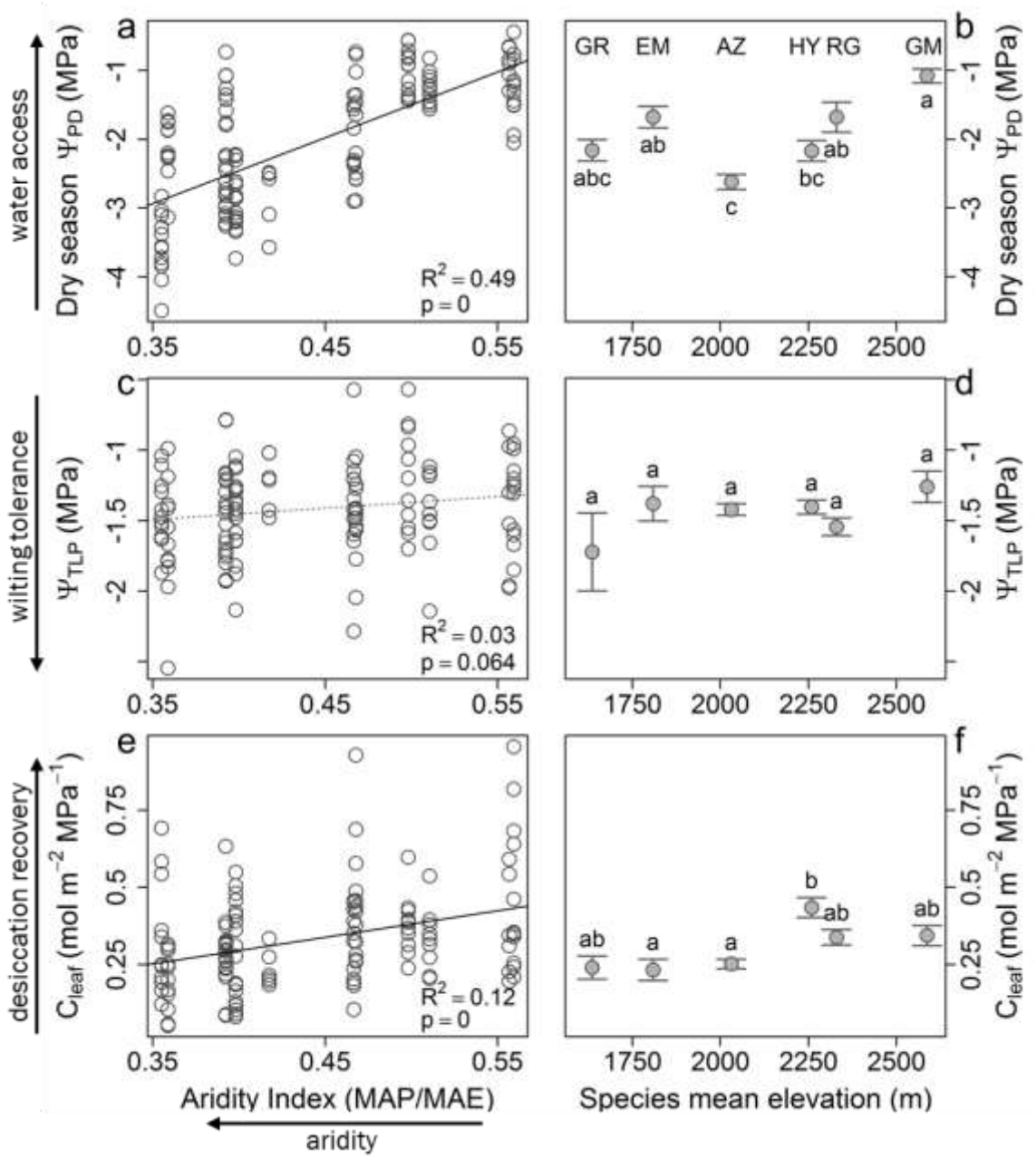

Figure 4. Oak species freezing vulnerability, T_{50} (species by site means). Species are Q. grisea (GR), Q. emoryi (EM), Q. arizonica (AZ), Q. hypoleucoides (HY), Q. rugosa (RG), Q. gambelii (GM). a) Summer-collected stem T_{50} mean temperature 14 days prior to collection (N = 24 species x site combinations). b) T_{50} of winter collected stems (N = 23 species x site combinations). c) Mean T_{50} for each species by mean elevation. Species codes, in upper part of plot, Q. grisea (GR), Q. emoryi (EM), Q. arizonica (AZ), Q. hypoleucoides (HY), Q. rugosa (RG), Q. gambelii (GM). Letters signify significant comparisons (at $p<0.05$ from post-hoc Tukey test) and upper two letter codes denote species.

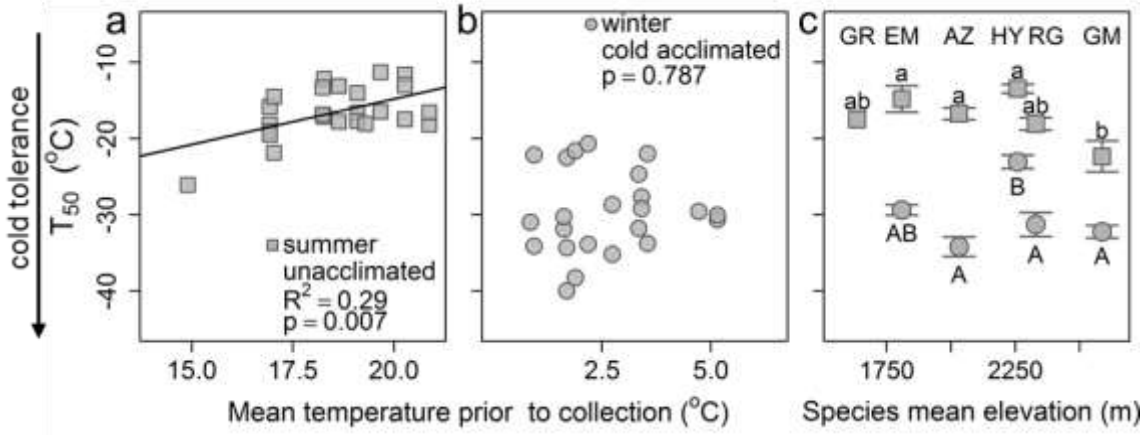

Figure 5. Percentage of leaves retained (marked in preceding wet season) by species mean aridity index, species mean SLA, and species mean absolute leaf capacitance. Seasonal evergreen status (E) and seasonal deciduousness (D) are shown at 100% and 0% retention. Error bars show SE of the phenology model (a,d) or SE of the mean. a – c) Leaf retention during the cold season (N = 6 species) d-f) Leaf retention in the dry season (N = 5 species).

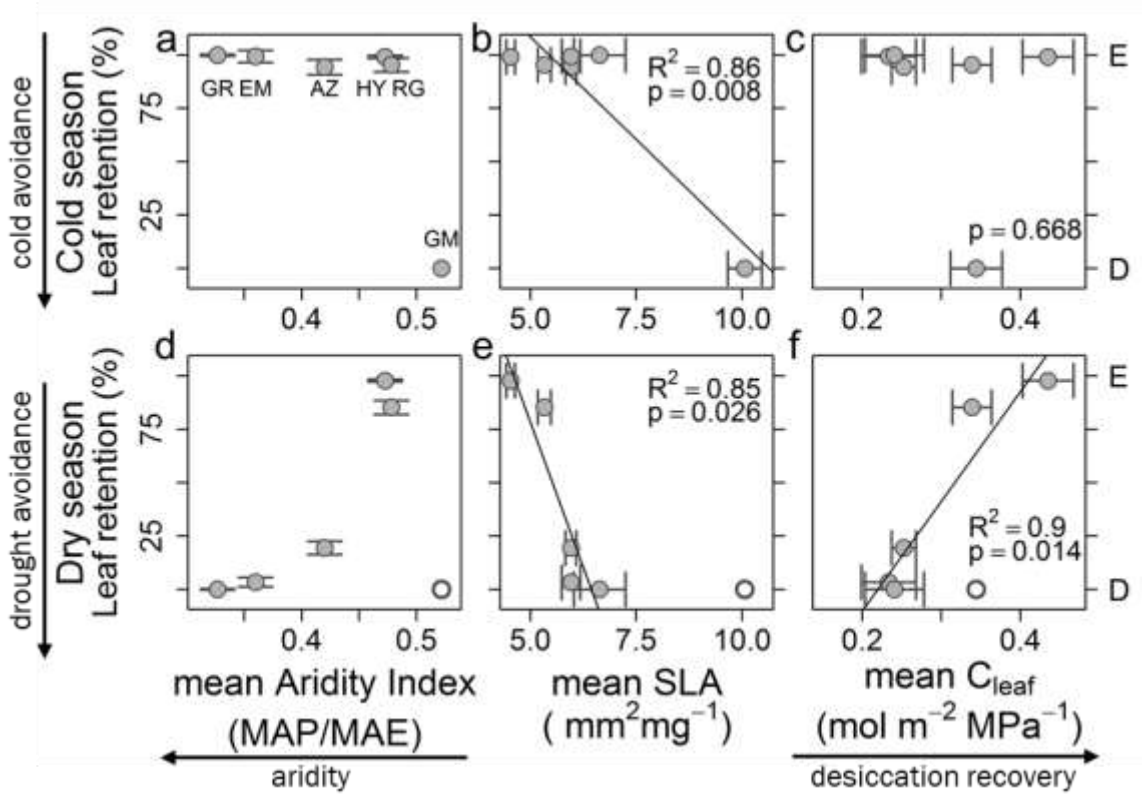

Chapter 2. Precipitation seasonality and leaf habit result in decoupled stem and leaf drought resistances among American oaks

Summary

Drought frequently occurs as short term or localized events, yet vulnerability to drought influences species ranges at large scales. Tree drought resistances are bounded by an inherent trade-off between maintaining gas exchange and efficient hydraulic conductance, while avoiding embolism formation within conducting tissues. The greater frequency and intensity of droughts occurring with global climate change increase the risks of trees encountering fatal drought stress. We used a set of 21 species of American oaks to ask how climate of origin is correlated with stem vulnerability to drought (vulnerability curves) and leaf stomatal closure (during an imposed drought), and how leaf habit affects resistances. We found that stem and leaf drought avoidance strategies are decoupled from one another by a stronger influence of precipitation seasonality, rather than annual aridity, on leaf resistance. Longer-lived woody stems showed greater embolism resistance in more arid environments, but water potential at stomatal closure—and overall leaf habit—was most strongly correlated with precipitation seasonality. We classified these stomatal closure and leaf loss strategies along a precipitation seasonality gradient: acquisitive (drought deciduous), conservative (evergreen), and opportunistic (winter deciduous). We found that oak species ranges are influenced by drought resistances and that seasonality of precipitation separately favors different overall leaf habits and stomatal closure strategies.

Introduction

Water availability in the environment shapes whole biomes (Stephenson 1990) and influences range shifts under warming (Crimmins et al. 2011). Woody plants have contended with and adapted to historical droughts within current ranges (Pockman and Sperry 2000, Williams et al. 2012). Increasing drought stress under global warming (IPCC 2013) is likely to increase tree mortality globally (Breshears et al. 2005, Allen et al. 2015, Greenwood et al. 2017). Understanding how drought resistances, both to short-term and long-term water stress, shape tree ranges is important in understanding the potential consequences of high temperature droughts exacerbated by global change (Breshears et al. 2005).

Plants face fundamental tradeoffs during drought between carbon acquisition and reducing water loss through transpiration (Sperry 2003, McDowell et al. 2008). As plants maintain open stomata, water stress increases the risk of hydraulic failure (Tyree and Sperry 1988). Highly negative pressures that form in a drought stressed plant can lead to the expansion of air bubbles into and between vessels, causing embolism formation and disrupting hydraulic flow (Tyree and Sperry 1988, Pockman et al. 1995). Broadly, trees may resist drought and avoid hydraulic disruption by 1) maintaining xylem that is less vulnerable to embolism formation, 2) slowing or halting transpiration via stomatal closure or 3) leaf dehiscence (Sperry 1995).

Strategies for drought resistance may differ based upon the severity and length of drought within a species range. less vulnerable xylem can lead to lower efficiency in water movement and an overall loss of hydraulic potential in woody angiosperms, reducing potential growth rate during wet seasons (safety- efficiency tradeoff, Sperry 2003; Hacke *et al.* 2006; Sperry *et al.* 2008). Closing stomata to reduce negative pressure gradients can may avoid embolism (Tyree and Cochard 1996, Hochberg et al. 2017) but the hydraulic safety conferred by closure may be incomplete (Brodribb and Holbrook 2003a) and lead to additional risks of carbon starvation during prolonged drought (Jones and Sutherland 1991, McDowell et al. 2008). Leaf abscission in response to drought can serve as a protective mechanism, and may be promoted if more disposable or distal parts of a plant (i.e. leaves, petioles) are more vulnerable to embolism than proximal parts (i.e. twigs, stems) (Tyree et al. 1993, Tsuda and Tyree 1997, Tyree and Zimmermann 2002, Choat et al. 2005, Bartlett et al. 2016). Leaf abscission during drought may be a way to keep stomata in any remaining leaves at least partially open for longer periods of time until shedding (Jones and Sutherland 1991, Brodribb and Holbrook 2003b). However, leaf drop may not always serve to maintain stem hydration and embolism may continue to spread in some species (Wolfe et al. 2016). Additionally, evergreen species are by definition unable to use this hydraulic safety mechanism.

Oaks (Quercus, L. family Fagaceae), a globally distributed woody genus, and highly abundant and diverse woody genus in North and Central America (Nixon 2006) are more drought hardy than many other co-occurring angiosperms (Abrams 1990). Oaks have been found to both confirm and defy expectations of drought resistance mechanisms.

Fagaceous species have weak xylem safety-efficiency correlations (Gleason *et al.* 2016), but species specific studies have found evidence supporting safety-efficiency tradeoffs, (e.g. Hacke *et al.* 2006). Oaks have also been found to maintain open stomata at more negative water potentials (Abrams 1990, Klein 2014) than sympatric species, although partial stomatal closure in oaks has also been found to keep xylem water potential in deciduous oaks above cavitation potentials (Cochard et al. 1996). Oak species may also be exceptions to expectations of hydraulic segmentation with no significant differences between petiole and stem xylem vulnerability to embolism (Cochard et al. 1992). We used a set of 21 oak species to ask how species from across an aridity gradient use different strategies to respond to drought. Specifically, we asked 1) how stem xylem vulnerability (expressed as water potential at a given % stem embolism) and leaf drought avoidance (through stomatal closure or leaf abscission) are related to annual drought (aridity, temperature, and precipitation), and drought seasonality (the variation in precipitation) among American oaks, and 2) whether leaf loss and leaf habit (general leaf loss phenology) are critical mechanisms of drought resistance in oaks.

Methods

Greenhouse common garden

We grew *Quercus* saplings from a broad collection of species (Table 1), representing three subgenera (*Quercus* or white oaks, *Lobatae* or red oaks, and *Virentes* or live oaks) of the warm regions of North and Central America. We collected acorns from native ranges (Fig. 1) in late 2013 and stored them at 4^{o}C until planting in University of Minnesota greenhouse facilities February 2014. We transplanted one-year old saplings to

a 1:1 potting soil: sand mix in tree pots (TP616, Steuwe and Sons, Oregon USA) in 2015. Saplings were well watered and kept at constant temperature for the first year of growth, then exposed to a cooler winter in 2015, and returned to warm conditions (22^{o}C before measurements). Seedlings were regularly treated with a water-soluble acidic fertilizer (Peters Professional 21-7-7 Acid Special, Everris NA Inc., Dublin, Ohio USA).

Dry down experiment

We continuously monitored gas exchange before midday (8-11) for stomatal closure during a dry down experiment on two-year-old saplings (in June – July 2016) (Species = 21, N = 77, Table 1, Fig. 1). We reduced watering to dry out soils to near 0% volumetric soil water content (VWC) over the course of one month (Fig 2.). We monitored soil volumetric water content (VWC %) with a handheld soil moisture meter (Fieldscout TDR 300, Spectrum Technologies, Inc., Illinois, USA), and gas exchange for stomatal closure. We used a LiCor 6400XT portable photosynthesis system (LI-COR Biosciences, Nebraska USA) to monitor leaf photosynthesis (A_{max}) and stomatal conductance on study plants every 2-3 days throughout the dry down. We let leaves equilibrate in the leaf chamber until measurements stabilized in fixed conditions: PAR = 600 μmol m^{-2} s^{-1} (ambient light level in greenhouse), CO_2 = 400ppm, block temperature = 24^{o}C, relative humidity = 45% (±0.85). We defined the point of stomatal closure to be when g_s was less than 5% of maximum conductance (measured on each individual of well-watered plants) or less than 5 mmol m^{-2} s^{-1}, whichever was greater (Craine et al. 2012). We measured Ψ, the leaf water potential, collected immediately after g_s measurements and found Ψ_{crit} as the water potential at the point of stomatal closure (for list of measurements and

abbreviations, see Table 2). We recorded any leaf water potentials greater than the maximum capacity of our pressure chamber (8MPa, Soilmoisture Equipment Corp., California USA) as -8MPa. To determine experimental effectiveness, we tested for soil VWC differences among individuals that did and did not show stomatal closure using unpaired, one-sided t-tests.

Throughout the dry down experiment, we recorded qualitative leaf responses to drying soils for all leaf cohorts: i) immature or new flushes, ii) mature flushes, and iii) leaves older than two flushes. We recorded leaf loss as a binary state in each age class. We calculated 1) both the likelihood of leaf loss for each species using binomial generalized linear models and 2) percent leaf loss in each leaf age class, calculated as the percentage of individuals per species that lost leaves in that cohort by the end of the dry-down measurements. The two measures were highly correlated with each other for all age classes ($r > 0.92$) and we use percentage of individuals showing leaf loss (% leaf loss, Table 2) for all further analyses. We determined overall species leaf habit (evergreen, winter deciduous or drought deciduous) from the literature and classified semi-deciduous species by the seasonal timing of leaf loss (Table 1, Muller 1942a, 1942b, 1954, Bryant and Kothmann 1979, Nixon 1997, Williams-Linera 1997, Garcia Moscoso 1998, Cavender-Bares 2000, Romero Rangel et al. 2002, Cavender-Bares et al. 2004b, Fallon, unpublished).

Stem xylem vulnerability

We selected nine oak species from the greenhouse garden to represent a broad range of species climatic distributions (Table 1, Fig. 1). We measured stem embolism following the pneumatic protocol of Pereira et al. (2016). This method uses vacuum measurements of air discharge in woody stems as a proxy for xylem embolisms and is robust to stem section length (Appendix S2: Methods). P_{50} or the stem water potential at 50 percent embolism, a common and meaningful measure of xylem vulnerability was found to be highly correlated with measurements of PAD_{50}, the stem water potential at 50 percent air discharge (PAD) from the stem, in a diverse set of tropical species (Pereira et al. 2016). As a consequence, this method is likely to have advantages over other methods, such as centrifugation or bench-drying, that may be problematic for species, such as oaks, with long vessel lengths. We cut leafy stems > 50cm in length in air, immediately recut at least 10 cm from the ends in water, and left the stems to rehydrate for at least 1 hour (no more than 3) covered with heavy black plastic bags. We measured stems of six individuals of each species when fully hydrated and then used the bench drying method to let stems desiccate at ambient conditions (Sperry et al. 1988). We used plastic covered and dark equilibrated leaves to find stem water potential (Ψ_{stem}, MPa) and stopped when stems were fully dehydrated (Appendix S2: Methods). Each air discharge measurement was made for 3 minutes.

We calculated change in moles of air and converted to air discharged (AD, μL) for each measurement and adjusted for system leakage (mean $= 3.96 \mu L\ 3min^{-1} \pm 0.49$) (Appendix S2: Methods). We found a normalized percent air discharged (PAD, %) for each individual as:

$$\mathrm{PAD} = 100 \times (\mathrm{AD} - \mathrm{AD_{min}})/(\mathrm{AD_{max}} - \mathrm{AD_{min}}) \quad \text{Eq. 1}$$

where AD_{max} is the AD at which Ψ_{stem} was most negative (most desiccated) and AD_{min} was the AD of the most hydrated measurement (when $\Psi_{stem} \approx 0$ MPa) (Appendix S2: Fig. S2.1). We removed individuals from further analyses that had AD_{min} values greater than mean AD_{min} + one standard deviation, because those deviations likely indicated poor seals around the stem (leaks).

We used the packge *plcfit* to fit Weibull curves to PAD, as a proxy for percent loss conductivity (Duursma and Choat 2017). This package uses bootstrapping to fit a non-linear Weibull curve (following the parameters of Ogle *et al.* (2009)) and generate confidence intervals around predicted parameters. We choose the Weibull model because it can fit r- or s-shaped curves and r-shaped curves have been found in *Quercus* hydraulic vulnerability curves (Cochard et al. 1992, Cavender-Bares and Holbrook 2001). The Weibull model also incorporates parameters for P_x (susceptibility to drought, or here, Ψ_{stem} at x% PAD, which we call here PAD_x) and S_{50} (sensitivity, or slope of the curve at the fit value of PAD_{50}) (Pammenter and Willigen 1998). Additionally, the resulting model allows the curve to be fit at any value of PAD_x and other values of PAD_y can still be extracted from that model (Ogle et al. 2009, Duursma and Choat 2017). We fit two types of models to each species: 1) fixed effects only, pooling data from all individuals of a species and 2) non-linear mixed model, with each individual as a random effect (Appendix S2: Fig. S2.2). For a single species, *Q. lyrata*, the model fitting failed to converge and we dropped single individuals in an iterative model fitting (five individuals instead of six) and kept the model with the lowest error (σ). We also calculated PAD_{12}, as

an approximation of the air entry point or the Ψ_{stem} beyond which embolisms can propagate quickly through the xylem (Sparks and Black 1999, Domec and Gartner 2001) and PAD_{88}, or the water potential at full embolism (Domec and Gartner 2001), for each species. In the event of failure of model fit for these more extreme values, we used the values of PAD_{12} and PAD_{88} fit from the PAD_{50} model. We found a strong relationship between both model types (Appendix S2: Fig. S2.3) and used the non-linear mixed model results for all analyses because the fit should be less affected by outlier individuals (Duursma and Choat 2017).

Bioclimatic data

We used the point of maternal plant collection to find climate of origin and used herbarium and literature records to find mean climatic values for whole species range (climate of range). We downloaded specimen occurrence records, based upon collected specimens and occurrence in literature, from GBIF (GBIF 2013). We retained all specimens with location data and then randomly sampled one point per one degree grid. For both climate of origin and of range, we extracted long term publically available bioclimatic variables (temperature, precipitation, seasonality, and aridity) from high resolution (30 arc second) datasets for each maternal plant location of all study individuals (Hijmans et al. 2005, CGIAR-CSI 2008, Zomer et al. 2008) using packages *raster* and *dismo* (Hijmans 2016, Hijmans et al. 2016). We found the mean, minimum, and maximum value for each bioclimatic variable for climate of range and the species mean for climate of origin (Table 1). We tested for correlations between climate of origin and climate of range and found high correlations between means for these variables of

interest: aridity index (mean annual precipitation/mean annual evapotranspiration, higher values indicate less aridity), mean annual temperature and precipitation, and temperature and precipitation seasonality (Appendix S2: Table. S2.1). We used climate of origin for all analyses.

Analyses

We conducted all analyses in R (R Core Team 2016). We averaged data to species for all measured variables (Ψ_{crit}, PAD_x, and percent leaf loss, Table 1). We also included simple hydraulic safety margins as i) S_{50}, a sensitivity measure of the slope of embolism with declining Ψ_{stem} (Pammenter and Willigen 1998) , ii) leaf-stem safety margin ($\Psi_{crit} - PAD_x$), where larger, positive values indicate stomatal closure that to maintain Ψ_{stem} above the pressure at 50% embolism and iii) stem safety margin ($PAD_{12} - PAD_{50}$), where larger values have been found indicate a less rapid propagation of embolism and have been found to be correlated with stem drought tolerance (Meinzer et al. 2009).

We used simple linear regressions to test effects of climate of origin, subgenus (coarse phylogenetic similarity), leaf loss, and leaf habit (species mean habits from literature, Table 1) on all response variables. We fit simple linear models to relationships among PAD_x, Ψ_{crit}, S_{50}, and safety margins to test the relationships between these variables. When the predictors were a factor, we used post-hoc Tukey tests ($\alpha = 0.05$) to determine pairwise significance. We checked all models for normality and transformed if necessary.

Results

Soil volumetric water content and precipitation declined through dry down

Soil VWC, photosynthetic rate, and stomatal conductance declined throughout the experiment (Fig 2). The variance in final soil VWC (mean 3.79% (± 4.7)) was largely due to the fact that some pots never fully dried out during the monitoring period. Individuals of some species remained in soil VWC between 5 and 9%, even while most individuals experienced VWC below 3%. *Q. falcata* was the only species for which no individuals experienced extreme drought (minimum VWC 7.3%), likely because these were quite small trees, and thus water loss was limited and plants were not effectively drying down the soil.

Leaf loss correlation with climate differs by leaf cohort age class

Only four species (total N = 21) showed no leaf abscission at all during the measurement period. Mature cohort loss was positively correlated with mean annual temperature of origin ($F_{1,19} = 5.25$, $P = 0.034$, $R^2 = 0.22$). Early cohort leaf loss (more than two flushes prior to measurements) was weakly correlated with mean annual temperatures of origin ($F_{1,17} = 3.39$, $P = 0.083$, $R^2 = 0.16$). Abscission of the immature leaf cohort was positively predicted by aridity index ($F_{1,19} = 3.48$, $P = 0.078$, $R^2 = 0.15$). Subgenus was marginally significant predictive factor of immature leaf abscission; species of subgenus *Virentes* had greater percentages of immature leaf loss ($F_{2,18} = 2.67$, $P = 0.09$, $R^2 = 0.23$).

Stomatal closure correlated with precipitation seasonality and aridity index

Ψ_{crit} was negatively correlated with precipitation seasonality, such that plants experiencing greater seasonality closed stomata at more negative water potentials ($\ln(\Psi_{crit})$, $F_{1,15} = 4.65$, $P = 0.048$, $R^2 = 0.24$, Table 3, Fig. 3b). Ψ_{crit} was positively but not significantly correlated with aridity index ($\ln(\Psi_{crit})$, $F_{1,15} = 4.42$, $P = 0.053$, $R^2 = 0.23$) (Table 3, Fig. 3a), as well as mean annual precipitation ($\ln(\Psi_{crit})$, $F_{1,15} = 4.53$, $P = 0.05$, $R^2 = 0.23$). Ψ_{crit} was not significantly predicted by subgenus. Differences between individuals that closed stomata and those that did not were likely influenced by the effectiveness of drought imposition. Soil VWC was significantly different between closed and unclosed individuals (mean open soil VWC = 3.64, mean closed soil VWC = 1.04, $t_{49.9} = 3.7$, $p = 0$). Subgenus was not a significant factor in predicting stomatal closure.

$PAD_{50,}$ PAD_{12}, but not PAD_{88}, correlated with aridity gradient

Xylem vulnerability, or PAD_{50}, was positively correlated with aridity index of origin, such that plants from less arid environments had less negative PAD_{50} values ($F_{1,7} = 9.138$, $P = 0.019$, $R^2 = 0.57$, Fig. 4b, Table 3). PAD_{50} was also correlated with mean annual precipitation ($P = 0.029$, $R^2 = 0.52$). PAD_{50} was not significantly correlated with precipitation seasonality nor with temperature seasonality (Table 3). The air entry point, PAD_{12}, was also positively correlated with aridity index ($F_{1,7} = 10.93$, $P = 0.013$, $R^2 = 0.61$, Fig. 4a) and mean annual temperature ($F_{1,7} = 7.02$, $P = 0.033$, $R^2 = 0.50$), but not with precipitation or temperature seasonality. PAD_{88} was not strongly correlated with any climatic variables (Fig. 4c). Neither stem hydraulic safety margin ($PAD_{12} - PAD_{50}$) nor leaf-stem hydraulic safety margin ($\Psi_{crit} - PAD_{50}$) were significantly correlated with any

climatic variables. Xylem vulnerability (any PAD_x) and safety margins were not significantly predicted by subgenus. The xylem vulnerability curves were not strong model fits in all cases (*Q. lyrata*, Table 1). The median width of the confidence interval around PAD_{50} was 1.7MPa (Table 1, Appendix S2: Fig. S2.2).

Stomatal closure and stem vulnerability are uncoupled

Ψ_{crit} was not significantly correlated with any measurements of stem vulnerability (PAD_x) or stem safety margins (Appendix S2: Fig. S2.4). There was a positive, but non-significant relationship between Ψ_{crit} and PAD_{12} (P = 0.109, P = 0.117, Appendix S2: Fig. S2.4a) and PAD_{50} (P = 0.117, Appendix S2: Fig. S2.4b).

Stomatal closure and total stem embolism point (PAD_{88}) differ by leaf habit

Ψ_{crit} was significantly and negatively correlated with percent early cohort leaf loss in all individuals ($\ln(\Psi_{crit})$, $F_{1,14} = 7.10$, P = 0.018, $R^2 = 0.34$, Fig. 5a). There was no relationship with other leaf age classes. Ψ_{crit} was significantly lower among drought deciduous species than winter deciduous species (Fig. 5b, Table 3). Ψ_{crit} was also negatively correlated with leaf retention: species with more negative Ψ_{crit} values were more likely to lose early cohort leaves during the drought (Fig. 5d). PAD_{88}, complete stem embolism point, was significantly predicted by overall species leaf habit ($F_{2,6} = 8.06$, P = 0.020, $R^2 = 0.73$, Table 3). Evergreen species had significantly lower PAD_{88} than drought- or winter-deciduous species. Leaf habit (described from literature) was not

significantly correlated with other stem vulnerability or safety margins variables (Figure 6, Table 3).

Leaf habit correlated with precipitation seasonality

Precipitation and temperature seasonality was significantly different among leaf habits. Winter deciduous species were from origins of much lower precipitation seasonality than drought deciduous species ($F_{2,18} = 11.49$, $P = 0.001$, $R^2 = 0.56$, Fig. 5c). Drought deciduous species are of origins that have significantly less temperature seasonality than evergreen or winter deciduous species ($F_{2,18} = 6.79$, $P = 0.006$, $R^2 = 0.43$). Leaf habits were not significantly correlated with leaf loss observed during the experiment. However, drought deciduous species showed uniformly higher percentages of leaf loss (≥ 0.5) than winter deciduous species (range 0.0 – 1.0).

Discussion

We predicted that oak species distributions would be influenced by drought resistances and that these drought resistances would fall among three strategies 1) low xylem vulnerability, 2) stomatal closure to avoid shorter term droughts, and 3) leaf dehiscence. We see evidence that all species have xylem vulnerability correlated with aridity, but that stomatal closure and dehiscence are tradeoffs correlated with variability of precipitation rather than simply average aridity. The stem and leaf drought resistances are decoupled as each is better predicted by different precipitation related climate factors. In the long lived woody tissues of the stems, xylem vulnerability is highly correlated with annual average

aridity (the ratio of mean annual precipitation over estimated mean annual evapotranspiration, Fig. 4). In the shorter lived leaves, drought avoidance via stomatal closure is significantly correlated with precipitation seasonality (the annual coefficient of variation in precipitation, Fig. 3) and is significantly different between winter and drought deciduous leaf habits, which occupy low and high ends of the precipitation gradient, respectively (Fig. 5). There is a positive, but not significant, relationship between stem xylem resistance to embolism (PAD_{12} and PAD_{50}) and stomatal closure (Appendix S2, Fig. S2.4). Common hydraulic safety margins are not significantly correlated with either climate or leaf habit (Table 1, Fig. 6). Only evergreen species showed a significant connection with stem vulnerability: PAD_{88}, or the point of runaway embolism, was significantly lower among species of evergreen leaf habits.

We expected that stomatal closure and stem vulnerability would be correlated (Bartlett et al. 2016) as a consequence of coordination between stems and leaves in strategies of drought resistance. Aguilar-Romero *et al.* (2017) found that leaf habit and stem xylem resistance in a set of broadly sympatric subtropical oaks were correlated with an aridity gradient, wherein drought deciduous species occupied the most arid areas, while species with longer leaf lifespans occupied the more humid areas and also maintained less vulnerable stem xylem. Kröber *et al.* (2014) found that among a group of co-occurring species in China, stem hydraulic traits were not closely linked to stomatal conductance, but rather to morphological traits and that evergreen species had much lower P_{50} values. Our results concur with findings that stomatal closure and stem xylem vulnerability are decoupled, although most variation in stem xylem vulnerability was not explained by

expected leaf lifespan. We found more resistant xylem among our evergreen species, but only at the PAD_{88}, or near total stem embolism measure. We found no evidence of stem to leaf safety margins that aligned with leaf habit or local climate. Instead of evidence for similar drought resistance strategies among leaves and stems, that leaf lifespan and stomatal closure are tightly correlated and best predicted by precipitation seasonality, while stem drought resistance can be independently predicted by average aridity.

The greater embolism resistance of stems in more arid areas agrees with expectations of maintaining safer stems in areas with stronger drought pressures. While we did not observe evidence that would agree with hypotheses of hydraulic segmentation, for example stem to leaf safety margins such that leaves are more vulnerable than stems to embolism and are shed as a fuse to prevent stem embolism, we did find evidence supporting our expectation that longer lived, or less disposable, tissues should be more adapted to local conditions of water stress (Tyree and Zimmermann 2002). Woody species do not consistently maintain safety margins (minimum water potential – P_{50}) that are correlated with aridity (Choat et al. 2012). However, we did not examine the minimum annual water potentials that any species may be expected to reach in their native environments, so we cannot definitively assert that each species is maintaining xylem safe from embolism.

Like other woody angiosperms, oaks have a wide array of leaf habits. Among oaks, aridity gradients have been found to separate drought deciduous species from evergreen species on smaller spatial scales (Aguilar-Romero et al. 2017). However, oaks also demonstrate intraspecific variation in response to differences in seasonal severity of

drought, where populations experiencing more severe drought are more likely to be deciduous (Ramírez-Valiente and Cavender-Bares 2017). Precipitation seasonality, rather than aridity, of the whole species ranges has been found to be more strongly correlated with specific leaf area (itself tightly correlated with timing of leaf dehiscence) among a subset of the winter, evergreen and drought deciduous species included in this study from Arizona, USA (Fallon and Cavender-Bares, unpublished). Stomatal closure has not been explicitly tied to aridity in a diverse set of grass species (Craine et al. 2012), so leaf stomatal responses to intra-annual variability in precipitation rather than mean annual aridity may result from the relatively short lifespans of leaves, compared to stems, and the timing of stress in the lifespans of the leaves. Winter deciduous species almost uniformly occupy low precipitation seasonality environments, while drought deciduous species occur in the most seasonal environments. Winter deciduous species generally experience more temperature variability and uniform precipitation, and winter precipitation (in the form of rain or snow) is less available because of low temperatures. Stomatal closure may be most advantageous in short term droughts, when plants can preserve leaf and stem water while not incurring large carbon deficits (Jones and Sutherland 1991, McDowell et al. 2008). In our study, winter deciduous species had closed stomata at less negative leaf water potentials and avoided drought induced desiccation; these species were the least likely to occupy habitats of large intra-annual variation in precipitation. Drought deciduous species occupy the highest seasonality environments, and may be more likely to experience carbon starvation if stomatal closure is a strategy to maintain leaf or plant water status. Recent work by Martin-StPaul *et al.* (2017) found that -4MPa was standard point of stomatal closure in woody plants. We find

values near or just below that value for some drought deciduous species. This may be due to leaf desiccation rather than stomatal closure during dry down among some of the drought-deciduous oak species. Among our species, the drought deciduous species with the highest Ψ_{crit} value, *Q. lancifolia*, is from the cloud forests of Honduras, which experiences a high annual rainfall, but a dry season that brings stretches of 1-2 months in which less than 3% of annual rainfall is received (Stadtmuller and Agudelo 1990). Therefore *Q. lancifolia* may be able to close stomata earlier and without serious starvation costs for shorter periods of time because the drought is followed by high precipitation. In our set of species, the two winter deciduous species that showed the highest precipitation seasonality (Fig. 5a) are from the semi-arid mountains of southern Arizona where they are relegated to high elevation areas, where they experience less water stress, or low elevation intermittent streams, where they may benefit from summer rain run-off during the warmer season (Fallon and Cavender-Bares, unpublished). These Arizona species close stomata at similar values to other winter deciduous species of less seasonal environments, possibly because of having access to root water that reduces the severity of precipitation seasonality (Ehleringer and Phillips 1996).

Conclusions

The distributions of American oak species are influenced by drought resistances and the timing of precipitation deficits, resulting in three strategies associated with broad differences in leaf habit. All species have stem xylem vulnerabilities that are well predicted by annual aridity, although they may not be safe from embolism at that mean level of aridity. Winter deciduous species occupy areas of significantly lower

precipitation seasonality and are opportunistic in gas exchange. These species close stomata at lower water potentials likely because longer term droughts are unlikely to lead to carbon starvation. Drought deciduous species live in habitats of high precipitation seasonality and are carbon-acquisitive at the expense of water loss. These species are most likely to experience severe droughts more frequently and thus might experience losses of opportunity for carbon fixation frequently if they closed stomata at high water potentials. They sacrifice leaf desiccation, and possible stem hydraulic failure, for continued gas exchange. Evergreen species are the most conservative in approach. These species close stomata at intermediate water potentials, relative to the shorter-lived leaf habits, occupy areas of medium seasonality, and maintain less vulnerable stem xylem to avoid stem hydraulic dysfunction.

Acknowledgements

This work was funded by a National Science Foundation grant (DEB-1146380, PI J.C.B.), and by University of Minnesota funding to B.F. (Charles J. Brand Fellowship, Dayton Bell Museum Fund). We thank Antonio Gonzalez-Rodriguez, Frank Hoerner, and Esau Zuniga for acorn collection. We are grateful for the work of Ian Carriere, Melat Weldesalasie, and Alec Scollard in helping establish and monitor the greenhouse garden and to Matthew Kaproth and Jose Ramírez-Valiente for their advice in oak rearing.

Chapter 2 Tables

Table 1. Oak (*Quercus*) species, authorities, subgenera (Lobatae = red, Quercus = white, Virentes = live), leaf habit, mean values of annual temperature (MAT, ^{o}C), annual precipitation (MAP, cm), and aridity index (AI, MAP/mean annual evapotranspiration) of maternal plant origins, mean values of Ψ_{crit}, leaf water potential (MPa) at stomatal closure, and PAD_{50}, stem water potential (MPa) at 50% embolism. Standard deviation of Ψ_{crit} is shown for species with more than one individual having closed stomata (Closed = n/total). Bootstrapped model 95% CI values follow PAD_{50}. n(VC) = total individuals measured to build xylem vulnerability curve. [1] Garcia Moscoso 1998, [2] Nixon 1997, [3] Fallon, unpublished, [4] Cavender-Bares et al. 2004b, [5] Cavender-Bares 2000, [6] Muller 1942a, [7] Romero Rangel et al. 2002, [8] Muller 1954, [9] Muller 1942b, [10] Williams-Linera 1997, [11] Bryant and Kothmann 1979

Table 1.

species	subgenus	leaf habit	MAT	MAP	AI	Ψ_{crit}	Closed	PAD_{50}		n(VC)
elliptica Née	Lobatae	drought[1]	22.3	101.3	0.64	-4.59	(1/4)	-3.89	(-2.78,-4.18)	5
emoryi Torr.	Lobatae	drought[2,3]	13.1	48.0	0.33	-3.93 (±0.15)	(2/4)	-4.75	(-2.41,-5.22)	6
falcata Michx.	Lobatae	winter[4,5]	20.2	132.2	0.86		(0/2)			
hemisphaerica Bartram ex Willd	Lobatae	winter[4,5]	20.3	128.5	0.83	-3.72 (±0.73)	(3/4)	-3.49	(-1.9,-4.17)	5
mexicana Bonpl.	Lobatae	drought[6, 7]	14.5	79.4	0.57	-3.77	(1/3)			
velutina Lam.	Lobatae	winter[2]	13.1	109.7	0.89		(0/4)			
ajoensis C.H. Mull.	Quercus	evergreen[8]	20.1	27.8	0.18	-3.83 (±0.66)	(3/4)			
arizonica Sarg.	Quercus	drought[2,3]	12.3	51.9	0.38	-5.98 (±2.86)	(2/4)	-3.98	(-3.14,-4.87)	4
austrina Small	Quercus	winter[4]	20.3	131.6	0.87	-2.40	(1/4)			
chapmanii Sarg.	Quercus	winter[4]	20.5	119.2	0.77	-1.75	(1/4)			
gambelii Nutt.	Quercus	winter[2,3]	10.5	59.6	0.48	-2.54	(1/4)			
insignis Mart. & Gal.	Quercus	drought[9,1,10]	17.0	149.4	1.19	-3.67 (±1.52)	(2/4)			
lancifolia Schltdl.&Cham.	Quercus	drought[9,1]	17.0	149.4	1.19	-2.00 (±1.04)	(2/4)	-2.72	(-2.23,-3.21)	4
lyrata (Walter) Dippel	Quercus	winter[2]	20.1	116.3	0.76	-2.47 (±0.88)	(4/4)	-3.26	(-1.48,-5.57)	5
margarettae (Ashe) Small	Quercus	winter[4]	20.1	127.3	0.82	-2.82	(1/4)			
michauxii Nutt.	Quercus	winter[2]	20.2	129.0	0.84	-3.14 (±0.85)	(2/4)	-3.69	(-3.03,-4.18)	5
pungens Liebm.	Quercus	winter[2,3, 11]	13.5	45.6	0.31		(0/4)			
rugosa Née	Quercus	evergreen[2,3]	8.9	66.6	0.57	-3.27	(1/4)	-4.09	(-3.69,-4.56)	6
stellata Wang.	Quercus	winter[4]	20.2	121.8	0.78		(0/2)			
geminata Small	Virentes	winter[4,5]	20.2	122.1	0.79	-2.64	(1/2)			
virginiana Miller	Virentes	evergreen[4,5]	20.2	129.2	0.84	-3.43 (±0.36)	(4/4)	-3.85	(-2.6,-5.22)	6

Table 2. Responses measured and abbreviations.

abbrev.	measurement	description
g_s	stomatal conductance, mol m^{-2} s^{-1}	water movement out of the leaf
Ψ_{crit}	stomatal closure, MPa	water potential of leaf at g_s < 5mmol m^{-2} s^{-1}
Ψ_{stem}	stem water potential, MPa	water potential of stem, measured with covered, equilibrated, leaf
leaf loss	leaf abscission, %	percent of individuals within a species showing any leaf wilt or senescence
PAD	percent air discharge, %	stem embolism, or air discharged from stem as a percentage of total air lost
PAD_{12}	air entry point, MPa	Ψ_{stem} at which embolisms begin to form in stem xylem
PAD_{50}	50% stem embolism point, MPa	Ψ_{stem} at which 50% of xylem is embolized
PAD_{88}	total stem embolism point, MPa	Ψ_{stem} of full stem embolism
S_{50}	sensitivity of xylem embolism, PAD MPa^{-1}	slope of xylem vulnerability curve at PAD_{50}
PAD_{12} - PAD_{50}	stem hydraulic safety margin, MPa	slope of change between air entry point and 50% embolism
Ψ_{crit} - PAD_{50}	leaf-stem hydraulic safety margin, MPa	difference of water potential at stomatal closure and 50% stem embolism

Table 3. Linear model summary statistics: stomatal closure, stem vulnerability, and safety margins as responses, climate of origin and leaf habit as predictors. DF = 1,15 (Ψ_{crit} x climate models); 2,14 (Ψ_{crit} x leaf habit); 1,7 (stem vulnerability x climate); 2,6 (stem vulnerability x leaf habit).

		MAT	temperature seasonality	MAP	precipitation seasonality	aridity index	leaf habit
$\ln(\Psi_{crit})$	R^2	0.05	0.00	*0.23*	**0.24**	*0.23*	*0.33*
	P	0.399	0.994	*0.050*	**0.048**	*0.053*	*0.058*
	F	0.76	0.00	*4.53*	**4.65**	*4.42*	*3.50*
PAD_{50}	R^2	0.26	0.41	**0.52**	0.01	**0.57**	0.30
	P	0.161	0.063	**0.029**	0.768	**0.019**	0.338
	F	2.45	4.85	**7.45**	0.09	**9.14**	1.31
PAD_{12}	R^2	0.04	0.05	**0.50**	0.24	**0.61**	0.25
	P	0.620	0.577	**0.033**	0.186	**0.013**	0.421
	F	0.27	0.34	**7.02**	2.15	**10.93**	1.00
PAD_{88}	R^2	0.12	0.32	0.08	0.05	0.08	**0.73**
	P	0.358	0.112	0.473	0.579	0.454	**0.020**
	F	0.97	3.30	0.57	0.34	0.63	**8.06**
S_{50}	R^2	0.24	0.46	0.00	0.25	0.00	0.20
	P	0.184	0.044	0.917	0.168	0.882	0.509
	F	2.18	5.99	0.01	2.36	0.02	0.76
Ψ_{crit} - PAD_{50}	R^2	0.00	0.00	0.19	0.20	0.26	0.02
	P	0.947	0.986	0.245	0.222	0.162	0.945
	F	0.00	0.00	1.61	1.80	2.44	0.06
PAD_{12} - PAD_{50}	R^2	0.02	0.05	0.08	0.22	0.12	0.47
	P	0.703	0.576	0.449	0.200	0.357	0.152
	F	0.16	0.34	0.64	2.00	0.97	2.63

Chapter 2 Figures

Figure 1. Mean maternal plant locations for each species measured. Symbol shapes are oak subgenera (Quercus or white oaks = circles, Lobatae or red oaks = triangles, and Virentes or live oaks = squares). Dark symbols show species for which xylem vulnerability curves were also measured, white symbols were only used for stomatal closure and leaf drought response measurements. Points are randomly dispersed when clustered for easier viewing.

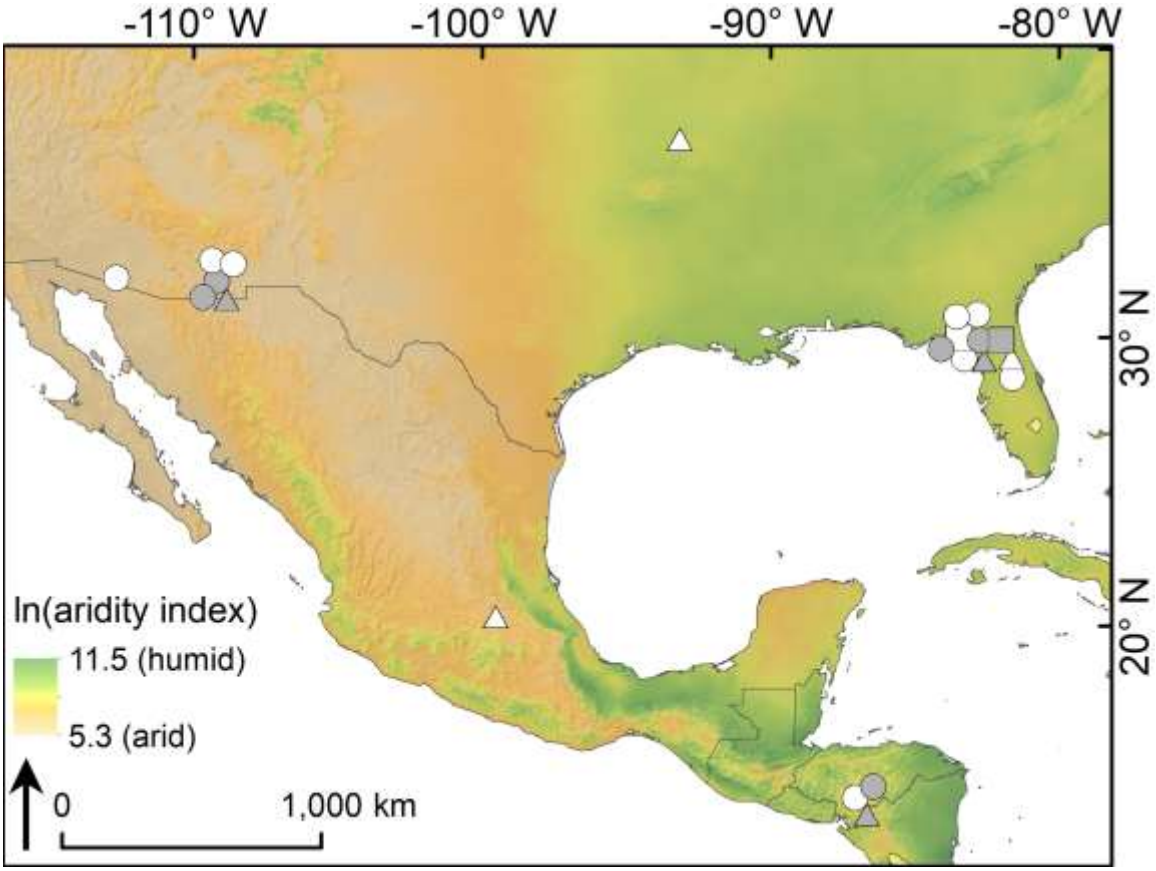

Figure 2. Mean soil water content (VWC), photosynthetic rate (A_{max}), and stomatal conductance (g_s) throughout the dry-down period. Error bars around VWC show standard error of the mean.

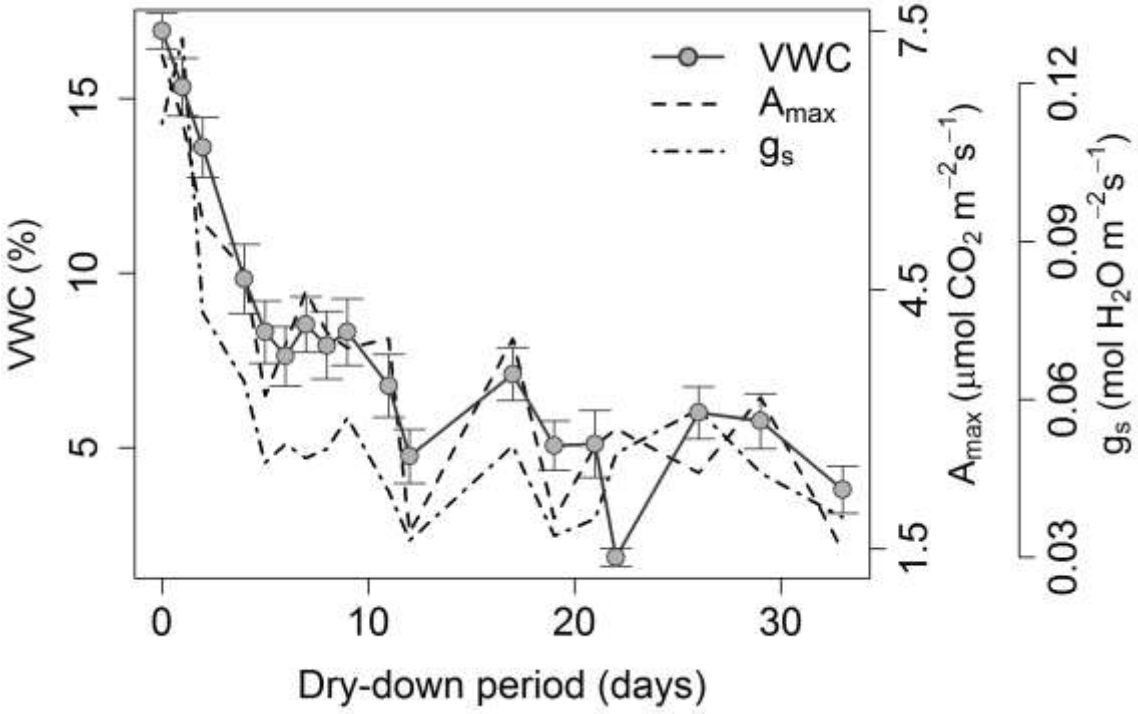

Figure 3. Stomatal closure by climate of origin**.** a**)** Water potential Ψ_{crit} *(*MPa) by aridity index (mean annual precipitation/mean annual evapotranspiration). b**)** Ψ_{crit} by precipitation seasonality (coefficient of variation, mm). Symbols are subgenera (Quercus = circles, Virentes = squares, Lobatae = triangles). Models were fit to natural log of Ψ_{crit}. Shaded areas show 95% confidence interval of model. Bars are standard error of the mean and no bars indicates stomatal closure was observed in only one individual.

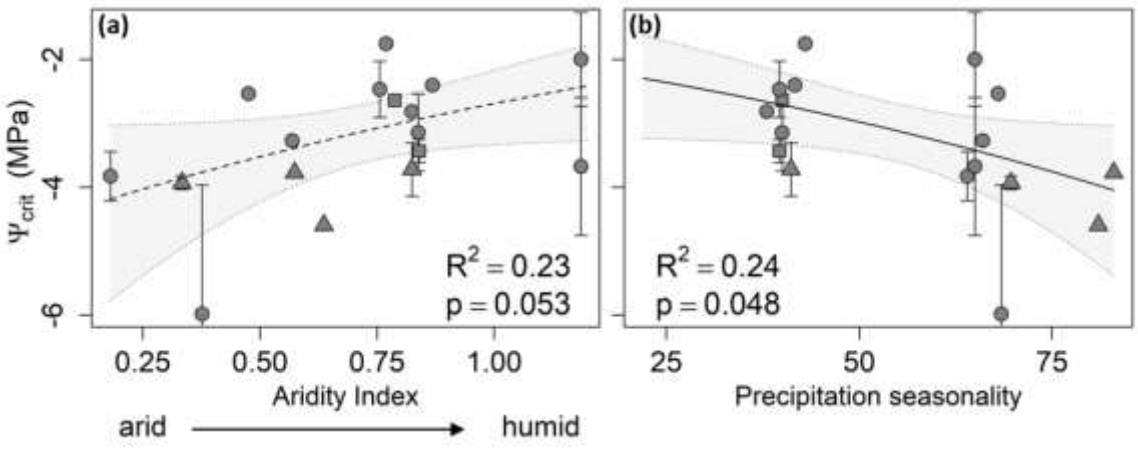

Figure 4. Stem xylem vulnerability, PAD_x (MPa), by mean aridity index of species origin. a) $PAD_{12,}$ Ψ_{stem} at 12% embolism, b) $PAD_{50,}$ Ψ_{stem} at 50% embolism, c) $PAD_{88,}$ Ψ_{stem} at 88% embolism. Shaded areas show 95% confidence interval of models with significant fits. Symbols are subgenera (Quercus = circles, Virentes = squares, Lobatae = triangles). Bars are upper and lower confidence intervals and bars are absent in some individuals where the PAD_{12} or PAD_{88} confidence intervals exceed the data on lower or upper estimation.

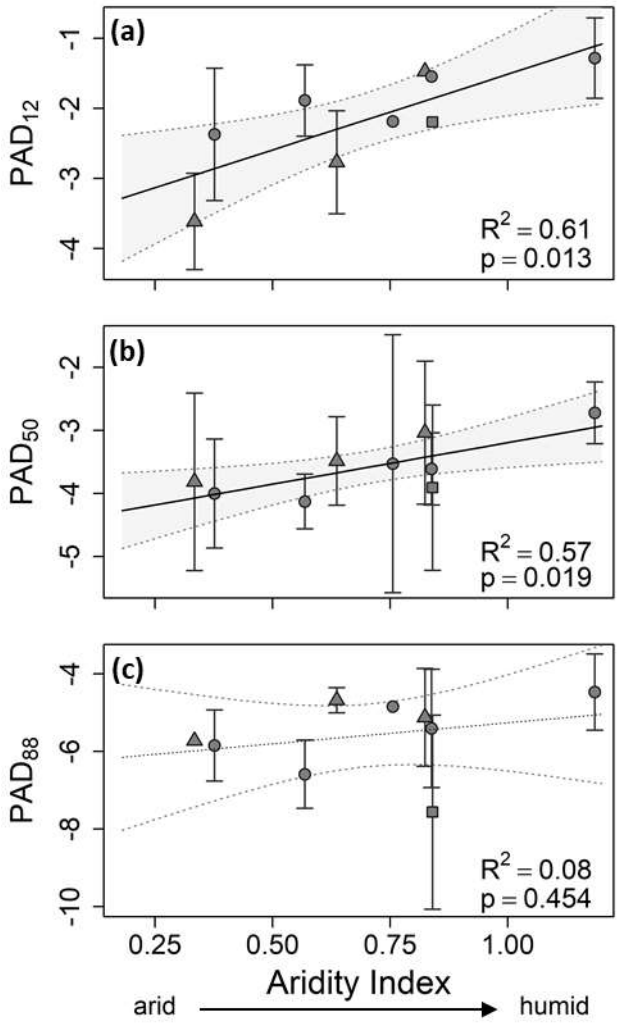

Figure 5. Leaf habits, precipitation seasonality, and stem and leaf vulnerability. a) Precipitation seasonality of origin differences by leaf habit and b) PAD_{88}, or water potential of complete stem embolism, by leaf habit. c) Ψ_{crit} (MPa) by overall species leaf habit and d) by percentage of early cohort leaf loss (oldest leaves) during drought. Bars are standard error of the mean and no bars indicates stomatal closure was observed in only one individual. Symbols are subgenera (Quercus = circles, Virentes = squares, Lobatae = triangles).

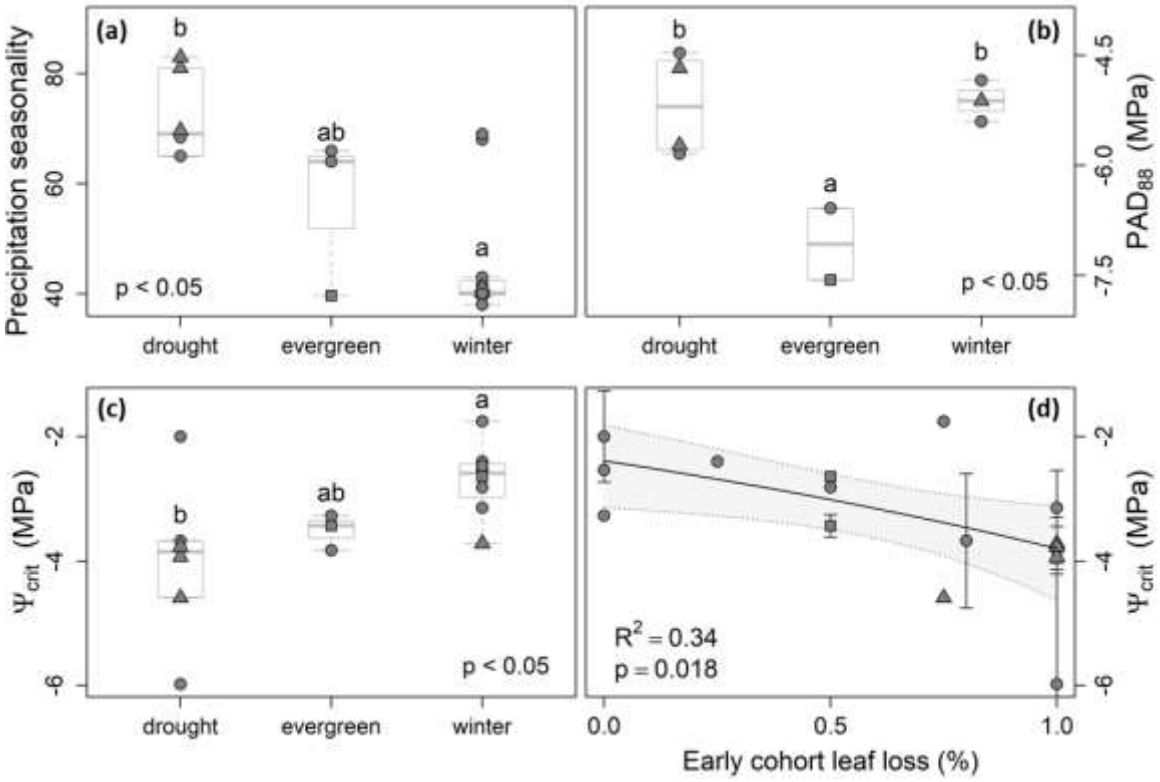

Figure 6. Leaf habit and a) air entry point (PAD_{12}) and b) leaf to stem safety margin. Symbols are subgenera (Quercus = circles, Virentes = squares, Lobatae = triangles).

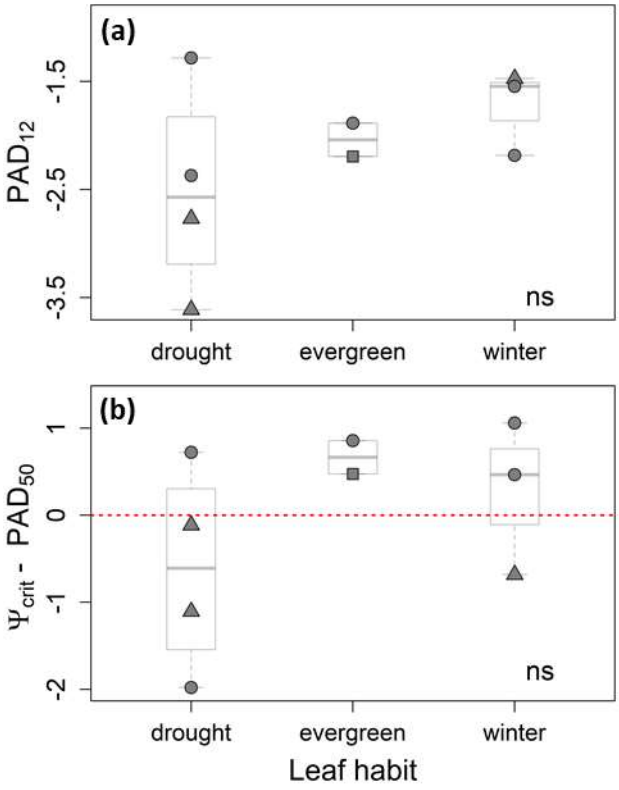

Chapter 3. Leaf phenological responses to cooling determine spectral detection of chlorophyll fluorescence

(This work was done in collaboration with José Eduardo Meireles and Jeannine Cavender-Bares)

Summary

Correctly and rapidly determining plant responses to cold stress can help us understand potential range expansions under global change. We exposed 14 species (N = 69) of American oaks, varying from warm temperate to tropical species, to cooling stress to examine how chlorophyll fluorescent responses (F_v/F_m and Φ_{PSII}), and derived chlorophyll fluorescent measures, differ among plants from different climates, subgenera, and winter leaf habits. We then tested whether leaf chlorophyll fluorescent responses (measured on dark- and light-adapted material) could be predicted from hyperspectral measurements on light-adapted leaves of the same individuals. We found that responses to initial cooling (from 22^{o}C to 8^{o}C) were similar among oak species, but that changes in dark-adapted Fv/Fm, photosynthetic yield (Φ_{PSII}), and electron transport rate during cold acclimation were best explained by with leaf loss propensity rather than by climate of origin or subgenus. We successfully modeled Fv/Fm and Φ_{PSII} from single hyperspectral reflectance measurements taken on plants on the same day as fluorescence measurements, but we were not able to predict responses as well from models created during other periods of the experiment. Predictive ability of spectral models increased when greater variation in fluorescent responses among the measured leaves was encompassed by the data. We could also successfully predict overall rates of change in Fv/Fm and Φ_{PSII}, but

not but the models of best fit were constructed from measurements made after the imposition of cooling stress.

Introduction

Responses to cold are important factors in determining tree range extents (MacArthur 1972, Osmond et al. 1987, Friedman et al. 2008, Koehler et al. 2012, Kreyling et al. 2014) and yet woody plants from different climates may be able to tolerate cold in similar ways (Sakai 1970, Fallon, unpublished). Plants from the same climate may resist cold using different strategies leading to different responses and cold resistances (Cavender-Bares et al. 1999). Understanding how and why stress responses to cold differ among plants is important for predicting range expansions and contractions that are likely under climate change (Parmesan and Yohe 2003, Crozier 2003). Common leaf stress response measurements of chlorophyll fluorescence require multiple measurements of light- and dark- adapted tissues (Cavender-Bares and Bazzaz 2004). Using single hyperspectral measurements to successfully model these fluorescent responses will speed assessment of plant stress responses and evaluations of plant performance in changing environments (Peñuelas and Filella 1998).

Plant cold tolerance, photosynthesis, and chlorophyll fluorescence

The long-lived tissues of woody species exposed to cooler temperatures must have some form of cold resistance in their leaves to survive (Levitt 1980, Lichtenthaler 1996). Immediate responses to cooling are usually a depression of photosynthetic function,

although plants may successfully acclimate to new lower temperatures over time (Berry and Bjorkman 1980, Huner et al. 1993). Metabolic restraints on photosynthetic processes at low temperatures may make plants more vulnerable to light damage (photoinhibition) and thus damage to the photosynthetic apparatus of the initial photosynthetic reaction centers, PSII (Berry and Bjorkman 1980, Cavender-Bares et al. 1999). Cooling may also result in changes to the lipid membranes of the chloroplasts in which photosynthesis takes place, providing a physical obstacle to efficient photosynthetic function (Berry and Bjorkman 1980). To cope with cold stresses plants may undergo winter senescence, have a semi-deciduous leaf habit (often deciduous after damage), or have evergreen leaves that are either able to function well at colder temperatures or which become functionally dormant. Evergreen species may adjust xanthophyll compounds in their leaves to reduce stress to PSII and increase non-photochemical quenching to reduce damage by photoinhibition, while deciduous species may experience more damage and be less able to recover from cold stress (Adams III and Demmig-Adams 1995, Verhoeven et al. 1996, Cavender-Bares et al. 1999, 2005).

Photosynthetic function, and thus plant response to cold stress, can be measured through two different measurements of chlorophyll fluorescence. Plants use light-harvesting complexes of chlorophyll within the chloroplasts to capture photons and move received light energy. The light-harvesting complexes of photosystems can deal with the high energy inputs in four ways: photochemistry, fluorescence, non-photochemical quenching, and decay (Muller 2001). Letting energy passively decline through electron decay can result in oxidative damage, so other pathways of handling the high energy inputs may be

prioritized in excess light or stressful conditions (Muller 2001). Fluorescence releases excess energy though the excitation of an electron in the form of red and far-red light. Chlorophyll is constantly fluorescing, though the amount of fluorescence increases in stressed or photo-damaged leaves (Bolhar-Nordenkampf et al. 1989). The ratio of minimum (basal or steady state) and maximal fluorescence provides measures of photosynthetic efficiency and photosynthetic yield (Cavender-Bares and Bazzaz 2004). Non-photochemical quenching (NPQ), or the amount of energy that must be dissipated through, primarily, heat, can be calculated from the dark and light adapted measurements, while electron transport rate (ETR), or electron movement from PSII, is a function of the light applied and photosynthetic yield (Maxwell and Johnson 2000, Cavender-Bares and Bazzaz 2004, Kalaji et al. 2014). In practice, these measurements are made on the same plants at pre-dawn or on artificially dark-adapted tissues (for quantum efficiency measurements and calculation of NPQ) and in light adapted tissues (realized yield, ETR, and calculation of NPQ). Collecting both measurements requires either separation in space (some individuals kept in dark conditions) or time (measurements collected in the dark, often before dawn) of tissues.

Leaf level spectral detection

The profile of light reflected from a leaf is an integrated measure of aspects of plant morphology, physiology and chemistry (Peñuelas and Filella 1998). Leaf level spectra have been used to detect changes in leaf function following chlorophyll content transitions (Gitelson and Merzlyak 1998, Gitelson et al. 2001). Hyperspectral reflectance, or high resolution reflectance across a broad range of wavelengths, can be a highly useful

tool in detecting multiple leaf properties from a single measurement and detecting between species differences (Cavender-Bares et al. 2017). Leaf hyperspectral reflectance measurements have been successfully used to determine the leaf water potentials of oak leaves (Cotrozzi et al. 2017), to predict gas exchange responses at different temperatures (Serbin et al. 2012), and to differentiate oak populations and predict functional traits (Cavender-Bares et al. 2016). Using hyperspectral reflectance, especially using remote sensing technology, to predict chlorophyll fluorescence, and thus plant stress, is a continuously developing field of study and some simple indices have been created to model fluorescence, yet these models cannot directly predict yield or potential photosynthetic efficiency (Gamon et al. 1990, 1997, Zarco-Tejada et al. 2001, 2013, Dobrowski et al. 2005, Grace et al. 2007, Meroni et al. 2009). Correctly predicting chlorophyll fluorescent responses (measured in dark and light adapted leaves) throughout the imposition of stress from a single spectral measurement would allow insight into multiple aspects of plant physiological resistance to cold while avoiding the multiple measurements required for accurate measures of chlorophyll fluorescence.

We use a system of diverse oaks (*Quercus* L.), from three subgenera, to investigate leaf chlorophyll fluorescence cold responses and whether leaf hyperspectral reflectance can accurately predict these responses. Oaks are a globally distributed woody genus that is highly diverse within North America (Nixon 2006). The species occupies a broad range of environments and occupies latitudes from 50^{o}N to the tropics (Axelrod 1983). Oak species diversity is greatest in warm temperate to subtropical locations, despite the species origins being boreal (Hipp et al. 2017). Oaks also exhibit a range of leaf

phenological responses to cold, from winter deciduous, evergreen and brevideciduous responses (Nixon 1997, Cavender-Bares and Holbrook 2001, Cavender-Bares et al. 2004b). Species leaf responses to cooling may be a consequence of 1) evolutionary history, 2) climate, and 3) seasonal leaf habits. Similar cooling tolerances may be achieved through different physiological strategies. We ask, 1) do a) clades (oak subgenera), b) climate, or c) deciduousness best predict cooling responses? 2) Can photosynthetic responses to cooling (measured by chlorophyll fluorescence) among a diverse set of oaks be predicted from leaf reflectance spectra?

Methods

We grew *Quercus* saplings of 14 species representing three subgenera (*Quercus* (white), *Virentes* (live), *Lobatae* (red)) from acorns collected (October - December 2013) from wild populations in native ranges (Fig. 1, Table 1). We stored acorns at 4^{o}C until planting in University of Minnesota greenhouse facilities in February 2014. We planted acorns in a 1:1 mix of sand:potting soil, kept seedlings at constant temperature after planting and later transplanted year-old seedlings to tree pots (TP616, Steuwe and Sons, Oregon USA) in 2015. Seedlings were regularly treated with a water-soluble acidic fertilizer (Peters Professional 21-7-7 Acid Special, Everris NA Inc., Dublin, Ohio USA).

We subjected 1.5 year old seedlings to cooling treatments in November and December of 2015. We lowered temperatures in stages from 22^{o}C to 18, 14, 10, and 8^{o}C over the course of eleven days, measuring plant responses at each temperature (Fig. 2). We then

held plants at 8^{o}C for 26 days, measuring the plants repeatedly (three fluorescence measurements and two hyperspectral reflectance measurements) during the acclimation period. We used growth lamps to maintain a 12 hour photoperiod prior to and during the experiment. We monitored leaf loss over the course of the experiment by counting leaves in pots at the end of the acclimation period and calculating percent loss from abscised leaves as a percentage of total leaves at the start of the experiment.

At all cooling and acclimation stages we measured the leaf level responses on the adaxial surface of mature, undamaged, upper-canopy leaves of healthy individuals (Table 1, Fig. 2, total N = 69). Tree pots were thoroughly watered the evening before any data collection. We measured chlorophyll fluorescence with an FMS2 Field Portable Pulse Modulated Chlorophyll Fluorometer (Hansatech, King's Lynn, UK). Chlorophyll fluorescence in dark adapted leaves (F_v/F_m) provides a measure of the potential quantum efficiency of PSII and is a general indication of plant health (Cavender-Bares and Bazzaz 2004). Chlorophyll fluorescence measured in a light adapted leaf provides a measure of realized photosynthetic yield (Φ_{PSII}) in a plant, which may also be experiencing non-photochemical quenching, thermal energy dissipation of excess absorbed light (Cavender-Bares and Bazzaz 2004). Additionally, we can calculate non-photochemical quenching (NPQ) and electron transport rates (ETR) from the dark- and light-adapted fluorescence measurements. We measured leaf-level hyperspectral reflectance (350 - 2500nm) using an SVC HR1024i spectroradiometer and reflectance probe (SpectraVista Corporation, Poughkeepsie, NY, USA) on three sections of a single leaf blade. We selected single leaves of each individual for measurement for either chlorophyll

fluorescence or hyperspectral reflectance and repeated measurements on the same leaves throughout the experiment. We measured F_v/F_m on plants before dawn light exposure and all other measurements between 8:30 and 11am.

Analyses

We performed all analyses in R version 3.4.1 (R Core Team 2016). We removed spectra with low reflectance (< 0.3) in the near infrared and resampled the spectra at each nanometer from 400 -2400nm (package *spectrolab*, Meireles et al. 2017). We averaged leaf level spectra for each individual at each measurement time point to obtain a single mean spectrum. We created three subsets of the measured spectra: full (400-2400nm), reduced to visible (400-700nm), and surrounding the peak of chlorophyll fluorescence of photosystem II (640-800nm, peak at 683nm Pedrós et al. 2008) (Fig. 3). We then fit models between each spectrum and the physiological measurements made at the same time point using jack-knifed, cross-validated, partial least squares regression (PLSR, package *pls*, Mevik, Wehrens, & Liland, 2016). PLSR analysis is a standard approach in hyperspectral data analysis, as it reduces the many correlated values of spectra into uncorrelated predictive variables (Wold et al. 1984, Serbin et al. 2012, Cotrozzi et al. 2017). We selected a minimum of three model components and then added subsequent model components that minimized the prediction residual sum of squares (PRESS) to reduce the likelihood of overfitting the models (Chen et al. 2004, Cotrozzi et al. 2017). We evaluated model fit by magnitude of effect size (R^2) between predicted and measured variables. We analyzed effect of different experimental times and spectral regions in type III ANOVA (package *car* Fox and Weisberg 2011) and tested for differences in effect

size between experimental times with post-hoc Tukey tests. We additionally tested for the predictive quality of spectral PLSR between measurement periods by testing the predictive power of models constructed from data at different experimental times (non-contemporary measures). Finally we fit a model of all hyperspectral reflectance (full spectra) measures with data from all experimental times.

We calculated rates of change of each fluorescent measurement in simple linear models (response ~ time) for each individual and each species in three time periods: over the whole experiment (total), during the cooling period, and during the acclimation period at 8^{o}C (Fig. 2). We used species-level rates of change to evaluate effects of climate of origin (minimum temperature of coldest period, Hijmans, Cameron, Parra, Jones, & Jarvis, 2005), leaf phenology (percent leaf loss during the experiment), and clade (oak subgenus) in additive linear models and found the effects of each predictor using a type III ANOVA (package *car*, Fox & Weisberg, 2011). We fit PLSR models of full spectra to rates of change per individual and evaluated model fit at each experimental time.

Results

Differences in photosynthetic function during acclimation due to differences in leaf loss

We observed declines in all fluorescence measures during the cooling period (Fig. 4, Table 2), with most measurements then stabilizing at slightly depressed levels. The mean rates of decline in all fluorescent measurements were greatest during the cooling period, and were significantly lower or near zero during the acclimation period (Table 2).

Overall declines were observed during the whole experiment, but the mean rates of total decline were less than the initial cooling suggesting some degree of acclimation to the cold.

Percent leaf loss was a significant predictor of rates of photosynthetic change during the experiment and more important than clade or climate of origin (Table 2). Neither mean minimum temperature of climate of origin nor percent leaf loss were significantly different among subgenera (post-hoc Tukey test, $\alpha = 0.05$). Minimum temperature and percent leaf loss were correlated with marginal significance and weak effect ($R^2 = 0.27$, $p = 0.057$, $F_{1,12} = 4.42$). We observed greater rates of decline in Fv/Fm during cooling, acclimation, and in the overall experiment in species that showed higher percentages of temperature-associated leaf loss. We also found that the minimum temperature of the coldest month was a significant predictor of declines during cooling in Fv/Fm. Percent leaf loss was also a significant predictor of rates of change in realized fluorescent yield and electron transport rate (ETR) during the acclimation period. Species showing greater leaf loss had greater rates of decline in yield and ETR (Table 2). Non-photosynthetic quenching (NPQ) was not significantly predicted by clade, climate of origin, or leaf loss. Subgenus was marginally significant ($P < 0.1$) in explaining some differences between red and white oaks in Fv/Fm responses during cooling (less negative rates of change in white oaks than red), and realized yield and ETR (more negative declines in white oaks). Mean minimum temperature of origin was a marginally significant predictor of rates of change in ETR, and NPQ. Species from warmer climates experienced greater declines in ETR during cooling and less overall change in NPQ during the same period. During

acclimation, climate of origin had a different effect: species from warmer climates experienced greater declines in NPQ and less negative declines in ETR (Table 2).

Spectral model fit changes in experimental time

Experimental time (date of measurement) was more often a significant factor in accurate model fitting than spectral region used to make the model. The experimental period after some degree of cooling, but not the final measurement, generated the best predictive models for all responses (Fig. 5). Spectral region used to create the model was only a significant factor in predicting differences in ETR models fits, however full spectra and fluorescent spectra generated the best models overall, though neither was consistently better than the other (Table 3, Fig.5). Models generated from different spectral regions had similar predicted by observed relationships (slopes and intercepts, Table 3). Model coefficients were consistently the largest in the visible, fluorescent, and near infrared regions (Fig. 6.i). Models from different experimental times and temperatures had the greatest variance in the visible and fluorescent regions for Fv/Fm and ETR, while NPQ and Φ_{PSII} models also had large variance in coefficients in the water balance (near infrared and shortwave infrared) and far SWIR (> 1900nm) regions of the spectra (Fig. 6.e-h).

Contemporary measures of spectra and fluorescence construct best models

All fluorescent measurements could be predicted from spectral measurements taken during the same experimental period, although the best fits (R^2 > 0.75) were only found

in quantum efficiency and yield measurements (Fv/Fm and Φ_{PSII}) of the acclimation periods at 8^{o}C (Fig. 7). These better model predictions coincided with increased coefficient of variation in the response values (Fig. 5). NPQ was not strongly predicted from spectra (maximum $R^2 = 0.6$) and PLSR models of ETR had high adjusted error rates (adjusted coefficients of variation in the moel) (Fig. 7).

Fluorescent responses were not well-predicted by models fit to responses at different experimental times, with the exception of rare cases (Fig. 8). All simultaneous models were stronger (higher R^2) with the exception of Fv/Fm at 22^{o}C, which could be predicted with a similar fit from a model created at 14^{o}C (simultaneous $R^2 = 0.37$, P = 0; non-contemporary model $R^2 = 0.44$, P = 0), and NPQ. NPQ had poor model fits from full spectra at 14^{o}C ($R^2 = 0.06$, P = 0.056) and final 8^{o}C acclimation ($R^2 = 0.12$, P = 0.003), but could be only marginally better predicted by non-contemporary full spectral models made at initial 8^{o}C ($R^2 = 0.1$, P = 0.011) and the middle acclimation step at 8^{o}C ($R^2 = 0.15$, P = 0.001), respectively. Models fit to data and spectra from the whole experiment predicted Fv/Fm and Φ_{PSII}, significantly and with strong effect, while models of ETR and NPQ were poorer predictors (Table 4).

Rates of response to cooling can be predicted from non-simultaneous measures

Individual rates of change in fluorescent measurements of realized (Φ_{PSII}) and maximum (Fv/Fm) photosynthetic yield could be well predicted ($R^2 > 0.5$) by full spectral models, but ETR and NPQ could not (Table 5). Fv/Fm changes during acclimation and total

changes were best predicted by spectral models fit from spectra collected after plants were exposed to 8°C and during acclimation ($R^2 > 0.85$ for all). Fv/Fm individual rates of change during acclimation and total change during the experiment were best predicted by models made at the end of the experiment ($R^2 = 0.97$, P = 0, PLSR adj CV = 0.002; and $R^2 = 0.99$, P = 0, PLSR adj CV = 0.001, respectively, Fig. 9). The models of best fit for F_v/F_m and Φ_{PSII} rates of acclimation included larger model coefficients in the NIR and SWIR1 regions (800 – 1400nm) than were observed in predictions of simple fluorescent measurements, as well as larger coefficients in the peak chlorophyll and fluorescent reflectance regions. Fv/Fm cooling response rates could be marginally well predicted by spectral measurements made at 14°C, in the middle of cooling ($R^2 = 0.55$, P = 0, PLSR adj CV = 0.001). Rates of change in Φ_{PSII} during acclimation and the total experiment were best predicted by measurements taken as the greenhouse temperature reach 8°C ($R^2 = 0.87$, P = 0, PLSR adj CV = 0.003; and $R^2 = 0.81$, P = 0, PLSR adj CV = 0.002, respectively, Fig. 9). Rates of change in Φ_{PSII} during cooling were very poorly predicted ($R^2 < 0.16$) as were all rates of change in NPQ and ETR.

Discussion

Our research shows that oak species have common responses to initial cooling, but that they acclimate in different ways (Fig. 4), primarily influenced by winter deciduous habits rather than climate of origin or oak subgenus (Table 2). Importantly, we can predict fluorescent responses, especially Fv/Fm (a pre-dawn, dark-adapted measurement) and Φ_{PSII}, from leaf level hyperspectral reflectance measured at a similar time, but not simultaneously, using full spectra or a fluorescent region subset (Table 3). We can predict

the responses best when plants are exposed to a cooling stress for a longer period of time, increasing variation in response (Fig. 5, 7). And while we cannot predict fluorescent responses as well from spectral models constructed at different experimental times (Fig. 8), we can predict rates of acclimation in fluorescent response from measurements made at single time points (Fig. 9). This will allow us to predict species overall responses to cooling before a prolonged acclimation period.

Differences in photosynthetic function during acclimation due to differences in leaf loss

Chlorophyll fluorescence and photosynthetic function showed common evidence of decline in all measurements. Only in the cooling response rates of quantum efficiency (F_v/F_m, a measure of photosynthetic function and plant stress) was minimum temperature of origin a significant factor, where rates of decline were greater in plants of warmer temperatures (although electron transport rate showed a similar, marginally significant effect in cooling response). This lack of association was surprising because our experiment includes oaks from tropical climate and because temperature of origin should predict photosynthetic function (Berry and Bjorkman 1980, Huner et al. 1993). However, an initial cooling shock response is expected among cold-tolerant plants before any acclimation which may explain the lack of effect of minimum temperature of origin and the general lack of effect of leaf habit, with the exception of F_v/F_m, on predicting cooling responses (Huner et al. 1993).

Percent leaf loss, an immediate measure of leaf habit, was a significant predictor in rates of response during acclimation. Quantum efficiency response rates were negatively associated with percent leaf loss while realized photosynthetic yield (Φ_{PSII}) and ETR were positively associated with leaf loss. Even as stress may increase during prolonged cooling (declines in F_v/F_m), increases in yield and electron transport rates have been observed in cold-hardy plants--even among senescing leaves—as evidence of acclimation or beginning processes of senescence (Adams et al. 1990, Huner et al. 1993). Non-photochemical quenching was the single measure where response rates were not well predicted by clade, minimum temperature, or leaf habit. NPQ has been found to increase in cold-hardy evergreens like pines and winter grasses during acclimation (Savitch et al. 2002, Rapacz et al. 2004), and we did observe less-negative declines in plants from cooler climates during acclimation. However, NPQ and photochemical quenching strategies can differ among plants and may be additionally variable among the oaks, wherein similar NPQ values can be the result of different non-photochemical quenching pathways (Cavender-Bares et al. 1999, Savitch et al. 2002). In our case, increased yield and ETR during acclimation among winter deciduous species may signal an increase in photosynthetic productivity as these plants prepare for the controlled process of leaf senescence, while hardier evergreen and brevideciduous species adjust or experience lower photosynthetic rates in the cooler period.

None of the tropical species in our experiment experienced high leaf loss, and all showed evidence of acclimation. All of the tropical species are montane oaks and may experience some degree of cooling in native ranges, though the minimum temperature for most is

greater than 8^{o}C. Tropical species of live oaks have been found to be freezing-intolerant (Koehler et al. 2012), but perhaps simple chilling rather than freezing among the tropical oaks of the red and white subgenera is not enough to induce significant stress.

Quantum efficiency and yield are better predicted from spectra than NPQ and ETR

Quantum efficiency and yield were the best-predicted fluorescent responses at all experimental times from spectral models. This is perhaps unsurprising as both are measures that are directly collected from chlorophyll fluorescence data, though each requires an initial, steady state, or background fluorescence measurement, followed by a high light exposure maximal fluorescence measurement (Cavender-Bares and Bazzaz 2004, Kalaji et al. 2014). However, in collecting hyperspectral measurements, we have only a measure of light-exposed tissue at a single standard illumination without prolonged dark exposure to allow recovery of PSII and electron transporters, so the spectral measurements provide some estimate of reflectance correlated with compounds that affect chlorophyll fluorescence. The primary regions of important coefficients in the models for yield and quantum efficiency were in the visible and near-infrared regions, with most models including the fluorescent region (Fig. 6). These coefficients include wavelengths corresponding to carotenoids, important in photoprotection, in models of quantum efficiency; xanthophylls, important in stress response and photoprotection and found to be correlated to cold response in evergreen leaves, in both yield and quantum efficiency models; chlorophyll content; and direct measures of fluorescence (Gamon et al. 1990, 1997, Verhoeven et al. 1996, Peñuelas and Filella 1998, Sims and Gamon 2002, Dobrowski et al. 2005, Sun et al. 2008). Some spectral models of yield also have higher

coefficients related to water balance. Yield and ETR have been found to be sensitive to water stress, as might occur in some leaves nearing senescence (Peñuelas and Filella 1998, Cavender-Bares and Bazzaz 2004, Sun et al. 2008, Thenkabail et al. 2011). Perhaps because most of the spectral models have the highest model coefficients in the visible and near infrared range there were few differences in model performance between those that used full spectra as variables and those that used only visible or fluorescent subsets.

The models of yield and quantum efficiency, while not direct measurements of dark- and light-adapted chlorophyll fluorescence ratios, may be more direct proxies than ETR and NPQ, both of which are calculated from fluorescent measurements. ETR coefficients were primarily related to chlorophyll content and fluorescence wavelengths. Realized yield, and therefore electron transport rates, increase non-linearly with chlorophyll content (Adams et al. 1990). Models of NPQ, while not highly predictive in our work, do include more carotenoids that may be associated with increased photoprotection and also more consistently include areas of longer wavelength short-wave infrared. Surprisingly NPQ model coefficients did not emphasize xanthophyll pigment reflectances which have been found to be correlated with NPQ in cold stressed evergreens (Verhoeven et al. 1996).

Predictive ability of spectral models differs by experimental time and response variance

Our spectral models were able to robustly predict quantum efficiency (F_v/F_m) and realized yield, however the model fits were better after cold exposure and some acclimation (Fig. 5, Fig. 7). This better fit coincides with higher coefficients of variation among the fluorescent measurements. As eventual leaf loss drives this variation among our species, the model fit increases as leaf responses, due to different leaf habits, change with the onset of winter senescence or cold acclimation. Additionally, spectral models fit to measurements at different experimental times did not perform as well as models made from same day (and same temperature) measurements. This experimental time sensitivity may limit the application in predicting quantum yield and efficiency. However, strong spectral models have been fit to photosynthetic performance among plants experiencing a range of temperatures and to water potential of oak leaves under different watering treatments (Serbin et al. 2012, Cotrozzi et al. 2017), so constructing models from highly variable data may result in better models. Our predictive ability from all data was again the best in modeling quantum efficiency and yield (Table 4), although both could be better predicted by models of specific experimental times (Table 3). The larger models may have strong fits because of the increased variability in response in the full data set, but lose some predictive power because that variability is due to different stress responses over time. Models more robust to time might be constructed from controlled experiments on plants of the same age experiencing different stresses.

Rates of response to cooling can be predicted from non-contemporary measures

While non-contemporary models were not strong predictors of fluorescent responses, rates of quantum efficiency and yield could be modeled from single spectral

measurement periods. Both could be robustly predicted from measurements at initial cooling to 8^{o}C and changes in F_v/F_m could be predicted by all cold acclimation measures. Importantly, we could predict rates of overall change from measurements made before imposing the stress. However, the predictive ability of these measurements was not as strong ($0.58 < R^2 < 0.76$). The coefficients of these models included more high values in the 800-1400nm range, which includes areas of the spectra that best model leaf and cell structure (Govender et al. 2007). As the rates of decline are primarily predicted by leaf habit and leaf habit is directly linked to structure, the rate models are including variable components that represent leaf habit rather than simply photosynthetic function spectra.

Conclusions

We find that hyperspectral reflectance measurements taken on light-exposed leaves can accurately model dark-adapted quantum efficiency and light-adapted realized photosynthetic yield measurements. But we include the caveat that, even among plants of varied evolutionary history, leaf morphology, and leaf habit, the models are more accurate when made on individuals with higher variance in responses. In our study this variance was due to differences in cold-induced leaf phenology and resulting differences in physiological responses.

Acknowledgements

Funding for the project was provided by the National Science Foundation (DEB-1146380 JCB PI). Andrew Latimer and Melis Akman contributed to discussions on the selection of

species for sampling. We thank Anna Schweiger, Shan Kothari, and Vinicius Marcilio-Silva for help with data collection.

Chapter 3 Tables

Table 1. Oak species used in this experiment. Mean latitude and longitude and mean minimum temperatures are of maternal origin of plants. Percent leaf loss shows actual observed leaf loss by the conclusion of the experiment (± 1 standard deviation). Overall species leaf habits (if deciduous, season of leaf loss) are derived from literature: [1]Muller 1954, [2]Nixon 1997, [3]Fallon, unpublished, [4]Aguilar-Romero et al. 2017, [5]Garcia Moscoso 1998, [6]Cavender-Bares et al. 2004b, [7]Cavender-Bares 2000, [8]Muller 1942b, [9]Williams-Linera 1997, [10]Muller 1942a, [11]Romero Rangel et al. 2002

species	section	n	latitude	longitude	min. temperature (C)	% leaf loss	leaf habit
ajoensis C.H. Mull.	Quercus	5	32.07	-112.71	4.3	1.2 (± 1.6)	evergreen[1]
arizonica Sarg.	Quercus	5	31.96	-109.23	-4.2	0.2 (± 0.5)	drought[2,3]
castanea Née	Lobatae	5	16.96	-92.76	10.9	0.3 (± 0.6)	evergreen[4]
elliptica Née	Lobatae	5	13.94	-87.01	14.3	0.6 (± 1.4)	drought[5]
emoryi Torr.	Lobatae	5	31.89	-109.19	-4.0	0.4 (± 0.8)	drought[2,3]
gambelii Nutt.	Quercus	5	31.93	-109.27	-4.8	77.9 (± 15.3)	winter[2,3]
hemisphaerica Bartram ex Willd	Lobatae	5	29.78	-82.63	5.1	0.3 (± 0.6)	winter[6,7]
insignis Mart. & Gal.	Quercus	5	14.03	-87.07	9.8	9.3 (± 9)	drought[5,8,9]
lancifolia Schltdl. & Cham.	Quercus	4	14.03	-87.07	9.8	0.0 (± 0)	drought[5,8]
mexicana Bonpl.	Lobatae	5	20.31	-99.55	3.7	0.0 (± 0)	drought[10,11]
michauxii Nutt.	Quercus	5	29.90	-82.73	4.8	12.0 (± 8.1)	winter[2]
rugosa Née	Quercus	5	31.91	-109.27	-5.8	1.4 (± 3.1)	evergreen[2,3]
velutina Lam.	Lobatae	5	36.88	-93.16	-6.9	87.1 (± 7.1)	winter[2]
virginiana Miller	Virentes	5	29.90	-82.64	4.9	0.2 (± 0.2)	evergreen[6,7]

Table 2. Mean rates of change during experimental periods across all species and effects of subgenus, coldest mean temperature at climate of origin, and percent of leaf loss observed during the experiment. Fv/Fm = maximum potential photosynthetic yield, Φ_{PSII} = realized photosynthetic yield, ETR = electron transport rate, and NPQ = non-photosynthetic quenching. Significance of terms is indicated by * ($P < 0.05$) or ɨ ($P < 0.1$).

						intercept and section effects			slope	
variable	period	mean	SD	R^2	$F_{4,9}$	intercept (Lobatae)	Quercus	Virentes	Min. temp	% leaf loss
Fv/Fm	cool	-0.002	(±0.001)	0.61	3.55	-0.002	*0.001ɨ*	0.000	**-8.82E-06***	**-0.002***
	acclim	-0.001	(±0.004)	0.71	5.39	-0.001	0.002	0.001	-9.68E-06	**-0.012***
	total	-0.001	(±0.003)	0.70	5.27	-0.001	0.002	0.001	-6.82E-06	**-0.008***
Φ_{PSII}	cool	-0.009	(±0.002)	0.53	2.49	-0.010	0.001	-0.002	1.42E-05	*0.005ɨ*
	acclim	-0.002	(±0.003)	0.66	4.29	-0.003	*-0.002ɨ*	-0.002	1.64E-05	**0.009***
	total	-0.004	(±0.002)	0.69	4.97	-0.006	-0.001	-0.001	*1.83E-05ɨ*	**0.008***
ETR	cool	-0.300	(±0.317)	0.37	1.35	-0.104	-0.092	0.108	*-3.59E-03ɨ*	-0.350
	acclim	-0.129	(±0.088)	0.54	2.69	-0.141	*-0.074ɨ*	-0.086	*7.88E-04ɨ*	**0.223***
	total	-0.183	(±0.074)	0.31	1.03	-0.169	-0.042	-0.017	-1.64E-04	0.096
NPQ	cool	-0.022	(±0.013)	0.48	2.08	-0.034	0.010	0.015	*1.42E-04ɨ*	0.013
	acclim	-0.013	(±0.009)	0.52	2.40	-0.008	-0.004	-0.001	*-9.17E-05ɨ*	0.001
	total	-0.014	(±0.004)	0.04	0.09	-0.013	0.001	-0.002	-8.50E-06	-0.001

Table 3. PLSR model results of spectra and contemporary fluorescence measurements during the cooling period, models fit from different spectral regions are shown in column sections. T = temperature setting and c/a indicate cooling or acclimation period. We fit models using the number of components (com) shown, resulting in the adjusted coefficient of variation (CV) and prediction residual error sum of squares (PRESS) values. R^2 (R^2 values greater than 0.5 in **bold**) and *F* statistics show fit of predicted to observed values for each model. Predicted by observed model significance are shown as P < 0.1 (ɪ), P < 0.05 (*), P < 0.01 (**), P < 0.001 (***).

				visible 400-700nm					fluorescent 640-800nm					full 400-2400nm				
resp	T	n	com	CV	PRESS	**R2**		F	com	CV	PRESS	**R2**		com	CV	PRESS	**R2**	
Fv/Fm	c	22	67	6	0.014	0.01	0.45***	52.4	4	0.014	0.01	0.30***	27.5	4	0.014	0.01	0.37***	38.5
	c	14	66	8	0.011	0.01	**0.62*****	105.8	7	0.012	0.01	**0.52*****	70.4	8	0.011	0.01	**0.66*****	125.0
	c	8	68	3	0.018	0.02	**0.54*****	78.8	5	0.017	0.02	**0.58*****	92.9	5	0.018	0.02	**0.58*****	90.3
	a	8	69	5	0.030	0.04	**0.95*****	1246.0	8	0.021	0.03	**0.95*****	1197.0	5	0.023	0.04	**0.93*****	946.2
	a	8	67	3	0.063	0.25	**0.75*****	198.9	7	0.044	0.13	**0.92*****	705.1	11	0.033	0.06	**0.94*****	993.6
Φ_{PSII}	c	22	67	5	0.099	0.64	0.31***	28.6	7	0.101	0.68	0.33***	32.5	4	0.096	0.61	0.35***	35.3
	c	14	66	5	0.044	0.12	**0.51*****	66.7	7	0.047	0.14	**0.56*****	82.8	3	0.045	0.13	0.47***	56.5
	c	8	68	5	0.065	0.28	0.34***	33.9	12	0.060	0.24	**0.52*****	70.8	4	0.061	0.25	0.43***	50.7
	a	8	69	10	0.042	0.05	**0.89*****	539.2	12	0.032	0.07	**0.89*****	563.3	24	0.033	0.07	**0.97*****	2171.8
	a	8	67	4	0.038	0.09	**0.51*****	66.9	12	0.037	0.07	**0.72*****	165.2	8	0.039	0.09	**0.64*****	116.9
ETR	c	22	67	5	10.687	7597	0.16***	12.1	6	10.570	7222	0.15**	11.4	3	10.164	6776	0.13**	9.8
	c	14	66	5	1.350	120	0.34***	33.0	7	1.312	112	0.39***	41.3	3	1.339	119	0.27***	24.1
	c	8	68	4	4.737	1514	0.11**	8.0	8	4.649	1420	0.27***	23.9	3	4.586	1471	0.13**	9.9
	a	8	69	9	0.719	16.71	**0.69*****	146.2	12	0.375	9.32	**0.73*****	178.9	6	0.453	13.17	**0.66*****	128.5
	a	8	67	3	2.423	401	0.10**	7.4	11	2.607	348	0.34***	33.4	5	2.309	352	0.22***	18.5
NPQ	c	22	67	9	0.419	11.39	0.33***	32.5	4	0.388	10.07	0.14**	10.4	3	0.382	10.30	0.14**	10.5
	c	14	66	9	0.255	4.33	0.43***	48.0	3	0.251	4.57	0.03	2.2	3	0.249	4.06	0.06ɪ	3.8
	c	8	68	8	0.309	6.20	**0.57*****	86.0	3	0.377	9.08	0.22***	18.6	10	0.367	8.94	**0.57*****	89.1
	a	8	69	3	0.198	3.51	0.07*	5.2	3	0.201	2.84	0.04ɪ	2.9	13	0.192	2.56	**0.60*****	100.8
	a	8	67	3	0.279	5.42	0.09*	6.2	3	0.273	5.14	0.14**	10.6	3	0.279	5.19	0.13**	9.4

Table 4. Model fits of full spectra with all data collected during the experiment. Number of model components (com), adjusted CV, and PRESS are from PLSR model fitting. *F* statistic and R^2 value from models of predicted by observed responses. All models are significant at P << 0.001 (***)

resp	n	com	CV	PRESS	*F*	R^2
Fv/Fm	337	13	0.022	0.16	2768.7	**0.89*****
Φ_{PSII}	337	28	0.080	2.19	540.2	**0.62*****
ETR	337	12	5.732	10890	81.9	0.20***
NPQ	337	11	0.314	32.95	198.6	0.37***

Table 5. Predictive fits (R^2) of spectral models (full spectra) of fluorescent response rate changes during experiment. R^2 values greater than 0.75 are in bold and R^2 values between 0.5 and 0.75 are italicized.

		predicted by spectra				
		cooling		acclimation		
	rates	22°C	14°C	8°C	8°C	8°C
Fv/Fm	cooling	0.33***	*0.55***	0.45***	0.36***	0.43***
	acclimation	*0.58***	*0.56***	**0.88*****	**0.85*****	**0.97*****
	total	*0.60***	*0.57***	**0.84*****	**0.90*****	**0.99*****
Φ_{PSII}	cooling	0.12**	0.12**	0.17***	0.06*	0.18***
	acclimation	*0.75***	**0.79*****	**0.87*****	*0.67***	*0.60***
	total	*0.73***	0.47***	**0.81*****	*0.64***	*0.51***
ETR	cooling	0.11**	0.11**	0.08*	0.09*	0.05ǂ
	acclimation	0.11**	0.11**	0.14**	0.17***	0.16***
	total	0.16***	0.14**	0.12**	0.16***	0.09*
NPQ	cooling	0.13**	0.13**	0.08*	0.10**	0.11**
	acclimation	0.16***	0.16***	0.18***	0.34***	0.25***
	total	0.07*	0.07*	0.04	0.07*	0.16**

Chapter 3 Figures

Figure 1. Oak species acorn collection sites and subgenera by minimum temperature of coldest month at origin (Hijmans et al. 2005). Clustered points were dispersed for visibility.

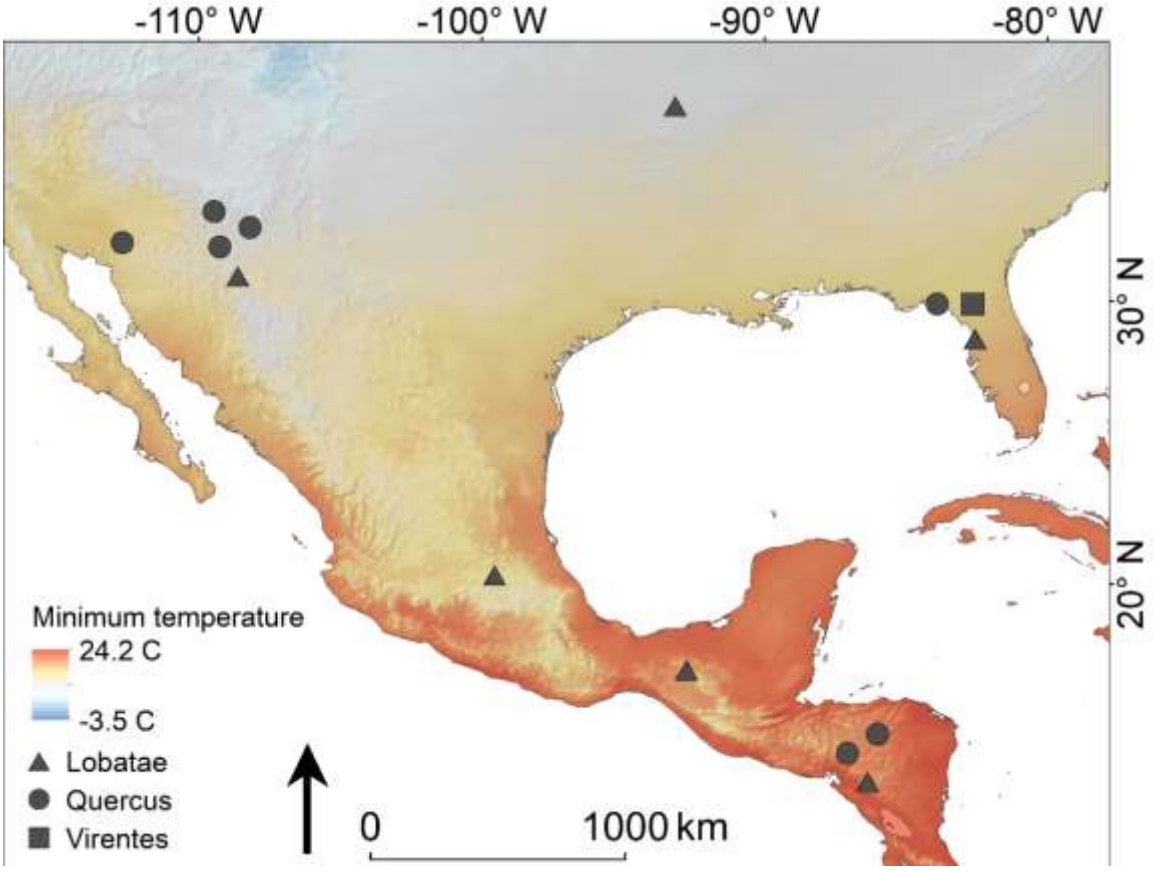

Figure 2. Greenhouse temperature settings and measurement times. Chlorophyll fluorescence was measured at each time point and leaf hyperspectral reflectance was measured at each point highlighted by a vertical gray bar.

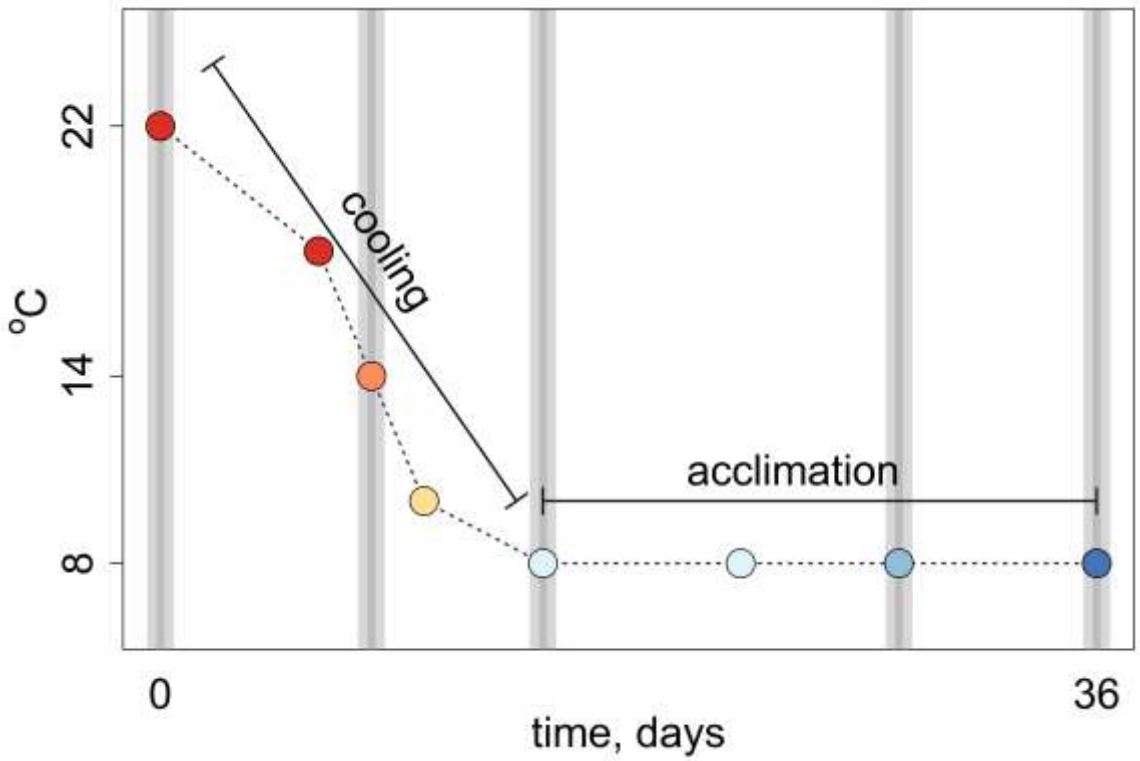

Figure 3. Spectra quantiles (P = .95) from all plants at three points during the experiment: initial measurements, after cooling to 8°C, and after being held at 8°C for 26 days. We created predictive models from the full spectral range (400-2400nm) and from the two subsets shown at vis (visible, 400-7s00nm) and fluor (PSII fluorescence, 640-800nm).

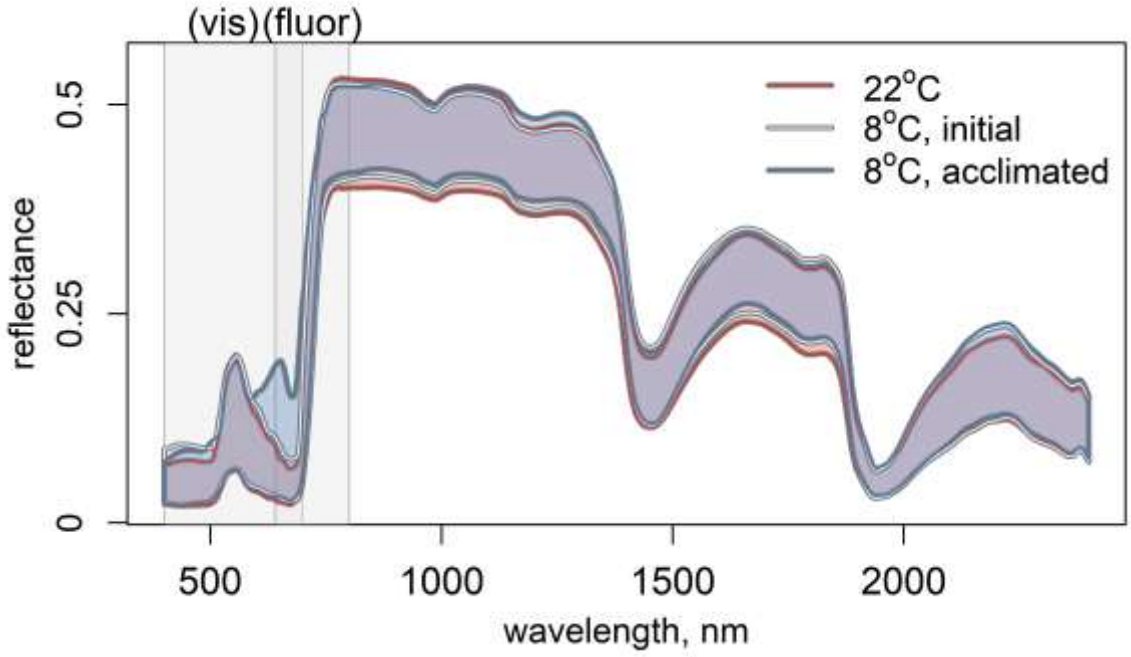

Figure 4. Chlorophyll fluorescence over time and by cooling or acclimation status of experiment (central bars). Species means are larger dots, all individual measurements are shown as gray points in background. Points are jittered slightly for visibility. a) Dark adapted predawn F_v/F_m, b) non-photochemical quenching, c) Φ_{PSII}, light-adapted realized photosynthetic yield, and d) electron transport rate.

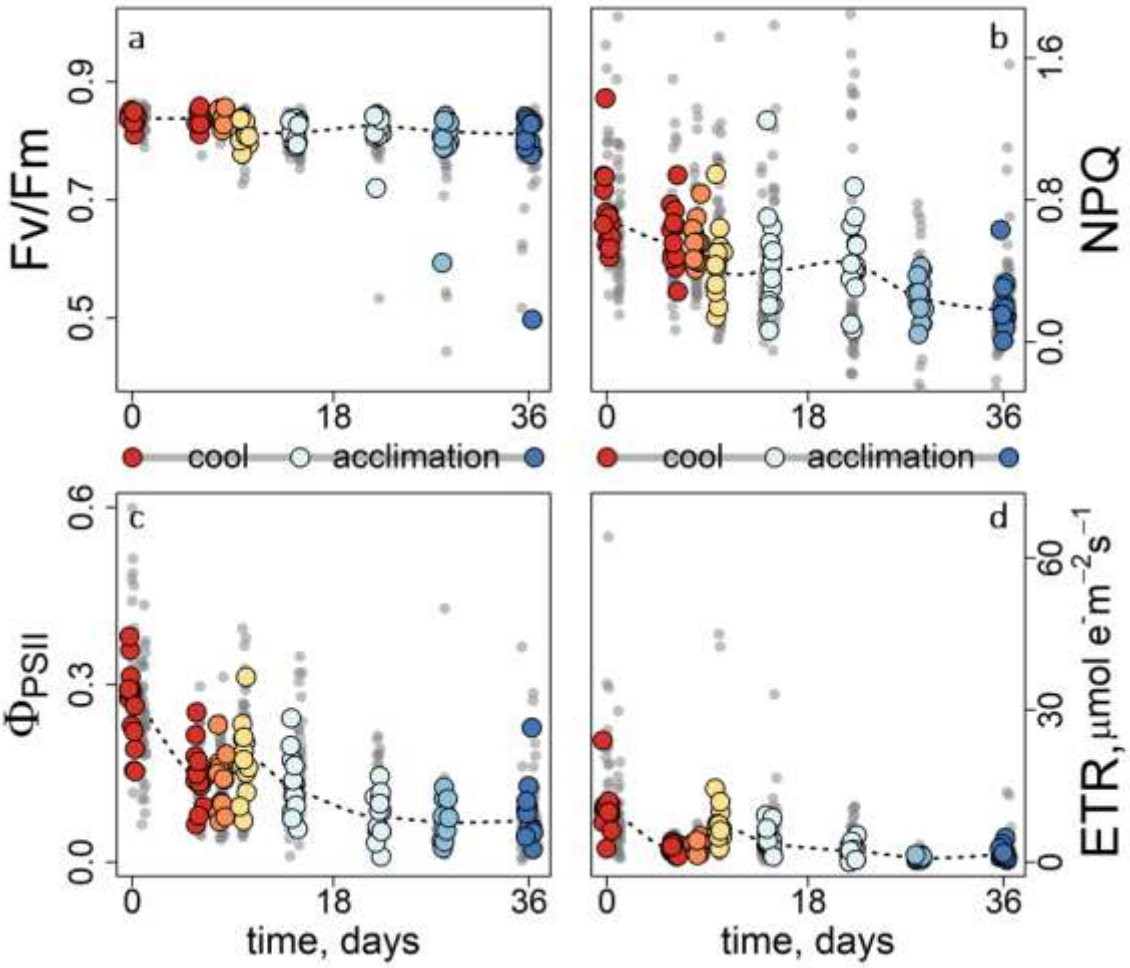

Figure 5. Effect size of fluorescence values predicted by observed values from PLSR models created from measurements taken on the same day. Spectral regions used to predict fluorescent observations are shown as visible (vis), fluorescent (fluor), and full a) R^2 of models of all responses, letters denote significant differences at $P < 0.05$). b) – e) Effect sizes of models for each fluorescent response. P-values show significance of experimental time and spectral region in effect size of prediction. Open triangles show coefficient of variation in each response variable at each experimental time. Dark squares in (e) denote models with low support ($P > 0.05$).

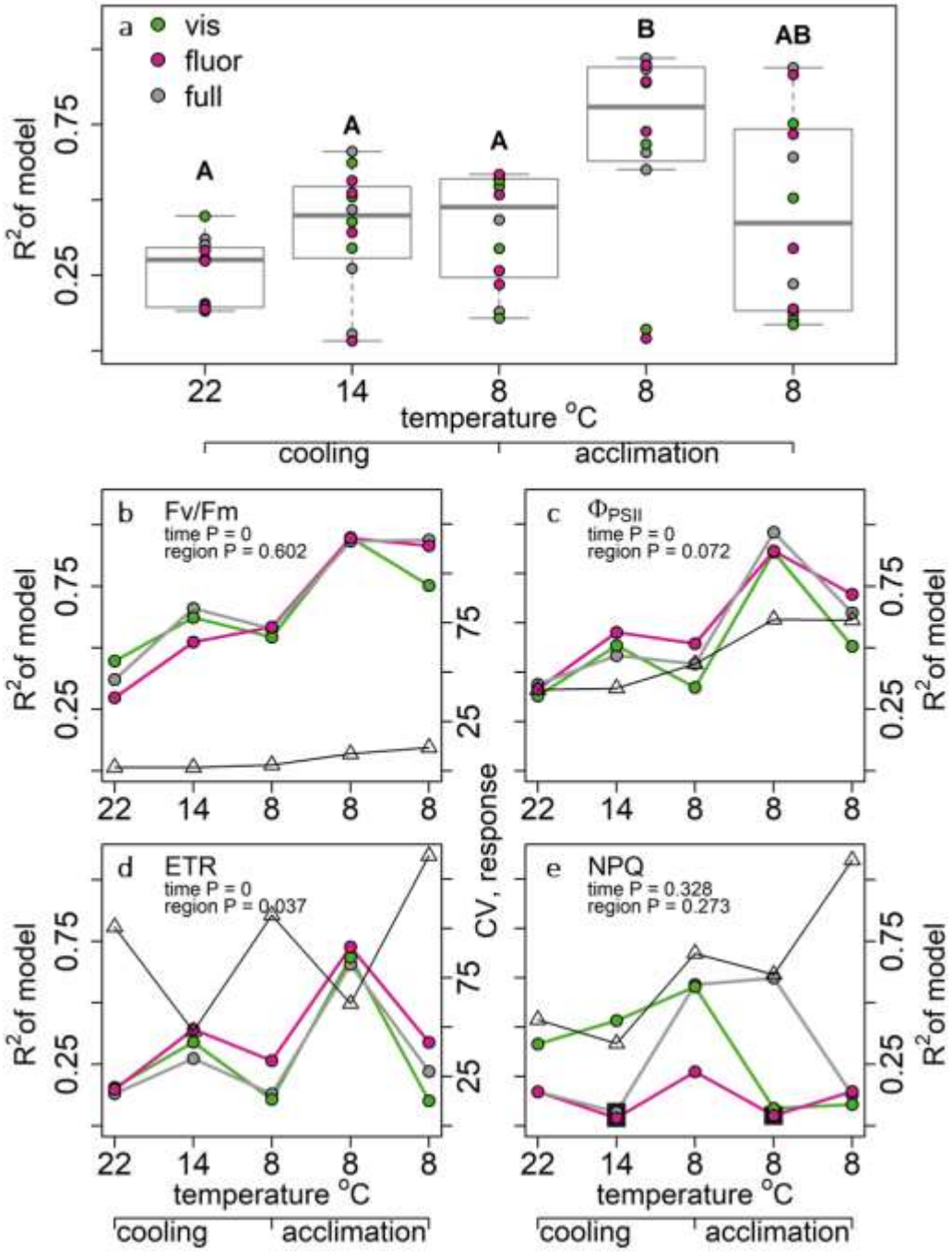

Figure 6. PLSR model coefficients from full spectra (a-d) and variance among model coefficients at different experimental times (e-f). Gray shading highlights spectral regions (V = visible, F = fluorescent, NIR = near infrared, SW1,2 = short-wave infrared 1 & 2). g) Model coefficients that exceed 95% of the coefficient value for each model. Dashed lines show areas of reflectance important for measuring carotenoids (Car), xanthophyll pigments (X), chlorophyll (Ch), fluorescence (Fl), and water (W).

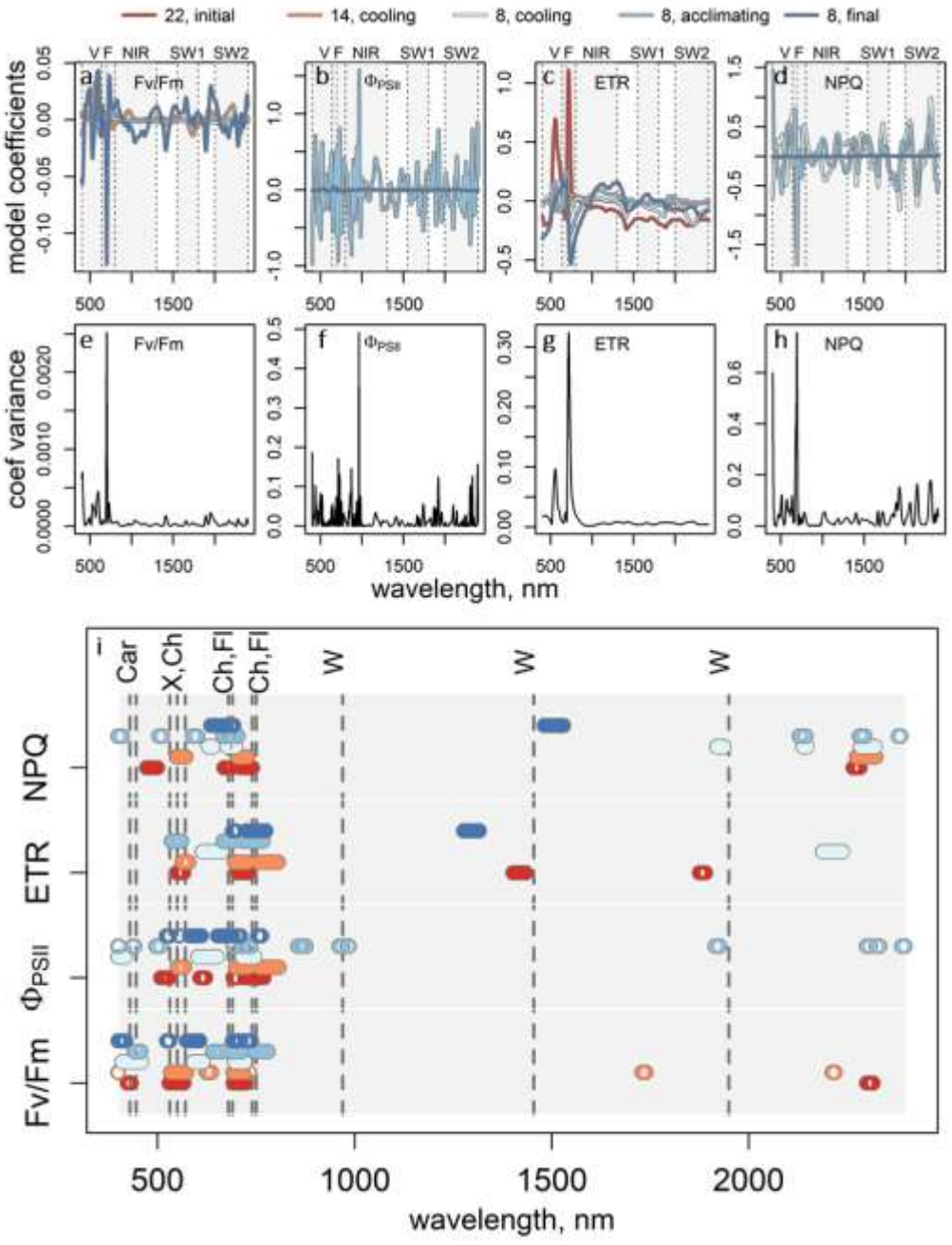

Figure 7. Predicted by observed fluorescent responses at each experimental time (left to right), shown with best model (maximum R^2), adjusted coefficients of variation, and predicted by observed R^2 and P values. Light gray background points are all predicted values from all spectra and dashed lines show 1:1 relationship.

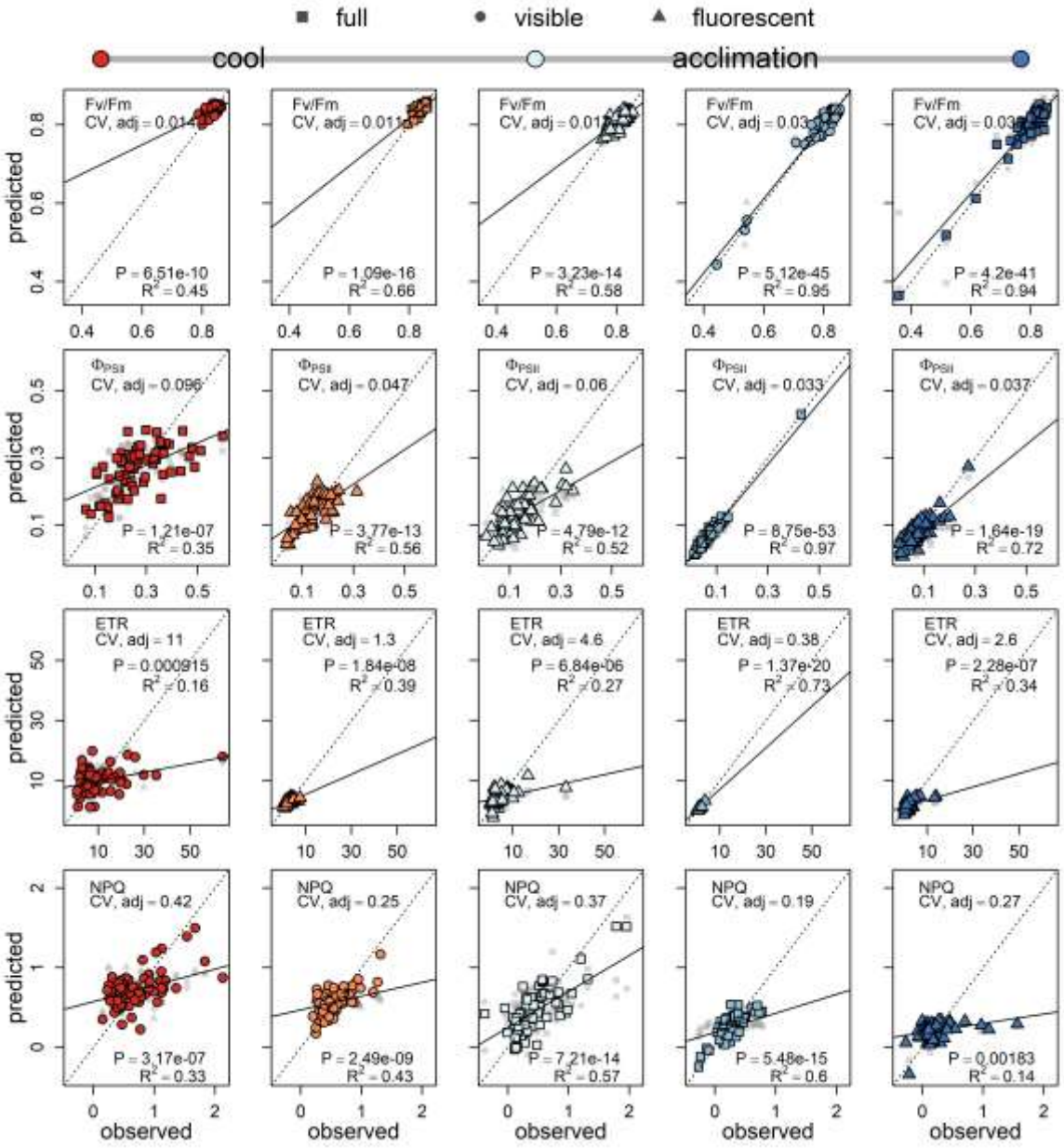

Figure 8. Model fits of predicted by observed fluorescent responses (all) predicted from non-simultaneous pls models (fit to spectra and observations measured at other experimental times) and simultaneous measurements. Dashed line is 1:1 relationship and colors show the experimental time step from which the pls models were constructed (using full spectra).

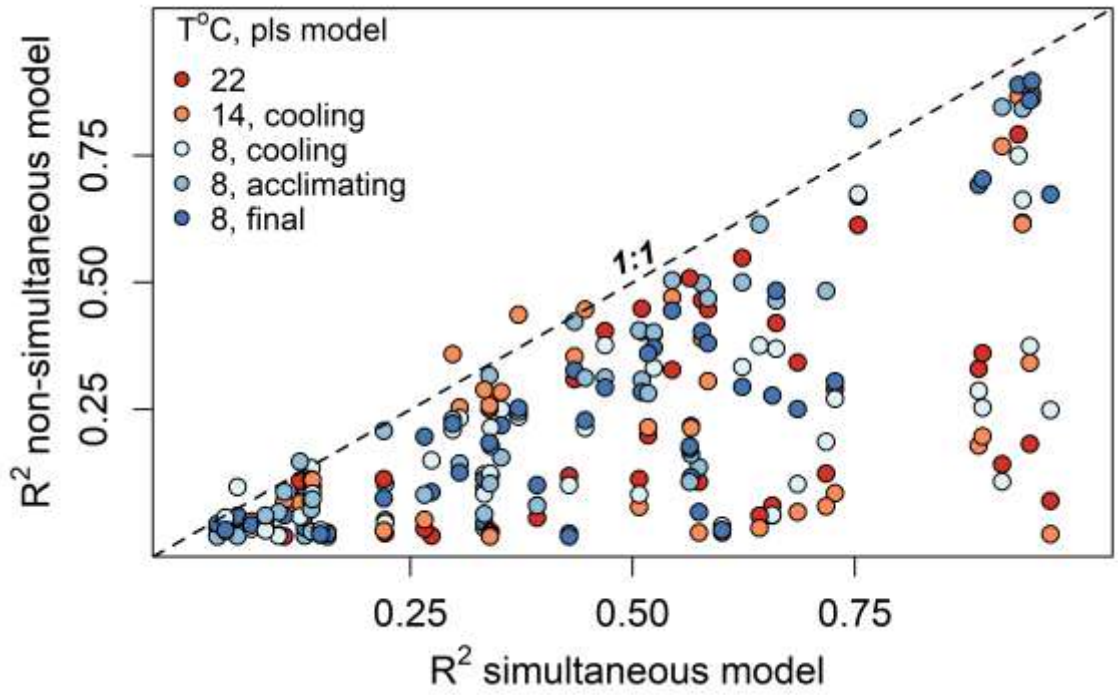

Figure 9. Rates of response predicted by models of best fit from full spectra collected at a-b) 8°C final after acclimation and c-d) 8°C upon initial cooling. Dashed line shows 1:1 relationship.

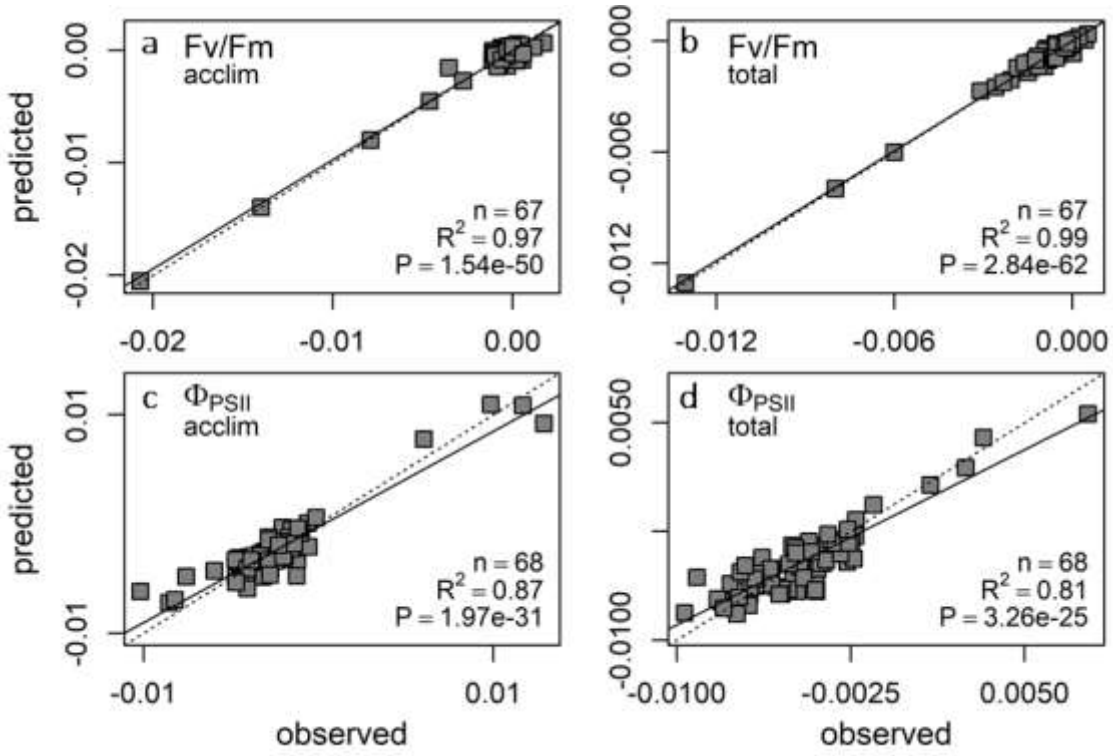

Bibliography

Abrams, M. D. 1988. Sources of variation in osmotic potentials with special reference to North American tree species. Forest Science 34:1030–1046.

Abrams, M. D. 1990. Adaptation and responses to drought in Quercus species of North America.

Adams, H. D., M. Guardiola-Claramonte, G. A. Barron-Gafford, J. C. Villegas, D. D. Breshears, C. B. Zou, P. A. Troch, and T. E. Huxman. 2009. Temperature sensitivity of drought-induced tree mortality portends increased regional die-off under global-change-type drought. Proceedings of the National Academy of Sciences 106:7063–6.

Adams, W. W., K. Winter, U. Schreiber, and P. Schramel. 1990. Photosynthesis and chlorophyll fluorescence characteristics in relationship to changes in pigment and element composition of leaves of Platanus occidentalis L. during autumnal leaf senescence. Plant Physiology 93:1184–1190.

Adams III, W. W., and B. Demmig-Adams. 1995. The xanthophyll cycle and sustained thermal energy dissipation activity in Vinca minor and Euonymus kiautschovicus in winter. Plant, Cell & Environment 18:117–127.

Aguilar-Romero, R., F. Pineda-Garcia, H. Paz, A. González-Rodríguez, and K. Oyama. 2017. Differentiation in the water-use strategies among oak species from central Mexico. Tree Physiology 37:1–11.

Allen, C. D., D. D. Breshears, and N. G. McDowell. 2015. On underestimation of global vulnerability to tree mortality and forest die-off from hotter drought in the Anthropocene. Ecosphere 6.

Araújo, M., and R. Pearson. 2005. Equilibrium of species' distributions with climate. Ecography 28:693–695.

Axelrod, D. I. 1983. Biogeography of Oaks in the Arcto-Tertiary Province. Annals of the Missouri Botanical Garden 70:629–657.

Banta, J. A., I. M. Ehrenreich, S. Gerard, L. Chou, A. Wilczek, J. Schmitt, P. X. Kover, and M. D. Purugganan. 2012. Climate envelope modelling reveals intraspecific relationships among flowering phenology, niche breadth and potential range size in Arabidopsis thaliana. Ecology Letters 15:769–777.

Bartlett, M. K., T. Klein, S. Jansen, B. Choat, and L. Sack. 2016. The correlations and sequence of plant stomatal, hydraulic, and wilting responses to drought. Proceedings of the National Academy of Sciences 113:13098–13103.

Bartlett, M. K., C. Scoffoni, and L. Sack. 2012. The determinants of leaf turgor loss point and prediction of drought tolerance of species and biomes: a global meta-analysis. Ecology Letters 15:393–405.

Bartlett, M. K., Y. Zhang, N. Kreidler, S. Sun, R. Ardy, K. Cao, and L. Sack. 2014.

Global analysis of plasticity in turgor loss point, a key drought tolerance trait. Ecology Letters 17:1580–1590.

Barton, A. 2008. Madrean pine-oak forest in Arizona: past dynamics, present problems. Page USDA Forest Service General Technical Report PSW-GTR-189.

Barton, A. M. 2002. Intense wildfire in southeastern Arizona: transformation of a Madrean oak–pine forest to oak woodland. Forest Ecology and Management 165:205–212.

Barton, A., and J. Teeri. 1993. The ecology of elevational positions in plants: drought resistance in five montane pine species in southeastern Arizona. American Journal of Botany 80:15–25.

Baty, F., C. Ritz, S. Charles, M. Brutsche, J.-P. Flandrois, and M.-L. Delignette-Muller. 2015. A Toolbox for Nonlinear Regression in R: The Package nlstools. Journal of Statistical Software 66:1–21.

Benjamini, Y., and Y. Hochberg. 1995. Controlling the false discovery rate: a practical and powerful approach to multiple testing. Journal of the Royal Statistical Society 57:289–300.

Berry, J., and O. Bjorkman. 1980. Photosynthetic response and adaptation to temperature in higher plants. Annual Review of Plant Physiology 31:491–543.

Betancourt, J., T. Van Devender, and P. Martin, editors. 1990. Packrat Middens: the last 40,000 years of biotic change. University of Arizona Press, Tucson.

Blackman, C. J., and T. J. Brodribb. 2011. Two measures of leaf capacitance: Insights into the water transport pathway and hydraulic conductance in leaves. Functional Plant Biology 38:118–126.

Blumer, J. C. 1909. On the Plant Geography of the Chiricahua Mountains. Science 30:720–724.

Bolhar-Nordenkampf, H. R., S. P. Long, N. R. Baker, G. Oquist, U. Schreiber, and E. G. Lechner. 1989. Chlorophyll fluorescence as a probe of the photosynthetic competence of leaves in the field: a review of current instrumentation. Functional Ecology 3:497.

Boyko, H. 1947. On the role of plants as quantitative climate indicators and the geo-ecological law of distribution. The Journal of Ecology 35:138–157.

Du Bray, E. A., J. S. Pallister, and D. B. Yager. 1995. Geologic map of the Turkey Creek caldera, Chiricahua Mountains, Cochise County, Arizona. Miscellaneous Investigations Series Map I-2544. United States Geological Survey.

Breshears, D. D., N. S. Cobb, P. M. Rich, K. P. Price, C. D. Allen, R. G. Balice, W. H. Romme, J. H. Kastens, M. L. Floyd, J. Belnap, J. J. Anderson, O. B. Myers, and C. W. Meyer. 2005. Regional vegetation die-off in response to global-change-type drought. Proceedings of the National Academy of Sciences 102:15144–8.

Brodribb, T., and N. Holbrook. 2003a. Stomatal closure during leaf dehydration, correlation with other leaf physiological traits. Plant Physiology 132:2166–2173.

Brodribb, T. J., and N. M. Holbrook. 2003b. Changes in leaf hydraulic conductance during leaf shedding in seasonally dry tropical forest. New Phytologist 158:295–303.

Brodribb, T. J., N. M. Holbrook, E. J. Edwards, and M. V. Gutiérrez. 2003. Relations between stomatal closure, leaf turgor and xylem vulnerability in eight tropical dry forest trees. Plant, Cell and Environment 26:443–450.

Brusca, R. C., J. F. Wiens, W. M. Meyer, J. Eble, K. Franklin, J. T. Overpeck, and W. Moore. 2013. Dramatic response to climate change in the Southwest: Robert Whittaker's 1963 Arizona Mountain plant transect revisited. Ecology and Evolution.

Bryant, F. C., and M. M. Kothmann. 1979. Variability in predicting edible browse from crown volume. Journal of Range Management 32:144–146.

Buja, K., and C. Menza. 2013. Sampling Design Tool for ArcGIS - for ESRI ArcGIS 10.0 Service Pack 3 or higher. NOAA, Silver Spring, MD.

Cavender-Bares, J. 2000. Physiological and evolutionary ecology of oaks: functional traits in relation to habitat, environmental stress, and global change. Harvard University, Cambridge, Mass.

Cavender-Bares, J. 2005. Impacts of freezing on long-distance transport in woody plants. Pages 401–424*in* N. Holbrook, M. Zwieniecki, and P. Melcher, editors.Vascular transport in plants. Elsevier, Oxford, UK.

Cavender-Bares, J. 2016. Diversity, distribution and ecosystem services of the North American oaks. International Oaks:37–48.

Cavender-Bares, J., D. D. Ackerly, D. A. Baum, and F. A. Bazzaz. 2004a. Phylogenetic overdispersion in Floridian oak communities. The American Naturalist 163:823–843.

Cavender-Bares, J., S. Apostol, I. Moya, J.-M. Briantis, and F. A. Bazzaz. 1999. Chilling-induced photoinhibition in two oak species: Are evergreen leaves inherently better protected than deciduous leaves? Photosynthetica 36:587–596.

Cavender-Bares, J., and F. A. Bazzaz. 2004. From leaves to ecosystems: using chlorophyll fluorescence to assess photosynthesis and plant function in ecological studies. Pages 737–755*in* G. Papageorgiou and Govindjee, editors.Chlorophyll fluorescence: a signature of photosynthesis. Kluwer Academic Publishers.

Cavender-Bares, J., P. Cortes, S. Rambal, R. Joffre, B. Miles, and A. Rocheteau. 2005. Summer and winter sensitivity of leaves and xylem to minimum freezing temperatures: a comparison of co-occurring Mediterranean oaks that differ in leaf lifespan. The New Phytologist 168:597–612.

Cavender-Bares, J., J. A. Gamon, S. E. Hobbie, M. D. Madritch, J. E. Meireles, A. K. Schweiger, and P. A. Townsend. 2017. Harnessing plant spectra to integrate the

biodiversity sciences across biological and spatial scales. American Journal of Botany 104:966–969.

Cavender-Bares, J., and N. M. Holbrook. 2001. Hydraulic properties and freezing-induced cavitation in sympatric evergreen and deciduous oaks with contrasting habitats. Plant, Cell and Environment 24:1243–1256.

Cavender-Bares, J., K. Kitajima, and F. A. Bazzaz. 2004b. Multiple trait associations in relation to habitat differentiation among 17 Floridian oak species. Ecological Monographs 74:635–662.

Cavender-Bares, J., J. E. Meireles, J. J. Couture, M. A. Kaproth, C. C. Kingdon, A. Singh, S. P. Serbin, E. Zuniga, G. Pilz, and P. A. Townsend. 2016. Associations of leaf spectra with genetic and phylogenetic variation in oaks: prospects for remote detection of biodiversity. Remote Sensing 8.

CGIAR-CSI. 2008. Global Aridity and PET Database. http://www.cgiar-csi.org/data/global-aridity-and-pet-database.

Chabot, B., and D. Hicks. 1982. The ecology of leaf life spans. Annual Review of Ecology and Systematics 13:229–259.

Chen, S., X. Hong, C. J. Harris, and P. M. Sharkey. 2004. Sparse Modeling Using Orthogonal Forward Regression With PRESS Statistic and Regularization. IEEE Transactions on Systems, Man, and Cybernetics, Part B: Cybernetics 34:898–911.

Choat, B., S. Jansen, T. J. Brodribb, H. Cochard, S. Delzon, R. Bhaskar, S. J. Bucci, T. S. Feild, S. M. Gleason, U. G. Hacke, A. L. Jacobsen, F. Lens, H. Maherali, J. Martínez-Vilalta, S. Mayr, M. Mencuccini, P. J. Mitchell, A. Nardini, J. Pittermann, R. B. Pratt, J. S. Sperry, M. Westoby, I. J. Wright, and A. E. Zanne. 2012. Global convergence in the vulnerability of forests to drought. Nature 491:752–5.

Choat, B., E. C. Lahr, P. J. Melcher, M. A. Zwieniecki, and N. M. Holbrook. 2005. The spatial pattern of air seeding thresholds in mature sugar maple trees. Plant, Cell and Environment 28:1082–1089.

Cochard, H., N. Bréda, and A. Granier. 1996. Whole tree hydraulic conductance and water loss regulation in Quercus during drought: evidence for stomatal control of embolism? Annales des Sciences Forestières 53:197–206.

Cochard, H., N. Breda, A. Granier, and G. Aussenac. 1992. Vulnerability to air embolism of three European species (Quercus petraea (Matt) Liebl, Q pubescens Willd, Q robur L). Annals of Forest Science 49:225–233.

Cotrozzi, L., J. J. Couture, J. Cavender-Bares, C. C. Kingdon, B. Fallon, G. Pilz, E. Pellegrini, C. Nali, and P. A. Townsend. 2017. Using foliar spectral properties to assess the effects of drought on plant water potential. Tree Physiology:1–10.

Craine, J. M., T. W. Ocheltree, J. B. Nippert, E. G. Towne, A. M. Skibbe, S. W. Kembel, and J. E. Fargione. 2012. Global diversity of drought tolerance and grassland climate-change resilience. Nature Climate Change 3:63–67.

Crimmins, S., S. Dobrowski, J. Greenberg, J. Abatzoglou, and A. Mynsberge. 2011. Changes in climatic water balance drive downhill shifts in plant species' optimum elevations. Science 331:324–327.

Crozier, L. 2003. Winter warming facilitates range expansion: cold tolerance of the butterfly Atalopedes campestris. Oecologia 135:648–56.

Davis, M. B., and R. G. Shaw. 2001. Range shifts and adaptive responses to Quaternary climate change. Science 292:673–9.

Van Devender, T. 1990. Late Quarternary vegetation and climate of the Sonoran Desert, United States and Mexico. Pages 134–165*in* J. Betancourt, T. Van Devender, and P. Martin, editors.Packrat Middens: The Last 40,000 Years of Biotic Change. The University of Arizona Press, Tucson.

Díaz, S., and J. Hodgson. 2004. The plant traits that drive ecosystems: evidence from three continents. Journal of Vegetation Science 15:295–304.

Dobrowski, S. Z., J. C. Pushnik, P. J. Zarco-Tejada, and S. L. Ustin. 2005. Simple reflectance indices track heat and water stress-induced changes in steady-state chlorophyll fluorescence at the canopy scale. Remote Sensing of Environment 97:403–414.

Domec, J. C., and B. L. Gartner. 2001. Cavitation and water storage capacity in bole xylem segments of mature and young Douglas-fir trees. Trees - Structure and Function 15:204–214.

Duursma, R., and B. Choat. 2017. fitplc - an R package to fit hydraulic vulnerability curves. Journal of Plant Hydraulics 4:2.

Ehleringer, J. R., and S. Phillips. 1996. Ecophysiological factors contributing to the distributions of several Quercus species in the intermountain west. Annals of Forest Science 53:291–302.

ESRI. 2011. ArcGIS Desktop: Release 10. Environmental Systems Research Institute, Redlands, CA.

Fick, S. E., and R. J. Hijmans. 2017. Worldclim 2: New 1-km spatial resolution climate surfaces for global land areas. International Journal of Climatology.

Flint, H. R., B. R. Boyce, and D. J. Beattie. 1967. Index of injury-a useful expression of freezing injury to plant tissues as determined by the electrolytic method. Canadian Journal of Plant Science 47:229–230.

Fox, J., and S. Weisberg. 2011. An {R} Companion to Applied Regression. 2nd ed. Sage, Thousand Oaks CA.

Freeman, B. G., and A. M. Class Freeman. 2014. Rapid upslope shifts in New Guinean birds illustrate strong distributional responses of tropical montane species to global warming. Proceedings of the National Academy of Sciences 111.

Friedman, J., J. Roelle, J. Gaskin, A. Pepper, and J. Manhart. 2008. Latitudinal variation

in cold hardiness in introduced Tamarix and native Populus. Evolutionary Applications 1:598–607.

Gamon, J. A., C. B. Field, W. Bilger, O. Björkman, A. L. Fredeen, and J. Peñuelas. 1990. Remote sensing of the xanthophyll cycle and chlorophyll fluorescence in sunflower leaves and canopies. Oecologia 85:1–7.

Gamon, J. A., L. Serrano, and J. S. Surfus. 1997. The photochemical reflectance index: An optical indicator of photosynthetic radiation use efficiency across species, functional types, and nutrient levels. Oecologia 112:492–501.

Garcia Moscoso, J. L. 1998. Caracterización dendrológica y ecológica del género Quercus L. en el bosque de la Montaña de Uyuca, Zamorano, Honduras. Zamorano.

GBIF. 2013. Global Biodiversity Information Facility. http://data.gbif.org/welcome.htm.

Gifford, M. E., and K. H. Kozak. 2012. Islands in the sky or squeezed at the top? Ecological causes of elevational range limits in montane salamanders. Ecography 35:193–203.

Gitelson, A. A., and M. N. Merzlyak. 1998. Remote sensing of chlorophyll concentration in higher plant leaves. Advances in Space Research 22:689–692.

Gitelson, A. a, M. N. Merzlyak, and O. B. Chivkunova. 2001. Optical Properties and Nondestructive Estimation of Anthocyanin Content in Plant Leaves Optical Properties and Nondestructive Estimation of Anthocyanin Content in Plant Leaves. Photochemistry and Photobiology 74:38–45.

Gleason, S. M., M. Westoby, S. Jansen, B. Choat, U. G. Hacke, R. B. Pratt, R. Bhaskar, T. J. Brodribb, S. J. Bucci, K. F. Cao, H. Cochard, S. Delzon, J. C. Domec, Z. X. Fan, T. S. Feild, A. L. Jacobsen, D. M. Johnson, F. Lens, H. Maherali, J. Martínez-Vilalta, S. Mayr, K. A. Mcculloh, M. Mencuccini, P. J. Mitchell, H. Morris, A. Nardini, J. Pittermann, L. Plavcová, S. G. Schreiber, J. S. Sperry, I. J. Wright, and A. E. Zanne. 2016. Weak tradeoff between xylem safety and xylem-specific hydraulic efficiency across the world's woody plant species. New Phytologist 209:123–136.

Gotelli, N. J., and A. M. Ellison. 2013. EcoSimR 1.00. http://www.uvm.edu/~ngotelli/EcoSim/EcoSim.html.

Govender, M., K. Chetty, and H. Bulcock. 2007. A review of hyperspectral remote sensing and its application in vegetation and water resource studies. Water SA 33:145–151.

Grace, J., C. Nichol, M. Disney, P. Lewis, T. Quaife, and P. Bowyer. 2007. Can we measure terrestrial photosynthesis from space directly, using spectral reflectance and fluorescence? Global Change Biology 13:1484–1497.

Greenwood, S., P. Ruiz-Benito, J. Martínez-Vilalta, F. Lloret, T. Kitzberger, C. D. Allen, R. Fensham, D. C. Laughlin, J. Kattge, G. Bönisch, N. J. B. Kraft, and A. S. Jump. 2017. Tree mortality across biomes is promoted by drought intensity, lower wood density and higher specific leaf area. Ecology Letters 20:539–553.

Grinnell, J. 1917. Field tests of theories concerning distribution control. The American Naturalist 51:115–128.

Hacke, U. G., J. S. Sperry, J. K. Wheeler, and L. Castro. 2006. Scaling of angiosperm xylem structure with safety and efficiency. Tree Physiology 26:689–701.

Harrell Jr, F. E., and C. Dupont. 2016. Hmisc: Harrell Miscellaneous. R package version 4.0-2.

Harrison, S., E. I. Damschen, and J. B. Grace. 2010. Ecological contingency in the effects of climatic warming on forest herb communities. Proceedings of the National Academy of Sciences of the United States of America 107:19362–19367.

Harsch, M. A., and J. HilleRisLambers. 2016. Climate warming and seasonal precipitation change interact to limit species distribution shifts across Western North America. PLoS ONE 11:e0159184.

Hijmans, R. J. 2016. raster: Geographic Data Analysis and Modeling. R package version 2.5-8.

Hijmans, R. J., S. E. Cameron, J. L. Parra, P. G. Jones, and A. Jarvis. 2005. Very high resolution interpolated climate surfaces for global land areas. International Journal of Climatology 25:1965–1978.

Hijmans, R. J., and J. Elith. 2013. Species distribution modeling with R Introduction.

Hijmans, R. J., S. Phillips, J. Leathwick, and J. Elith. 2016. dismo: Species Distribution Modeling. R package version 1.1-4.

Hipp, A. L., P. S. Manos, A. González-Rodríguez, M. Hahn, M. Kaproth, J. D. McVay, S. V. Avalos, and J. Cavender-Bares. 2017. Sympatric parallel diversification of major oak clades in the Americas and the origins of Mexican species diversity. New Phytologist.

Hochberg, U., C. W. Windt, A. Ponomarenko, Y. Zhang, J. Gersony, F. E. Rockwell, and N. M. Holbrook. 2017. Stomatal Closure, Basal Leaf Embolism, and Shedding Protect the Hydraulic Integrity of Grape Stems. Plant Physiology 174:764–775.

Holland, P. G., and D. G. Steyn. 1975. Vegetational responses to latitudinal variations in slope angle and aspect. Journal of biogeography 2:179–183.

Holmgren, C. A., J. L. Betancourt, and K. A. Rylander. 2006. A 36,000-yr vegetation history from the Peloncillo Mountains, southeastern Arizona, USA. Palaeogeography, Palaeoclimatology, Palaeoecology 240:405–422.

Huner, N. P. A., G. Oquist, V. M. Hurry, M. Krol, S. Falk, and M. Griffith. 1993. Photosynthesis, photoinhibition and low temperature acclimation in cold tolerant plants. Photosynthesis Research 37:19–39.

IPCC. 2013. Climate Change 2013: The Physical Science Basis. Contribution of Working Group I to the Fifth Assessment Report of the Intergovernmental Panel on Climate Change. Page (T. Stocker, D. Qin, G.-K. Plattner, M. Tignor, S. Allen, A. Boschang,

A. Nauels, Y. Xia, V. Bex, and P. Midgley, Eds.). Cambridge University Press, Cambridge United Kingdom and New York, NY, USA.

Jones, H. G., and R. A. Sutherland. 1991. Stomatal control of xylem embolism. Plant, Cell & Environment 14:607–612.

Kadmon, R., O. Farber, and A. Danin. 2003. A systematic analysis of factors affecting the performance of climatic envelope models. Ecological Applications 13:853–867.

Kalaji, H. M., G. Schansker, R. J. Ladle, V. Goltsev, K. Bosa, S. I. Allakhverdiev, M. Brestic, F. Bussotti, A. Calatayud, P. Dąbrowski, N. I. Elsheery, L. Ferroni, L. Guidi, S. W. Hogewoning, A. Jajoo, A. N. Misra, S. G. Nebauer, S. Pancaldi, C. Penella, D. Poli, M. Pollastrini, Z. B. Romanowska-Duda, B. Rutkowska, J. Serôdio, K. Suresh, W. Szulc, E. Tambussi, M. Yanniccari, and M. Zivcak. 2014. Frequently asked questions about in vivo chlorophyll fluorescence: Practical issues. Photosynthesis Research 122:121–158.

Kalnay, E., M. Kanamitsu, R. Kistler, W. Collins, D. Deaven, L. Gandin, S. S. M Iredell, G. White, J. Woollen, Y. Zhu, A. Leetmaa, R. Reynolds, M. Chelliah, W. Ebisuzaki, W. Higgins, J. Janowiak, K. C. Mo, C. Ropelewski, J. Wang, R. Jenne, and D. Joseph. 1996. The NCEP/NCAR 40-Year Reanalysis Project. Bulletin of the American Meteorological Society 77:473–471.

Kelly, A. E., and M. L. Goulden. 2008. Rapid shifts in plant distribution with recent climate change. Proceedings of the National Academy of Sciences 105:11823–6.

Klein, T. 2014. The variability of stomatal sensitivity to leaf water potential across tree species indicates a continuum between isohydric and anisohydric behaviours. Functional Ecology 28:1313–1320.

Koehler, K., A. Center, and J. Cavender-Bares. 2012. Evidence for a freezing tolerance-growth rate trade-off in the live oaks (Quercus series Virentes) across the tropical-temperate divide. The New Phytologist 193:730–44.

Koide, R. T., R. H. Robichaux, S. R. Morse, and C. M. Smith. 1989. Plant water status, hydraulic resistance, and capacitance. Pages 161–183*in* R. W. Pearcy, J. R. Ehleringer, H. A. Mooney, and P. W. Rundel, editors.Plant physiological ecology: Field methods and instrumentation. Chapman and Hall, London New York.

Kramer, P. J., and J. S. Boyer. 1995. Water relations of plants and soils. Academic Press, San Diego, CA.

Kreyling, J., S. Schmid, and G. Aas. 2014. Cold tolerance of tree species is related to the climate of their native ranges. Journal of Biogeography.

Kröber, W., S. Zhang, M. Ehmig, and H. Bruelheide. 2014. Linking xylem hydraulic conductivity and vulnerability to the leaf economics spectrum--a cross-species study of 39 evergreen and deciduous broadleaved subtropical tree species. PLoS ONE 9:e109211.

Lamont, B. B., and H. C. Lamont. 2000. Utilizable water in leaves of 8 arid species as derived from pressure-volume curves and chlorophyll fluorescence. Physiologia

Plantarum 110:64–71.

Legendre, P. 2014. lmodel2: Model II Regression. R package version 1.7-2.

Lenoir, J., J. C. Gégout, P. A. Marquet, P. de Ruffray, and H. Brisse. 2008. A significant upward shift in plant species optimum elevation during the 20th century. Science 320:1768–71.

Lenz, A., G. Hoch, Y. Vitasse, and C. Körner. 2013. European deciduous trees exhibit similar safety margins against damage by spring freeze events along elevational gradients. The New Phytologist.

Lenz, T. I., I. J. Wright, and M. Westoby. 2006. Interrelations among pressure-volume curve traits across species and water availability gradients. Physiologia Plantarum 127:423–433.

Levitt, J. 1980. Responses of Plants to Environmental Stresses. 2nd ed. Academic Press, Inc, New York, NY.

Lichtenthaler, H. K. 1996. Vegetation stress: an introduction to the stress concept in plants. Journal of Plant Physiology 148:4–14.

Little Jr., E. L. 1971. Atlas of United States trees: Volume 1, Conifers and important hardwoods. U.S. Department of Agriculture Miscellaneous Publication 1146.

Livingston, B. E., and F. Shreve. 1921. The distribution of vegetation in the United State, as related to climatic conditions. Carnegie institution of Washington. Publication no. 284, Carnegie Institution of Washington, Washington, D.C.

MacArthur, R. H. 1972. Geographical Ecology: Patterns in the Distribution of Species. Harper & Row, New York, NY.

Martin-StPaul, N., S. Delzon, and H. Cochard. 2017. Plant resistance to drought relies on early stomatal closure. Ecology Letters:1–23.

Maxwell, K., and G. N. Johnson. 2000. Chlorophyll fluorescence--a practical guide. Journal of Experimental Botany 51:659–68.

McDowell, N., W. T. Pockman, C. D. Allen, D. D. Breshears, N. Cobb, T. Kolb, J. Plaut, J. S. Sperry, A. West, D. G. Williams, and E. A. Yepez. 2008. Mechanisms of plant survival and mortality during drought: Why do some plants survive while others succumb to drought? New Phytologist 178:719–739.

Medeiros, J. S., and W. T. Pockman. 2011. Drought increases freezing tolerance of both leaves and xylem of Larrea tridentata. Plant, Cell and Environment 34:43–51.

Meinzer, F. C., D. M. Johnson, B. Lachenbruch, K. A. McCulloh, and D. R. Woodruff. 2009. Xylem hydraulic safety margins in woody plants: coordination of stomatal control of xylem tension with hydraulic capacitance. Functional Ecology 23:922–930.

Meireles, J. E., A. Schweiger, and J. Cavender-Bares. 2017. spectrolab: Class and Methods for Hyperspectral Data. R package version 0.0.2.

Meroni, M., M. Rossini, L. Guanter, L. Alonso, U. Rascher, R. Colombo, and J. Moreno. 2009. Remote sensing of solar-induced chlorophyll fluorescence: Review of methods and applications. Remote Sensing of Environment 113:2037–2051.

Merriam, C. H. 1894. Laws of temperature control of the geographic distribution of terrestrial animals and plants. National Geographic Magazine 6:229–238.

Mevik, B.-H., R. Wehrens, and K. H. Liland. 2016. pls: Partial Least Squares and Principal Component Regression.

Mitchell, S. G., and K. A. Ober. 2013. Evolution of Scaphinotus petersi (Coleoptera: Carabidae) and the role of climate and geography in the Madrean sky islands of southeastern Arizona, USA. Quaternary Research 79:274–283.

Mohler, C. L. 1990. Co-Occurrence of Oak subgenera: implications for niche differentiation. Bulletin of the Torrey Botanical Club 117:247–255.

Muller, C. H. 1942a. Notes on the American flora, chiefly Mexican. American Midland Naturalist 27:470–490.

Muller, C. H. 1942b. The Central American species of Quercus.

Muller, C. H. 1954. A new species of Quercus in Arizona. Madroño 12:140–145.

Muller, P. 2001. Non-photochemical quenching: a response to excess light energy. Plant Physiology 125:1558–1566.

NCEI, and NOAA. (n.d.). Land-based Station Data, National Centers for Environmental Information, National Oceanic and Atmposheric Administration. http://www.ncdc.noaa.gov/data-access/land-based-station-data.

Nixon, K. C. 1997. Quercus. Pages 445–506*in* Flora of North America Editorial Committee, editor.Flora of North America North of Mexico. v. 3, 1993. Oxford University Press, New York, NY.

Nixon, K. C. 2002. The oak (Quercus) biodiversity of California and adjacent regions. USDA Forest Service 184:3–20.

Nixon, K. C. 2006. Global and Neotropical Distribution and Diversity of Oak (genus Quercus) and Oak Forests. Ecology and Conservation of Neotropical Montane Oak Forests 185:3–13.

NOAA. 2016. National Climatic Data Center, National Oceanic and Atmospheric Administration. http://www.ncdc.noaa.gov/.

Nobel, P. S., and P. W. Jordan. 1983. Transpiration stream of desert species: resistances and capacitances for a C3, a C4, and a CAM Plant. Journal of Experimental Botany 34:1379–1391.

Ogle, K., J. J. Barber, C. Willson, and B. Thompson. 2009. Hierarchical statistical modeling of xylem vulnerability to cavitation. New Phytologist 182:541–554.

Osmond, C. B., M. P. Austin, J. A. Berry, W. D. Billings, J. S. Boyer, J. W. H. Dacey, P.

S. Nobel, S. D. Smith, and W. E. Winner. 1987. Stress Physiology and the Distribution of Plants. BioScience 37:38–48.

Pammenter, N. W., and C. Vander Willigen. 1998. A mathematical and statistical analysis of the curves illustrating vulnerability of xylem to cavitation. Tree Physiology 18:589–593.

Parmesan, C., and G. Yohe. 2003. A globally coherent fingerprint of climate change impacts across natural systems. Nature 421:37–42.

Pearson, R. G., and T. P. Dawson. 2003. Predicting the impacts of climate change on the distribution of species: are bioclimate envelope models useful? Global Ecology and Biogeography 12:361–371.

Pearson, R. G., and T. P. Dawson. 2004. Bioclimate envelope models: what they detect and what they hide — response to Hampe (2004). Global Ecology and Biogeography 13:469–472.

Pedrós, R., I. Moya, Y. Goulas, and S. Jacquemoud. 2008. Chlorophyll fluorescence emission spectrum inside a leaf. Photochemical & Photobiological Sciences 7:498.

Peñuelas, J., and L. Filella. 1998. Visible and near-infrared reflectance techniques for diagnosing plant physiological status. Trends in Plant Science 3:151–156.

Pereira, L., R. S. Oliveira, L. Pereira, P. R. L. Bittencourt, R. S. Oliveira, M. B. M. Junior, and F. V Barros. 2016. Plant pneumatics : stem air flow is related to embolism--new perspectives on methods in plant hydraulics. New Phytologist.

Pockman, W., and J. S. Sperry. 2000. Vulnerability to xylem cavitation and the distribution of Sonoran desert vegetation. American Journal of Botany 87:1287–1299.

Pockman, W. T., J. S. Sperry, and J. W. O'Leary. 1995. Sustained and significant negative water pressure in xylem. Nature 378:715–716.

Poulos, H., U. Goodale, and G. Berlyn. 2007. Drought response of two Mexican oak species, Quercus laceyi and Q. sideroxyla (Fagaceae), in relation to elevational position. American Journal of Botany 94:809–818.

Poulos, H. M. 2009. A review of the evidence for pine-oak niche differentiation in the American Southwest. Journal of Sustainable Forestry 28:92–107.

Poulos, H. M. 2014. Tree mortality from a short-duration freezing event and global-change-type drought in a Southwestern piñon-juniper woodland, USA. PeerJ 2:1–14.

Poulos, H. M., G. P. Berlyn, and U. M. Goodale. 2008. Physiological and stuctural mechanisms of niche differentiation for three sky island Oaks in relation to light and temperature. Desert Plants 24:3–12.

R Core Team. 2016. R: A language and environment for statistical computing. R Foundation for Statistical Computing, Vienna, Austria.

Ramírez-Valiente, J. A., and J. Cavender-Bares. 2017. Evolutionary trade-offs between

drought resistance mechanisms across a precipitation gradient in a seasonally dry tropical oak (Quercus oleoides). Tree Physiology 37:889–901.

Randin, C. F., J. Paulsen, Y. Vitasse, C. Kollas, T. Wohlgemuth, N. E. Zimmermann, and C. Körner. 2013. Do the elevational limits of deciduous tree species match their thermal latitudinal limits? Global Ecology and Biogeography 22:913–923.

Rapacz, M., D. Gasior, Z. Zwierzykowski, A. Lesniewska-Bocianowska, M. W. Humphreys, and A. P. Gay. 2004. Changes in cold tolerance and the mechanisms of acclimation of photosystem II to cold hardening generated by anther culture of Festuca pratensis x Lolium multiflorum cultivars. New Phytologist 162:105–114.

Reich, P. B. 2014. The world-wide "fast-slow" plant economics spectrum: A traits manifesto. Journal of Ecology 102:275–301.

Rodwell, M., and B. Hoskins. 2001. Subtropical anticyclones and summer monsoons. Journal of Climate 14:3192–3211.

Romero Rangel, S., C. Ezequiel, R. Zenteno, M. De Lourdes, and A. Enríquez. 2002. El Género Quercus (Fagaceae) en el Estado de México. Annals of the Missouri Botanical Garden 89:551–593.

Sack, L., P. D. Cowan, N. Jaikumar, and N. M. Holbrook. 2003. The "hydrology" of leaves: co-ordination of structure and function in temperate woody species. Plant, Cell and Environment 26:1343–1356.

Sack, L., J. Pasquet-Kok, and PrometheusWiki Contributors. 2013. Leaf pressure-volume curve parameters. http://www.publish.csiro.au/prometheuswiki/tiki-pagehistory.php?page=Leaf pressure-volume curve parameters&preview=16.

Sakai, A. 1970. Freezing Resistance in Willows from Different Climates. Ecology 51:485–491.

Savitch, L. V., E. D. Leonardos, M. Krol, S. Jansson, B. Grodzinski, N. P. A. Huner, and G. Öquist. 2002. Two different strategies for light utilization in photosynthesis in relation to growth and cold acclimation. Plant, Cell and Environment 25:761–771.

Sawyer, D. A., and T. B. Kinraide. 1980. The forest vegetation at higher altitudes in the Chiricahua Mountains, Arizona. American Midlands Nauralist 104:224–241.

Schneider, C. A., W. S. Rasband, and K. W. Eliceiri. 2012. NIH Image to ImageJ: 25 years of image analysis. Nature Methods 9:671–675.

Scholander, P. F., E. D. Bradstreet, E. A. Hemmingsen, and H. T. Hammel. 1965. Sap pressure in vascular plants. Science 148:339–46.

Schwilk, D., M. Gaetani, and H. Poulos. 2013. Oak bark allometry and fire survival strategies in the Chihuahuan Desert sky islands, Texas, USA. PLoS ONE 8:e79285.

Schwilk, D. W., and J. E. Keeley. 2012. A plant distribution shift: temperature, drought or past disturbance? PLoS ONE 7:e31173.

Serbin, S. P., D. N. Dillaway, E. L. Kruger, and P. A. Townsend. 2012. Leaf optical

properties reflect variation in photosynthetic metabolism and its sensitivity to temperature. Journal of Experimental Botany 63:489–502.

Sexton, J. P., P. J. McIntyre, A. L. Angert, and K. J. Rice. 2009. Evolution and ecology of species range limits. Annual Review of Ecology, Evolution, and Systematics 40:415–436.

Sheppard, P., and A. Comrie. 2002. The climate of the US Southwest. Climate Research 21:219–238.

Shreve, F. 1915. The vegetation of a desert mountain range as conditioned by climatic factors. Carnegie Institution of Washington, Washington D.C.

Sims, D. A., and J. A. Gamon. 2002. Relationships between leaf pigment content and spectral reflectance across a wide range of species, leaf structures and developmental stages. Remote Sensing of Environment 81:337–354.

Skelton, R. P., A. G. West, and T. E. Dawson. 2015. Predicting plant vulnerability to drought in biodiverse regions using functional traits. Proceedings of the National Academy of Sciences 112:5744–5749.

Smith, R. J. 2009. Use and misuse of the reduced major axis for line-fitting. American Journal of Physical Anthropology 140:476–486.

Sparks, J. P., and R. A. Black. 1999. Regulation of water loss in populations of Populus trichocarpa: the role of stomatal control in preventing xylem cavitation. Tree Physiology 19:453–459.

Sperry, J. S. 1995. Limitations on stem water transport and their consequences. Page 440*in* B. L. Gartner, editor.Plant Stems: Physiology and Functional Morphology. Academic Press, Inc, San Diego, CA.

Sperry, J. S. 2003. Evolution of water transport and xylem structure. International Journal of Plant Sciences 164:S115–S127.

Sperry, J. S., J. R. Donnelly, and M. T. Tyree. 1988. A method for measuring hydraulic conductivity and embolism in xylem. Plant, Cell and Environment 11:35–40.

Sperry, J. S., F. C. Meinzer, and K. A. McCulloh. 2008. Safety and efficiency conflicts in hydraulic architecture: scaling from tissues to trees. Plant, Cell and Environment 31:632–645.

Stadtmuller, T., and N. Agudelo. 1990. Amount and variability of cloud moisture input in a tropical cloud forest. Pages 25–32Hydrology in mountainous regions. I - Hydrological Measurements; the Water Cycle. Proceedings of Lausanne Symposia. IAHS Publication.

Stephenson, N. L. 1990. Climatic control of vegetation distribution: the role of the water balance. The American Naturalist 135:649–670.

Sun, P., A. Grignetti, S. Liu, R. Casacchia, R. Salvatori, F. Pietrini, F. Loreto, and M. Centritto. 2008. Associated changes in physiological parameters and spectral

reflectance indices in olive (Olea europaea L.) leaves in response to different levels of water stress. International Journal of Remote Sensing 29:1725–1743.

Swetnam, T. W., and J. L. Betancourt. 1998. Mesoscale disturbance and ecological response to decadal climatic variability in the American Southwest. Journal of Climate 11:3128–3147.

Thenkabail, P. S., J. G. Lyon, and A. Huete, editors. 2011. Hyperspectral Remote Sensing of Vegetation. CRC Press, Boca Raton, FL USA.

Tsuda, M., and M. T. Tyree. 1997. Whole-plant hydraulic resistance and vulnerability segmentation in Acer saccharinum. Tree Physiology 17:351–7.

Tyree, M. T., and H. Cochard. 1996. Summer and winter embolism in oak: impact on water relations. Annales des Sciences Forestières 53:173–180.

Tyree, M. T., H. Cochard, P. Cruiziat, B. Sinclair, and T. Ameglio. 1993. Drought-induced leaf shedding in walnut: evidence for vulnerability segmentation. Plant, Cell & Environment 16:879–882.

Tyree, M. T., and H. T. Hammel. 1972. The measurement of the turgor pressure and the water relations of plants by the pressure-bomb technique. Journal of Experimental Botany 23:267–282.

Tyree, M. T., and J. S. Sperry. 1988. Do woody plants operate near the point of catastrophic xylem dysfunction caused by dynamic water stress? Plant Physiology 88:574–80.

Tyree, M. T., and M. H. Zimmermann. 2002. Xylem Structure and the Ascent of Sap. Springer-Verlag, Berlin Heidelberg.

USDA. 2014. Coronado National Forest GIS DataService, USDA Forest. http://www.fs.usda.gov/detail/r3/landmanagement/gis/?cid=stelprdb5208076.

USGS. 2009. 1/3-Arc Second National Elevation Dataset. http://nationalmap.gov.

USGS. 2013. Digital representations of tree species range maps from “Atlas of United States Trees” by Elbert L. Little, Jr. (and other publications). http://esp.cr.usgs.gov/data/little/.

Venables, W. N., and B. D. Ripley. 2002. Modern Applied Statistics with S. 4th ed. Springer, New York.

Verhoeven, A., W. Adams, and B. Demmig-Adams. 1996. Close relationship between the state of the xanthophyll cycle pigments and photosystem II efficiency during recovery from winter stress. Physiologia Plantarum 96:567–576.

Wallmo, O. 1955. Vegetation of the Huachuca Mountains, Arizona. American Midland Naturalist 54:466–480.

Warshall, P. 1995. The Madrean sky island archipelago: a planetary overview. Pages 6–18*in* F. DeBano, P. Ffolliott, C. Edminster, A. Ortega-Rubio, G. Gottfried, and R. Hamre, editors.Biodiversity and Management of the Madrean Archipelago: The Sky

Islands of Southwestern United States and Northwestern Mexico. Rocky Mountain Forest and Range Experiment Station, Fort Collins, Colorado.

Whittaker, R., and W. Niering. 1964. Vegetation of the Santa Catalina Mountains, Arizona. I. Ecological classification and distribution of species. Journal of the Arizona Academy of Science 3:9–34.

Whittaker, R., and W. Niering. 1965. Vegetation of the Santa Catalina Mountains, Arizona: a gradient analysis of the south slope. Ecology 46:429–452.

Williams-Linera, G. 1997. Phenology of deciduous and broadleaved-evergreen tree species in a Mexican tropical lower montane forest. Global Ecology and Biogeography Letters 6:115–127.

Williams, A. P., C. D. Allen, A. K. Macalady, D. Griffin, C. A. Woodhouse, D. M. Meko, T. W. Swetnam, S. A. Rauscher, R. Seager, H. D. Grissino-Mayer, J. S. Dean, E. R. Cook, C. Gangodagamage, M. Cai, and N. G. McDowell. 2012. Temperature as a potent driver of regional forest drought stress and tree mortality. Nature Climate Change 2:1–6.

Wold, S., A. Ruhe, H. Wold, and W. J. Dunn III. 1984. The collinearity problem in linear-regression: the partial least-squares (PLS) approach to generalized inverses. SIAM Journal on Scientific and Statistical Computing 5:735–743.

Wolfe, B. T., J. S. Sperry, and T. A. Kursar. 2016. Does leaf shedding protect stems from cavitation during seasonal droughts? A test of the hydraulic fuse hypothesis. New Phytologist 212:1007–1018.

Wright, I. J., P. B. Reich, M. Westoby, D. D. Ackerly, Z. Baruch, F. Bongers, J. Cavender-Bares, T. Chapin, J. H. C. Cornelissen, M. Diemer, J. Flexas, E. Garnier, P. K. Groom, J. Gulias, K. Hikosaka, B. B. Lamont, T. Lee, W. Lee, C. Lusk, J. J. Midgley, M.-L. Navas, Ü. Niinemets, J. Oleksyn, N. Osada, H. Poorter, P. Poot, L. Prior, V. I. Pyankov, C. Roumet, S. C. Thomas, M. G. Tjoelker, E. J. Veneklaas, and R. Villar. 2004. The worldwide leaf economics spectrum. Nature 428:821–827.

Zarco-Tejada, P. J., J. R. Miller, G. H. Mohammed, T. L. Noland, and P. H. Sampson. 2001. Estimation of chlorophyll fluorescence under natural illumination from hyperspectral data. International Journal of Applied Earth Observation and Geoinformation 3:321–327.

Zarco-Tejada, P. J., A. Morales, L. Testi, and F. J. Villalobos. 2013. Spatio-temporal patterns of chlorophyll fluorescence and physiological and structural indices acquired from hyperspectral imagery as compared with carbon fluxes measured with eddy covariance. Remote Sensing of Environment 133:102–115.

Zomer, R., D. Bossio, A. Trabucco, L. Yuanjie, D. Gupta, and V. Singh. 2007. Trees and water: smallholder agroforestry on irrigated lands in Northern India. Colombo, Sri Lanka: International Water Management Institute. Page IWMI Research Report.

Zomer, R. J., A. Trabucco, D. A. Bossio, O. van Straaten, and L. V. Verchot. 2008. Climate change mitigation: A spatial analysis of global land suitability for clean

development mechanism afforestation and reforestation. Agriculture, Ecosystems & Environment 126:67–80.

Appendix S1. Chapter 1 Supplementary Methods and Results

Site selection and establishment

We surveyed a set of elevationally stratified random sites first for oak vegetation cover by elevation and selected a subset to use as longer term temperature and physiological data collection sites. We generated a random set of survey points within the eastern Chiricahua study area. We used only sites on high exposure sites to avoid the large differences in microclimate (water availability and temperature) and correlated occurring vegetation, that can occur with topographically diverse dry mountains (Boyko 1947, Holland and Steyn 1975, Pearson and Dawson 2003). We used a 10m-resolution digital elevation model (USGS 2009) to calculate aspect of exposure and total average solar irradiance during the dry season (Wh m^{-2}), June 1- July 31 in ArcMap (ESRI 2011) and generated a grid of points that were only of the highest 30% of irradiance values (lowest value: 130916 Wh m^{-2}) and either of primarily north (337.5 to 22.5^{o}) or south-facing aspect (and 157.5 to 202.5^{o}). We then excluded points near waterways (30m) or roads (100m) to avoid edge habitat-effects and human disturbance (USDA 2014). We assigned all points were than assigned to one of seven 200m elevation bands, proceeding from 1400m to 2800m.and randomly selected 20 points from each elevation and aspect (north or south) strata using the Sampling Tool Extension for ArcMap (Buja and Menza 2013). Then we randomly ordered each set and prioritized visits to the first five points in each elevation by aspect (north or south) stratum, only visiting the subsequent points if the initial points were inaccessible or did not meet the selection criteria (aspect, distance from road or stream).

Site temperature, water availability, leaf transpiration

At each site, we placed a piece of rebar (under special use permit USFS-DOU0149) in an unshaded location and affixed an aerated PVC pipe 0.75m above the ground. The pipe provided shade and relatively unimpeded air movement for exposed air temperature readings. We hung three iButtons inside the aerated housing at each site to log the temperature every three hours (0, 3, 6, 9, 12, 15, 18, 21 hours) from May 2014 to September 2015.

We determined, from a 24-hour period of sampling multiple individuals of the focal species, the daily period during which Ψ_{leaf} was at a minimum and stable, and we collected leaves for Ψ_{MD} measurements from 11am – 1pm. We removed petioled leaves from plants and immediately placed and sealed them into strong polyethylene bags, which included small, damp pieces of paper towel to reduce vapor pressure deficit and this water loss, and transported the bags in coolers.

Phenology--leaf marking

On all study individuals, we marked three fully-expanded, healthy, full-sun leaves of the most recent flush to monitor leaf retention, starting in October 2014. We loosely looped plastic-coated, flexible shape-retaining wire around leaf petioles and then looped the wire ends around the twigs to increase the chances of retention after leaf abscission. We checked leaves 3 times to 335 days after marking (following the next summer monsoons)

and used the timing of monitoring as a predictor in the leaf retention models (0, 90, 240, 335 days each coincidental with seasonal changes).

Turgor Loss Points

We measured Ψ_{TLP} as the osmotic potential at which leaf turgor is zero, following the relationship between the inverse of the leaf water potential and the leaf water lost, found by repeated measurements in a dehydrating leaf (Tyree and Hammel 1972, Koide et al. 1989). The results of these curves were also used to find absolute capacitance at full turgor, C_{leaf} (mol m^2 MPa^{-1}), a measure of the water storage within the leaf (Bartlett et al. 2012, Sack et al. 2013). We collected stems with recent, fully-expanded, healthy, full-sun leaves at the shoulder times of the day to minimize xylem cavitation, and transported the stems, wrapped in damp paper towels, in polyethylene bags and recut the stems under distilled water and rehydrated each for up to 18 hours in a dark and humid environment. We followed the bench-dry method to determine Ψ_{TLP} (Koide et al. 1989, Sack et al. 2013), allowing leaves to desiccate briefly and the equilibrate between leaf water potential measurements that were reduced by approximately 0.3MPa at each repeated measure. We placed the leaves in a loose plastic wrap and let them equilibrate for at least ten minutes between measurements in Whirl-Pak polyethylene bags (Nasco, Fort Atkinson, WI, USA) to reduce any water loss during the measurements. We additionally scanned the leaves just before measuring and dried the leaves for at least 72 hours before weighing for leaf dry weight and calculations of leaf water.

We removed saturated points, or points at which water loss did not reduce the Ψ_{leaf} by more than 0.01MPa, before Ψ_{TLP} calculation. We then plotted relationship curve and fit a

line to the linear portion of the curve, found using Reduced Major Axis regression techniques (package lmodel2 Legendre 2014) to allow for error in both water weight and Ψ_{leaf} measures (Smith 2009) and maximized linear fit of osmotic potential portion of the curve. We did not calculate the Ψ_{TLP} when we had fewer than 4 points after turgor loss point to fit (average support=7.4±1.8 points). We calculated C_{leaf} as the product of saturated water content (mol)/leaf area (m^2) and the slope of relative water content over declining Ψ_{leaf} (MPa^{-1}) before TLP (Bartlett et al. 2012, Sack et al. 2013). We dropped individuals from analysis which had R^2<0.8 values for lines of fit to osmotic potential declines.

Freezing injury

We cut stems under water to reduce any embolism, and then immediately placed the cut end of stems in rose tubes filled with distilled water. Distal stem ends were kept covered in polyethylene bags to maintain humid environments and kept cool (4-8^{o}C). We shipped samples back to the University of Minnesota and tested the live stems within 4 days of collection. We tested stems in two rounds (half of each species set from each site). We sectioned the stems into seven 1-cm segments, avoiding nodes as much as possible, and placed them in 15ml conical tubes containing 1ml of nanopure water (<1 μS specific conductivity). Stem sections from each individuals were allotted to an unfrozen control and the other tubes were allotted to a treatment temperature (-5, -10, -15, -20, -25, and -38^{o}C). Tubes were frozen at a rate of -5^{o}C/hour in a programmable freezing chamber (Cole-Parmer Instrument Co. , Vernon Hills, IL, USA) and removed after being held at their assigned temperature for 30 minutes. Because of equipment limitations, we

achieved the lowest temperatures (-25, -38^{o}C), by removing the tubes to stand-alone freezers. We monitored temperatures every minute in all environments with multiple copper-constantin thermocouples attached to a datalogger (Campbell Scientific, Inc., Logan, UT, USA). We added an additional 8ml of nanopure water to each tube after freezing, agitated for the tubes at 200rpm for 24 hours, and measured the specific conductivity of the solutions. We then autoclaved all of the tubes to heat kill the stems, agitated the tubes again for 24 hours, and again measured specific conductivity.

Appendix S1 Tables

Table S1.1. Study site species and environmental data. Number of species per site shown following species name and sites without species were used only for temperature data collection. Mean temperatures for study duration, including mean summer maximum (mean of daily summer maxima) and absolute winter minimum are shown.

elevation (m)	aspect	aspect (deg)	species	N	mean T (^{o}C)	mean summer max T (^{o}C)	winter minT (^{o}C)
1612	N	14	--	0	14.9 (±10.2)	35.2	-10.5
1665	S	169	--	0	16.1 (±9.3)	33.7	-7.8
1735	S	174	*Q. arizonica* (2), *Q. emoryi* (6), *Q. grisea* (4)	12	14.5 (±11.5)	36.5	-11.5
1761	N	353	*Q. arizonica* (6), *Q. hypoleucoides* (6)	12	14.2 (±9.6)	34.6	-10.0
1807	S	159	--	0	15.4 (±10.5)	35.8	-10.5
1887	N	11	--	0	13.3 (±8.8)	30.8	-10.5
1947	N	12	*Q. arizonica* (6), *Q. hypoleucoides* (6)	12	13 (±9)	31.4	-10.3
1980	S	198	*Q. arizonica* (6), *Q. emoryi* (6)	12	15.4 (±8.9)	33.0	-7.0
2026	N	357	*Q. arizonica* (6), *Q. hypoleucoides* (6), *Q. rugosa* (6)	18	13.3 (±8.5)	31.4	-9.5
2140	S	170	*Q. arizonica* (6)	6	14 (±8.4)	31.9	-8.0
2303	S	199	*Q. arizonica* (6), *Q. hypoleucoides* (6)	12	13.3 (±9.4)	31.7	-10.8
2359	N	12	*Q. arizonica* (6), *Q. hypoleucoides* (6)	12	11.8 (±7.7)	27.8	-9.5
2481	N	338	*Q. gambelii* (6), *Q. rugosa* (6)	12	10.7 (±7.5)	27.8	-10.5
2495	S	189	*Q. hypoleucoides* (6), *Q. rugosa* (6)	12	11.3 (±8.5)	28.9	-12.8
2547	N	10	--	0	9.4 (±7.3)	24.6	-11.3
2586	S	163	*Q. gambelii* (6), *Q. hypoleucoides*(6)	12	11.3 (±8.5)	29.2	-12.0
2620	N	341	*Q. gambelii* (6)	6	9 (±7.2)	24.1	-11.5
			total individuals	**138**			

Table S1.2. Pearson correlations between locally collected temperature data (2014 – 2015), elevation, and extracted long-term climate variables. Temperature data was collected from June 2014 – June 2015 at all measurement sites (N=17) and local elevations and compared to bioclimatic variables of BIO1 (mean annual temperature), BIO6 (minimum temperature of coldest month) and AI (aridity index, MAP/MAE, Hijmans et al. 2005, CGIAR-CSI 2008). Significance values were adjusted to reduce the false discovery rate (Benjamini and Hochberg 1995) and shown as p<0.01 **, p<0.0001 ***.

	elevation	AI	BIO1	BIO6
annual mean	**-0.90*** **	**-0.91*** **	**0.90*** **	**0.90*** **
summer maximum	**-0.89*** **	**-0.89*** **	**0.88*** **	**0.86*** **
summer mean	**-0.97*** **	**-0.97*** **	**0.97*** **	**0.95*** **
winter mean	**-0.66** **	**-0.69** **	**0.66** **	**0.68** **
winter minimum	-0.44	-0.51	0.49	0.54
elevation	--	**0.99*** **	**-0.99*** **	**-0.97*** **

Table S1.3. Species mean (quadratic peak) elevation, calculated from presence data of site surveys (N=62) following Lenoir et al. (2008). Peak elevation are shown for each species in an overall model of presence by elevation (aspect=both) and in data subset to either aspect. Amplitude is the amplitude of the fitted normal curve and maximum is the maximum probability the peak. Chi-squared tests show significance (p-values) of comparison to quadratic model.

species	aspect	N	Peak elevation (m)	Amplitude	Maximum	χ^2 (null)	χ^2 (linear)
arizonica	both	30	2031.012	133.456	0.957305	0.000	0.000
arizonica	N	10	1971.836	143.0053	0.865168	0.000	0.006
arizonica	S	20	2075.279	85.9152	0.999962	0.000	0.000
emoryi	both	17	1808.574	115.7416	0.770255	0.000	0.000
emoryi	N	5	1799.378	57.83943	0.854863	0.000	0.035
emoryi	S	12	1828.342	116.0103	0.857677	0.000	0.000
gambelii	both	13	2586.903	177.4363	0.569839	0.000	0.182
gambelii	N	11	2572.663	183.9474	0.781605	0.000	0.252
gambelii	S	2	2556.581	3.011176	1	0.001	0.002
grisea	both	7	1635.689	62.35952	0.632243	0.000	0.031
grisea	N	3	1246.296	120.4997	0.999251	0.003	0.934
grisea	S	4	1633.367	68.86928	0.572564	0.003	0.121
hypoleucoides	both	20	2259.107	183.8011	0.668685	0.000	0.000
hypoleucoides	N	9	2129.971	147.5525	0.812217	0.002	0.001
hypoleucoides	S	11	2374.154	136.3639	0.835974	0.000	0.012
rugosa	both	7	2329.76	253.7643	0.21987	0.109	0.158
rugosa	N	4	2145.647	143.2551	0.500939	0.045	0.013
rugosa	S	3	2523.802	68.19184	0.494564	0.008	0.145

Table S1.4. ANOVA (Type III) of plant water access and leaf physiological measurements by average Aridity Index at collection site (MAP/MAE) and species. Interactive terms were dropped when not significant. Significance notations are p < 0.001 ***, p< 0.01**, p<0.05*.

		AI	species	AI x species	*residuals*
dry season Ψ_{PD}					
	SS	4.68	7.83	4.39	34.6
	df	1	5	4	124
	F stat	16.8***	5.6***	3.9**	
Ψ_{TLP}					
	SS	0.02	2.45	2.18	11.07
	df	1	5	4	118
	F stat	0.2	5.2***	5.8***	
C_{leaf}					
	SS	0.2	0.61	--	2.45
	df	1	5	--	122
	F stat	10.2**	6.1***	--	
dry season $\Delta\Psi$					
	SS	4.97	9.93	--	47.7
	df	1	5	--	128
	F stat	13.3***	5.3***	--	
wet season $\Delta\Psi$					
	SS	0.06	4.45	--	38.33
	df	1	5	--	131
	F stat	0.2	3*	--	
wet season Ψ_{PD}					
	SS	0.1	0.29	--	1.76
	df	1	5	--	131
	F stat	7.2**	4.3**	--	

Table S1.5. ANOVA (Type III) of T_{50} by climatic and species predictors, and test round (covariate), a) T_{50} of all collected stems, b) T_{50} in summer stems, unacclimated to cold, c) T_{50} in acclimated stems Term significance as denoted as $p < 0.001$ ***, $p < 0.01$**.

	a				b				c			
	all seasons, T_{50}				**unacclimated, T_{50}**				**acclimated, T_{50}**			
predictor variables	**SS**	**df**	***F* stat**		**SS**	**df**	***F* stat**		**SS**	**df**	***F* stat**	
BIO6	0.5	1	0		6.51	1	0.9		1.67	1	0.1	
previous mean temperature	--	--	--		19.82	1	2.7		1.1	1	0.1	
collection season	4404.5	1	275	***	--	--	--		--	--	--	
test group	144.2	1	9	**	451.11	1	61	***	18.18	1	1.4	
species	1086.9	5	13.6	***	244.68	5	6.6	***	1058.81	4	20.7	***
residuals	1313.3	82			280.93	38			459.88	36	0	

Table S1.6. Species trait correlations (means of species at each collection site, N = 24, except in leaf retention, when N in dry and wet seasons = 21), upper diagonal is Pearson's r and lower is Spearman's rho. Significant correlations ($p<0.05$, alpha adjusted for multiple comparisons) are in bold.

Pearson's r

Spearman's rho	cold leaf retention	dry leaf retention	wet leaf retention	dry Ψ_{PD}	wet Ψ_{PD}	dry $\Delta\Psi$	wet $\Delta\Psi$	Ψ_{TLP}	C_{leaf}	SLA	accli-mated T_{50}	unaccli-mated T_{50}	elev	AI	BIO6
cold leaf retention		0.37	0.35	**-0.45**	**0.67**	**0.54**	-0.16	-0.34	-0.01	**-0.89**	0.24	**0.63**	**-0.46**	**-0.52**	**0.50**
dry leaf retention	0.44		**0.99**	0.12	-0.35	0.04	-0.34	0.00	**0.67**	**-0.62**	**0.68**	0.31	0.45	0.45	-0.40
wet leaf retention	0.42	**1.00**		0.13	-0.31	0.07	-0.34	0.02	**0.69**	**-0.70**	**0.71**	0.38	0.42	0.43	-0.38
dry Ψ_{PD}	-0.36	0.00	0.02		**-0.57**	**-0.72**	-0.04	0.30	0.37	0.29	0.14	-0.45	**0.75**	**0.77**	**-0.78**
wet Ψ_{PD}	0.32	-0.22	-0.22	**-0.67**		**0.48**	0.34	**-0.45**	-0.36	**-0.56**	0.13	**0.62**	**-0.75**	**-0.74**	**0.71**
dry $\Delta\Psi$	0.45	0.31	0.31	**-0.67**	0.45		-0.06	-0.24	-0.15	**-0.52**	0.07	**0.53**	**-0.49**	**-0.52**	**0.50**
wet $\Delta\Psi$	-0.12	-0.33	-0.34	0.01	0.35	-0.14		0.20	-0.28	0.19	-0.07	0.03	-0.19	-0.12	0.12
Ψ_{TLP}	0.07	0.13	0.13	0.23	-0.22	-0.18	0.21		0.30	0.23	0.03	-0.09	0.37	0.32	-0.33
C_{leaf}	0.25	**0.77**	**0.77**	0.39	**-0.50**	-0.02	-0.26	0.29		-0.22	**0.63**	0.14	**0.52**	**0.52**	**-0.51**
SLA	**-0.47**	**-0.79**	**-0.80**	0.11	-0.18	**-0.48**	0.19	-0.13	**-0.51**		-0.43	**-0.73**	0.25	0.30	-0.28
acclimated T_{50}	**0.51**	**0.73**	**0.75**	0.15	0.10	0.13	-0.12	0.11	**0.55**	**-0.66**		0.47	0.14	0.14	-0.15
unacclimated T_{50}	**0.54**	0.34	0.34	**-0.48**	**0.65**	**0.54**	0.10	-0.01	0.07	**-0.62**	0.45		**-0.51**	**-0.52**	**0.48**
elev	-0.27	**0.48**	**0.50**	**0.71**	**-0.82**	-0.39	-0.23	0.40	**0.58**	-0.08	0.14	**-0.50**		**0.98**	**-0.97**
AI	-0.27	0.42	0.44	**0.76**	**-0.78**	-0.45	-0.22	0.37	**0.53**	-0.07	0.14	**-0.49**	**0.98**		**-0.99**
BIO6	0.28	-0.41	-0.43	**-0.76**	**0.83**	0.42	0.20	-0.42	**-0.57**	0.09	-0.18	**0.50**	**-0.98**	**-0.97**	

Appendix S1 Figures

Figure S1.1. Average annual (a) and average daily summer maximum (b) and winter minimum (c) temperatures by elevation of site for study period of 2014-2015. North-facing (circles) and south-facing (triangles) and their lines of fit are shown around the overall mean (solid line).

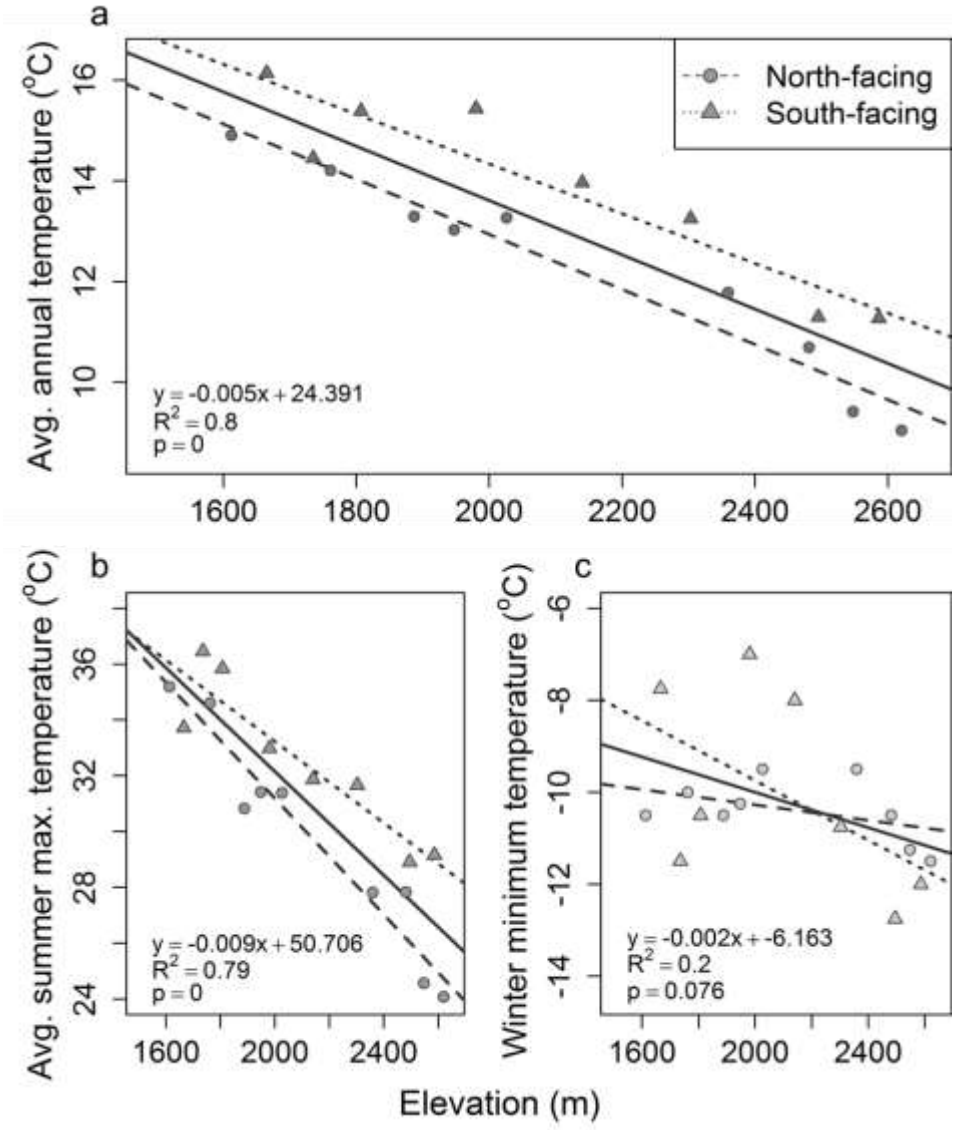

Figure S1.2. Mean annual temperatures (local observed MAT in light gray circles and WorldClim derived BIO1 in dark circles) by elevation of site (N=17). Open circles show local NOAA temperature stations (NOAA 2016). A 95% CI is shown around local MAT and the average difference between all fitted values of the model is shown as 1.93^{o}C, an estimate of local temperature anomalies over historic averages.

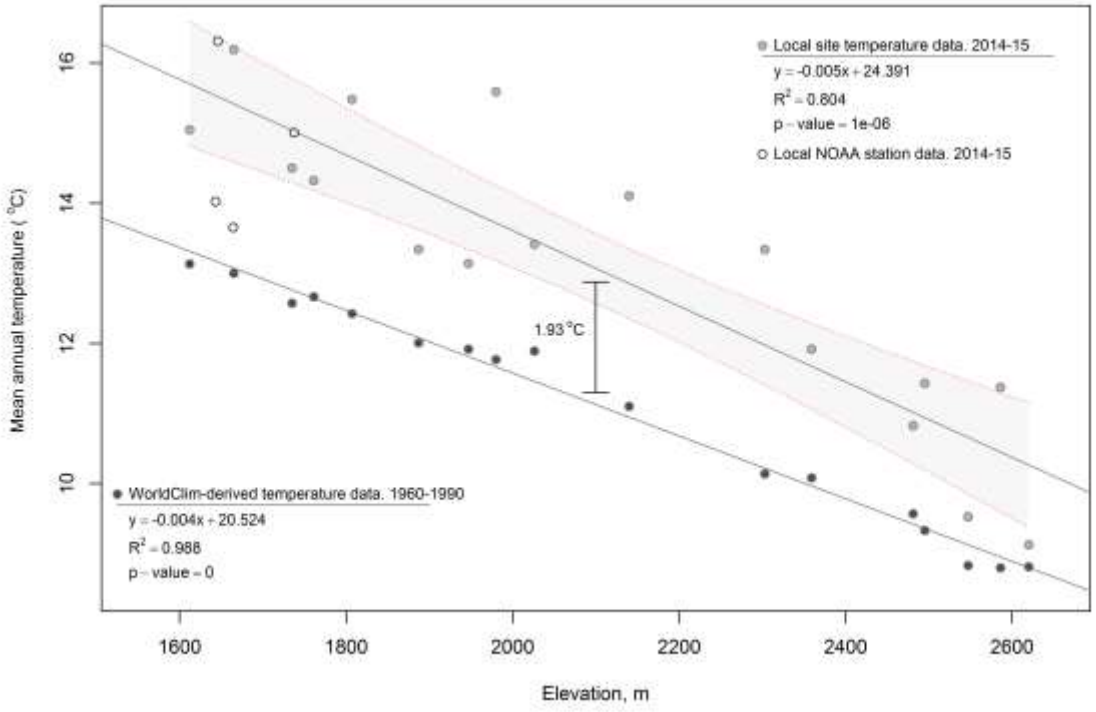

Appendix S2. Chapter 2 Supplementary Methods and Results

Methods

Pneumatic method

We calculated reservoir volume as the sum of all area between stem end and the pressure transducer. We used a vacuum gage pressure transducer (PX141-015V5V, Omega Engineering), which ranged from 1V at 0psi to 6V at -15psi, when supplied with an 8V input (repeatability ±.15% span of range). We kept input constant at 8V with a step-down voltage regulator with an output display reading accurately to one significant digit. Voltage and air temperature were recorded every second on a Campbell 850x Datalogger (Campbell Scientific, Utah USA). We converted voltage of start and end of each 180 second measurement to pressure (in kPa) using the manufacturers reported linearity, $y = 20.682 – 20.6842 * x$.

We found covered leaves to be in equilibrium with stem water potential. In several species of oaks, we covered multiple leaves with plastic and foil and let the stem desiccate. We measured leaf water potential (leaf pressure chamber, Soilmoisture Equipment Corp., California USA) of two covered leaves simultaneously from each stem after an hour of being covered and after the stem had been kept in a dark bag to equilibrate for up to an hour. We found an average difference of 0.1MPa ± 0.1 between any two covered leaves and no significant change in covered leaf water potential after the whole stem had been left to equilibrate for at least 15 minutes in a dark humid environment, indicating that covered leaves are equilibrated with stems with minimal

additional equilibration time. We then used covered leaves to measure stem water potential and we let stems equilibrate in a dark bag for 30 minutes after drying before measuring.

We covered 1-2 leaves were wrapped in plastic wrap and foil before leaving to rehydrate. Just before the initial (most hydrated) stem air volume test, we sampled one covered leaf to insure that plants were well-hydrated ($\leq$ -1MPa). We recut stem ends immediately before measuring and fit with a tight section of silicone tubing. We clamped the tubing to the stem with hose clamps or zipties and used latex glue to seal the edge of tubing to stem. We kept stems in a black polyethylene bags during measurements to reduce transpiration. Between measurements, we left stems to bench dry in ambient laboratory conditions (low interior light, mean air temperature of 21.5^{o}C) between measurements with the ends of the stems (with tubing still attached) loosely wrapped with Parafilm (Bemis, Wisconsin, USA).

We considered stems dehydrated when we reached the limit of the pressure chamber or when the sap emerging from the cut petiole was minimal. Most individuals measured had strongly wilted leaves by the end of measurements. We left stems to desiccate for up to 18 hours.

We recorded the initial pressure as the pressure immediately after opening the vacuum to the stem section, as there is a volume of air within that section that immediately lowers

the pressure. We found this by referencing the recorded start time and referencing a visual plot of the datalogger output to find the initial drop. End voltages (pressure) were recorded at 180 seconds after the initial pressure. Some measurements had large enough air volume that the vacuum chamber needed to be depressurized to finish a measurement. In those cases, the total air discharged (AD, μL) was added from subsequent measures until 180 seconds of measurement was achieved.

We found leakage following Pereira et al. (2016), as K_{leak}, a measure of air flow into the system from atmospheric pressure, for all leakage measurements (N=18). We measured system leakage on a cut and sealed stem (sealed with superglue) and mounted in the same way that samples were measured. The mean value of K_{leak} was used to adjust the AD values for each measurement as a function of K_{leak}, duration of testing, and change in pressure between atmosphere and vacuum system. We used the mean value of the internal vacuum throughout a single measurement as the mean internal pressure. Stem leakage was subtracted from each calculated value of AD (air discharge amount μL 3 min^{-1}). Some individuals were dropped due to very large leaks in the system (an order of magnitude larger than the average value). The mean AD of any stem leak test was 4.4μL $3min^{-1}$ ±1.26. The mean value of K_{leak} 2.932 $x10^{-7}$ μL s^{-1} MPa^{-1} and the mean amount of leakage subtracted from any measurement was then 3.96μL $3min^{-1}$ ± 0.49.

Before fitting curves, we dropped any individual stems from the analysis that had an AD_{min} of greater than the mean and one standard deviation. This was a conservative effort

to remove samples for which leakage may have been greater than the measured stem leakage.

Appendix S2 Tables

Table S2.1. Correlations of climate of origin and climate of range variables. AI = aridity index, mean annual precipitation/mean annual evapotranspiration (CGIAR-CSI 2008), BIO15 = precipitation seasonality, BIO12 = mean annual precipitation, BIO1 = mean annual temperature, BIO4 = temperature seasonality (Hijmans et al. 2005)

		climate of range		
		mean	max	min
climate of origin	AI	0.96	0.81	0.45
	BIO15	0.92	0.89	0.86
	BIO12	0.92	0.65	0.63
	BIO1	0.64	-0.02	0.64
	BIO4	0.86	0.87	0.70

Appendix S2 Figures

Figure S2.1. Percent air discharged (PAD) by stem water potential for each species. Different symbols represent individual stems.

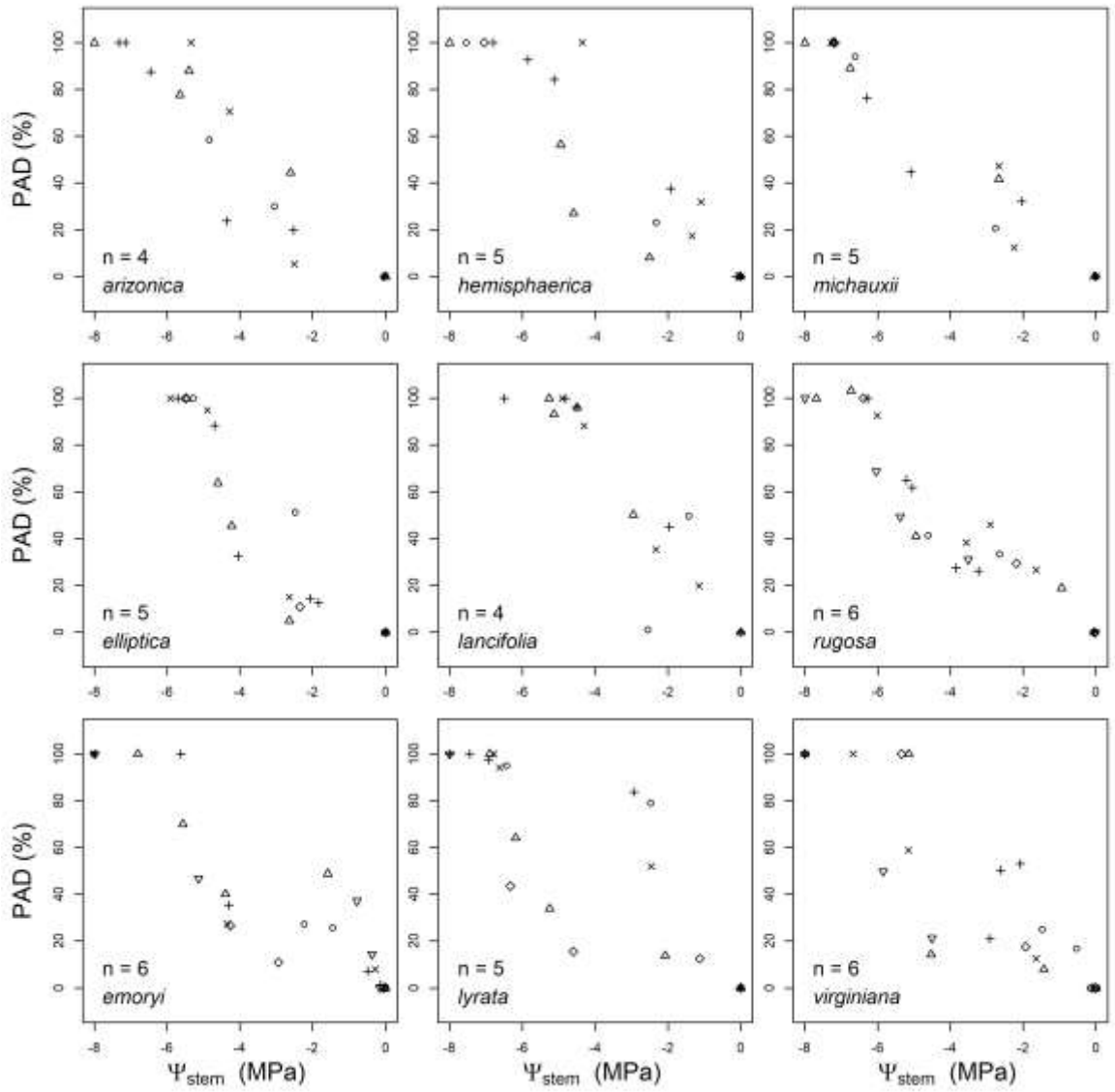

Figure S2.2. Percent air discharged (PAD) by stem water potential, with model fits. Curves fit as non-linear mixed models (individuals as random effect) to find PAD_{50} (P_{50}) for each species with a 95% bootstrapped CI (dotted upright lines). Data fit with package fitplc (Duursma and Choat 2017).

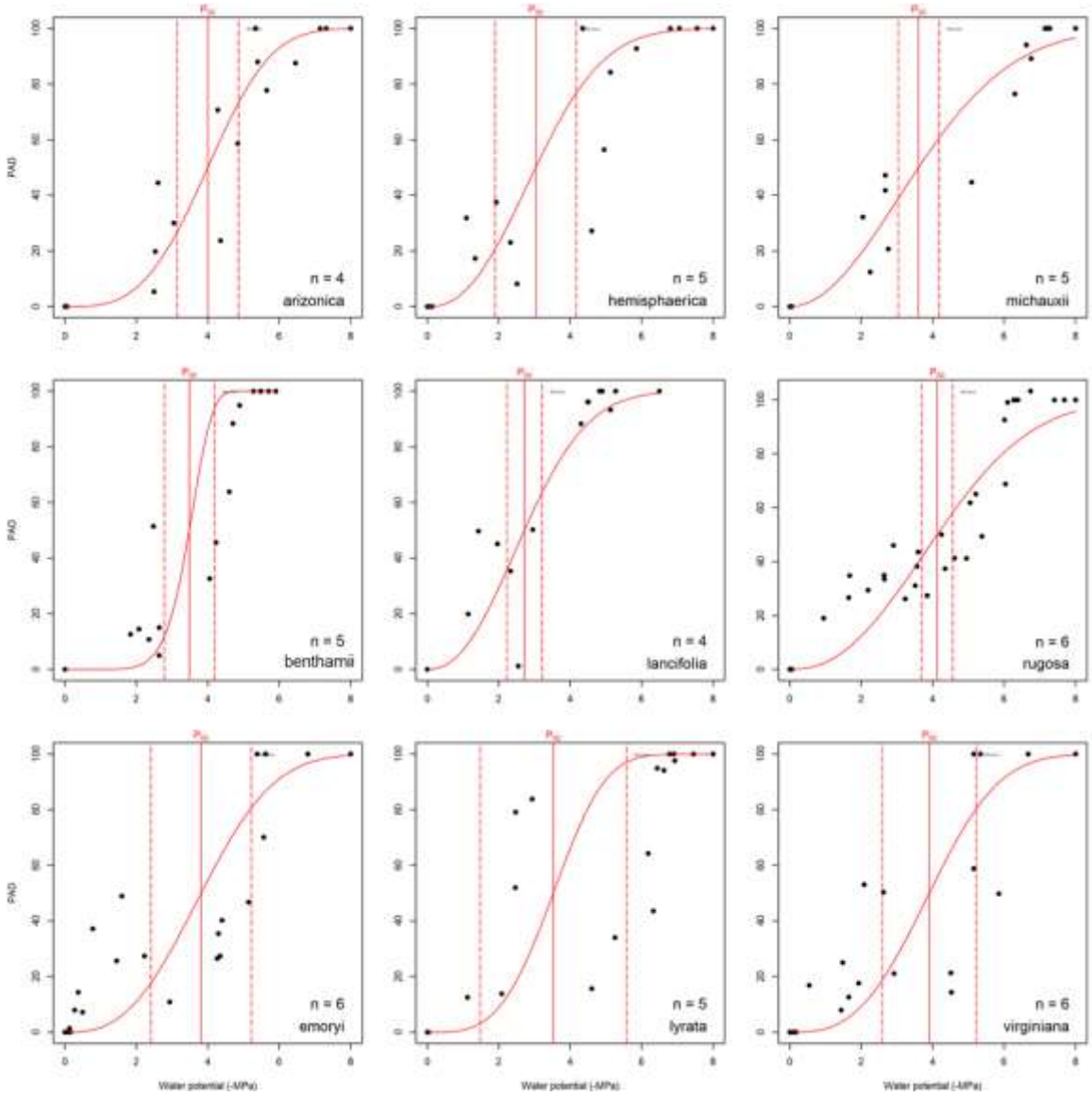

Figure S2.3. PAD_{50} predicted by non-linear mixed model and PAD_{50} predicted from model with only Ψ_{stem} as a fixed effect. Solid line shows linear fit between variables, dashed line shows 1:1 relationship. Grey polygon outlines 95% CI. Both species-level PAD_{50} were found using *plcfit* (Duursma and Choat 2017).

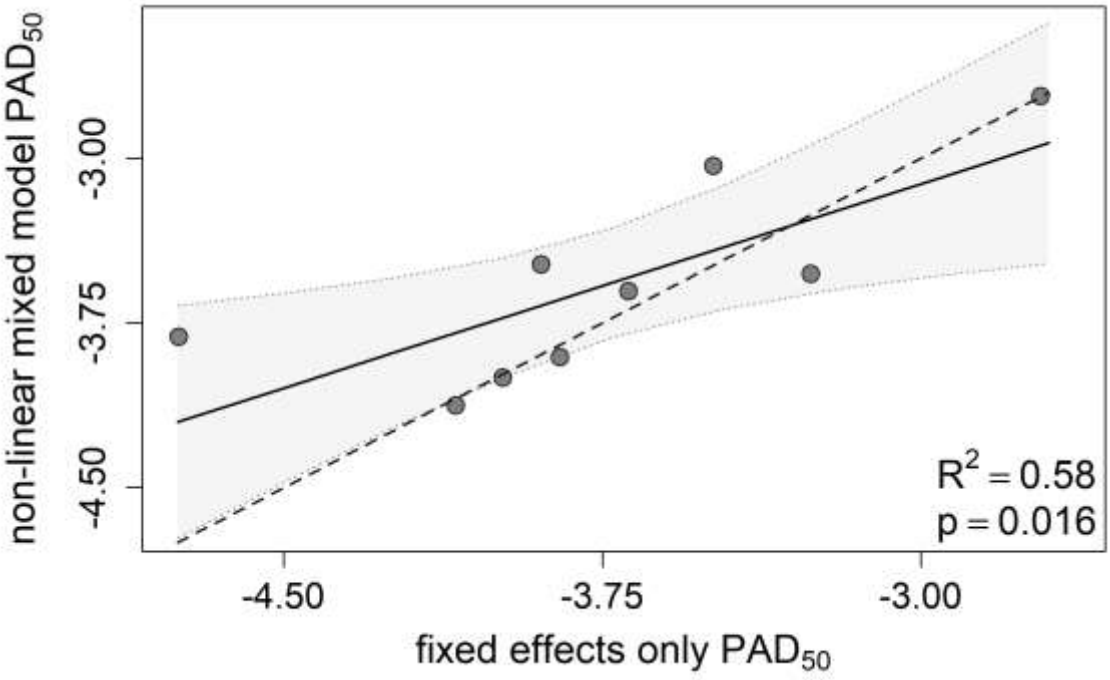

Figure S2.4. Stomatal closure by stem xylem vulnerability. Species mean leaf water potential at stomatal closure, Ψ_{crit} (MPa), by stem xylem vulnerability, $PAD_{x.}$ (MPa). a) $PAD_{12,}$ Ψ_{stem} at 12% embolism, dashed line indicates significant relationship at $p < 0.1$, b) $PAD_{50,}$ Ψ_{stem} at 50% embolism, c) $PAD_{88,}$ Ψ_{stem} at 88% embolism, relationship is not significant. Shaded areas show 95% confidence interval of model. Models were fit to natural log of Ψ_{crit}.

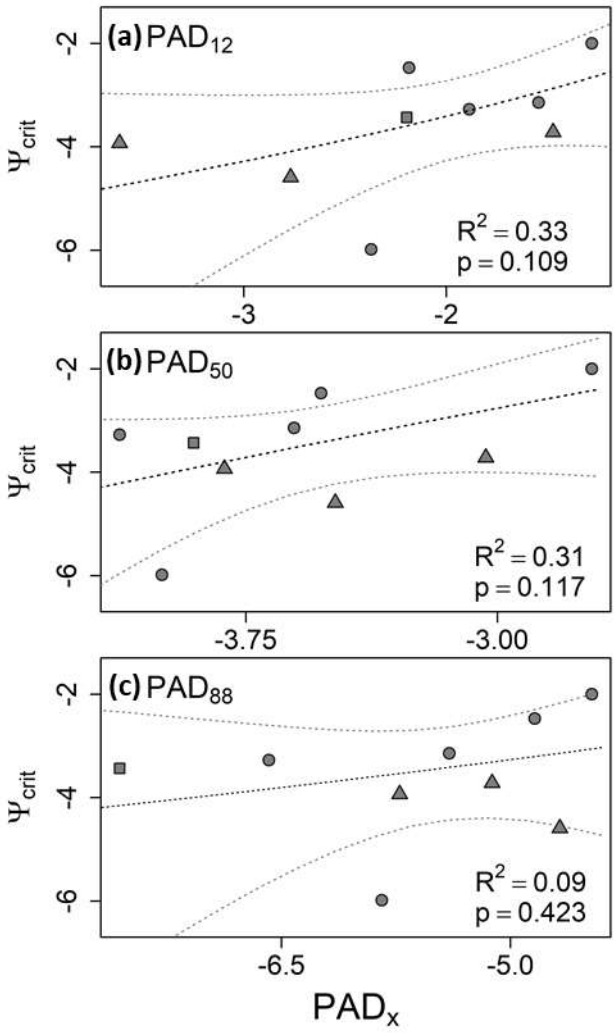

Appendix S3. Supplementary species monthly temperature and precipitation summaries

Methods

We downloaded species occurrence data, verified within the literature or with herbarium samples, for all oak species included in this dissertation (GBIF 2013). We used a subset of those occurrences (1 pt per 1 degree^2) and extracted the associated monthly average precipitation and temperature data from WorldClim v2 30 arc second raster files (Fick and Hijmans 2017). We found the mean values of monthly precipitation and temperature for each species. We also extracted the same values for each collection point for acorns used in our greenhouse experiments (Chapters 2 and 3) and from the study sites along the elevation gradient in the Chiricahua Mountains (Chapter 1) and found the mean monthly values for each species.

Appendix S3 Figures

Figure S3.1. Monthly precipitation and temperature for all oak species included in this dissertation (a - l this page, m - x, next page). Mean monthly precipitation (blue bars) and temperature (red points) for whole species ranges. Error bars show standard deviation for monthly temperature values. Solid lines are the mean monthly values from acorn collection sites (oaks in greenhouse experiment) and dashed lines are mean monthly values from sites in Arizona.

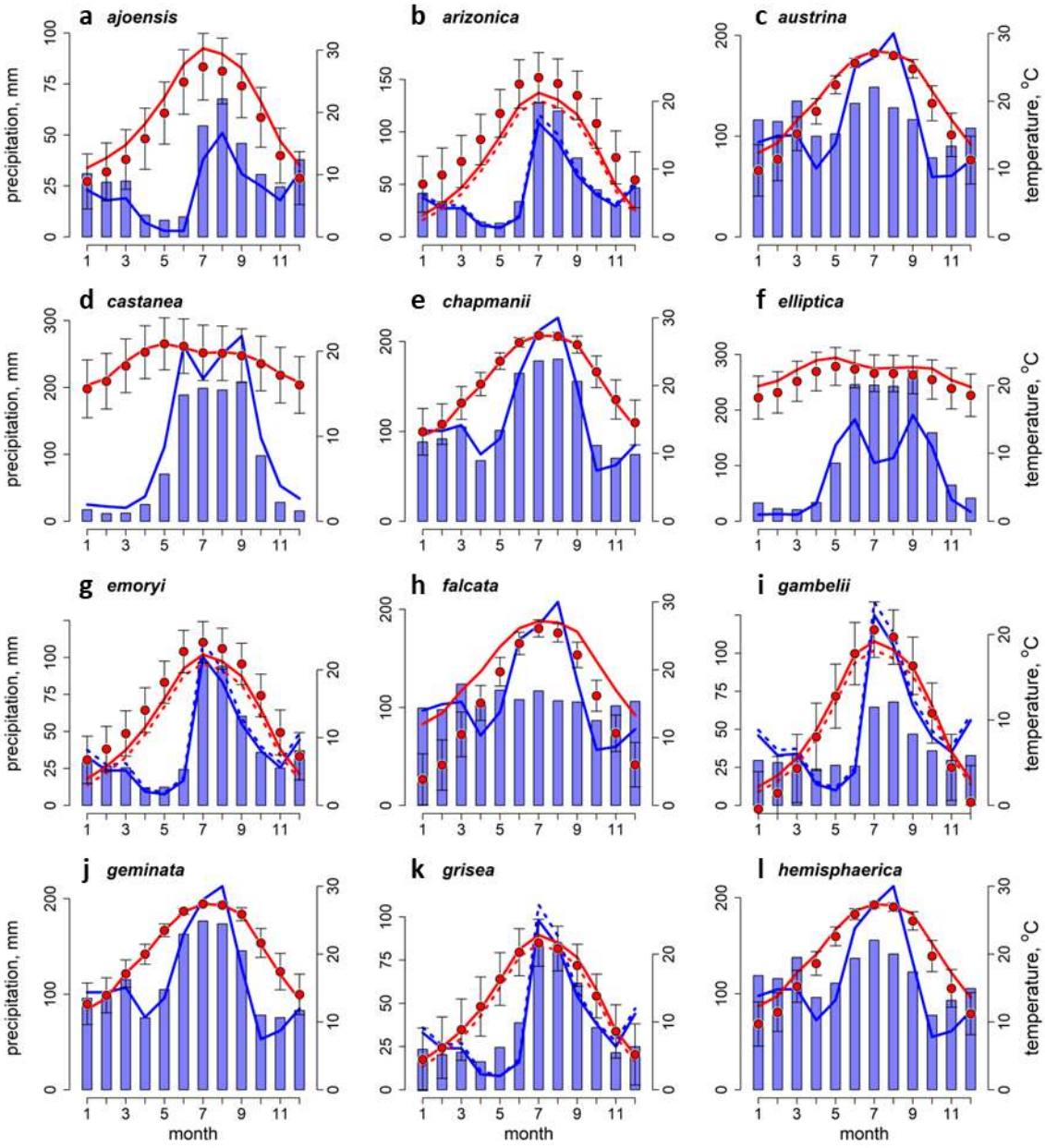

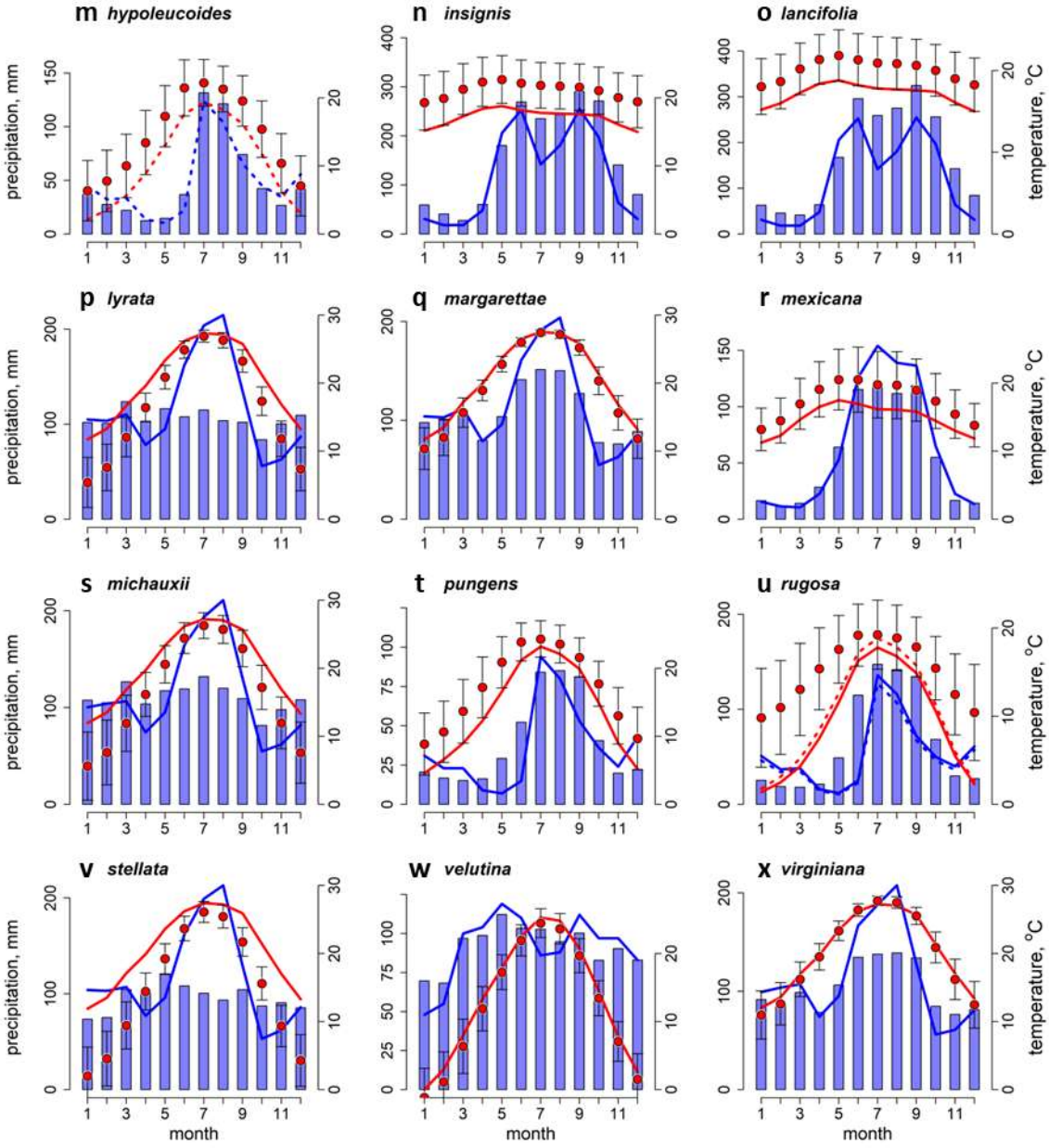
m hypoleucoides
n insignis
o lancifolia
p lyrata
q margarettae
r mexicana
s michauxii
t pungens
u rugosa
v stellata
w velutina
x virginiana
precipitation, mm
temperature, °C
month